

NON-LINEAR, SELF-CONSISTENT SCREENING APPLIED
TO SIMPLE METALS

By

MARK DOUGLAS WHITMORE, M. SC.

A Thesis

Submitted to the School of Graduate Studies
in Partial Fulfilment of the Requirements

for the Degree
Doctor of Philosophy

McMaster University

October 1978

NON-LINEAR SCREENING IN
SIMPLE METALS

DOCTOR OF PHILOSOPHY (1978)
(Physics)

McMASTER UNIVERSITY
Hamilton, Ontario.

TITLE: Non-linear Self-consistent Screening Applied to
Simple Metals

AUTHOR: Mark Douglas Whitmore, B.Sc. (McMaster University)
M.Sc. (McMaster University)

SUPERVISOR: Professor J.P. Carbotte

NUMBER OF PAGES: ix, 143

ABSTRACT

Non-linear, approximately self-consistent calculations of the electron density distribution around a proton and a helium nucleus in otherwise uniform electron gases of different densities have been performed, and applied to two types of problems.

One of these is the energies and equilibrium positions of isolated He in Al and Mg, and of pairs of both H and He in these metals. For the pair potential between the impurities an expression based on the density functional formalism has been used. Both perfect hosts and ones with single vacancies are considered. It is found that when occurring singly, each of these impurities is attracted at least to the vicinity of a vacancy in either metal, and that when two impurities are near a vacancy, the minimum energy configuration occurs with them bracketing the defect, relaxed towards it from the interstitial sites.

The superconductivity of metallic H has been considered, using non-linear calculations to determine the electron-proton and proton-proton potentials. It is found that this causes an enhancement of the transition temperature T_c over that obtained using linear response theory. T_c also depends strongly on the structure assumed, being computed as up to 280°K for the face-centered cubic structure, and less than 10°K for body-centered cubic.

ACKNOWLEDGEMENTS

It is a pleasure to thank my research supervisor Dr. J.P. Carbotte for his guidance, and in particular for his ever present enthusiasm, throughout the course of this work.

I also wish to thank Dr. F. Kus, Dr. G.R. Piercy, Dr. Z. Popović and Dr. R. Shukla as well as the students of the Theory Group for many helpful discussions.

I wish to acknowledge the financial assistance of the National Research Council of Canada as well as the family and estate of E. Dalley.

Many thanks go to Mrs. H. Kennelly for the speedy and accurate typing of most of this thesis.

And finally, I would like to thank my wife Eva, whose never failing support and encouragement have been of inestimable value, and who finished the typing of the thesis.

TABLE OF CONTENTS

		Page
CHAPTER I	INTRODUCTION	1
CHAPTER II	REVIEW OF MODEL POTENTIAL THEORY	5
	2.1 Introduction	5
	2.2 The Problem and the Assumptions	9
	2.3 The Model Potential	12
	2.4 Total Crystal Energy	21
	2.5 Effective Ion-ion Interaction	25
	2.6 Many Electron Effects and Effective Mass Corrections	26
	2.7 Model Potential Theory in the Local Limit	29
CHAPTER III	EXTENSIONS OF THE MODEL POTENTIAL THEORY: HYDROGEN AND HELIUM IMPURITIES IN SIMPLE METALS	33
	3.1 Introduction	33
	3.2 Theory of the Heat of Solution of a Single Impurity	35
	3.3 Approximate Non-linear Self-consistent Screening	42
	3.4 Energies and Equilibrium Sites of a Single He in Al and Mg	51
	3.5 Interatomic Potentials Using Non-linear Screening	58
	3.6 Energies and Equilibrium Sites of Pairs of H and He in Al and Mg	65

	Page
CHAPTER IV APPLICATION TO SUPERCONDUCTIVITY: METALLIC HYDROGEN	72
4.1 Introduction	72
4.2 Eliashberg Gap Equations and Func- tional Derivatives	76
4.3 Non-linear Screening Calculations and Potentials	82
4.4 Self-consistent Phonons in Hydro- gen	91
4.5 Transition Temperatures and Func- tional Derivatives	101
CHAPTER V SUMMARY AND CONCLUSIONS	114
APPENDIX I INTERATOMIC POTENTIALS FROM THE DENSITY FUNCTIONAL FORMALISM	117
AI.1 Relationship Between Inter- atomic Potentials Calculated Using Model Potentials and Using the Density Functional Formalism	117
AI.2 Applicability to Phonon Spectra	120
APPENDIX II ATOMIC FORCE CONSTANTS FOR METALLIC HYDROGEN	127
REFERENCES	139


LIST OF FIGURES

Figure No.		Page
2.1	Schematic view of model and ionic potentials	14
3.1	Displaced electron distributions around He in Al and Mg	49
3.2	Non-linear self-consistent potentials around He in Al and Mg	50
4.1	Displaced electron densities around a proton in metallic H	85
4.2	Screened electron-proton form factors	86
4.3	Screened proton-proton potentials	87
4.4	Displaced electron density about a proton using non-linear and linear response	88
4.5	Screened proton-proton potentials using non-linear and linear response	89
4.6	Phonon dispersion curves for fcc H, $r_s = 0.6$	94
4.7	Phonon dispersion curves for fcc H, $r_s = 0.8$	95
4.8	Phonon dispersion curves for fcc H, $r_s = 1.0$	96
4.9	Phonon dispersion curves for bcc H, $r_s = 0.6$	97
4.10	Phonon dispersion curves for bcc H, $r_s = 0.8$	98
4.11	Phonon dispersion curves for bcc H, $r_s = 1.0$	99
4.12	Phonon dispersion curves for fcc H, $r_s = 1.2$	100
4.13	Maximum phonon frequencies	102
4.14	$\alpha^2 F(\omega)$ for fcc H, $r_s = 0.6$	103
4.15	$\alpha^2 F(\omega)$ for fcc H, $r_s = 0.8$	104
4.16	$\alpha^2 F(\omega)$ for fcc H, $r_s = 1.0$	105
4.17	$\alpha^2 F(\omega)$ for bcc H, $r_s = 0.6$	106

Figure No.		Page
4.18	$\alpha^2 F(\omega)$ for bcc H, $r_s = 0.8$	107
4.19	$\alpha^2 F(\omega)$ for bcc H, $r_s = 1.0$	108
4.20	$\delta T_c / \delta \alpha^2 F(\omega)$ for fcc H	111

LIST OF TABLES

Table No.		Page
2.1	Notation used in total energy calculation	24
3.1	Structure and potential parameters for Al and Mg	37
3.2	Fermi level phase shifts for the electron-He potentials in Al and Mg	51
3.3	Trial potential parameters, and interaction and correlation energies for He in Al and Mg	52
3.4	Heats of solution of single He in Al and Mg	53
3.5	Energy barriers between interstitial sites for single He in Al and Mg	56
3.6	Energies of single H and He near a vacancy in Al and Mg	59
3.7	Energies of pairs of H and He in Al and Mg with one impurity at a vacancy	68
3.8	Energies of pairs of H and He bracketing a vacancy in Al and Mg	69
4.1	Fermi level phase shifts for the electron-proton potentials in metallic H	84
4.2	Superconductivity of fcc H	110
4.3	Superconductivity of bcc H	113
A.1	Various contributions to the Al interionic potential calculated using the density functional formalism	124



CHAPTER I

INTRODUCTION

Recent years have seen many calculations of properties of simple metals which depend on the basic electron-electron, electron-ion and ion-ion interactions. Pseudopotential, or model potential theories have been widely used primarily because of their success, and because they lend themselves readily to a perturbation theory approach, in which the unperturbed state of the metal is taken to be a collection of ions immersed in a uniform sea of conduction electrons.

This procedure is naturally based on a number of approximations, and is correspondingly subject to some limitations. While these are described more fully in the next chapter, it is appropriate to identify here those which primarily motivate the work described in the rest of this thesis.

The first of these is the assumption that an ion in a simple metal can be represented as a weak perturbation on the electron gas and treated in low order. Sometimes this is simply not the case, and to determine the behaviour of the electrons, a different approach must be used.

Second, even if this is valid, the actual modelling of the ion is subject to uncertainty. Generally one can either calculate the pseudopotential from first principles, or use a parametrized form fitted to some quantity. When using the former,

it is difficult to obtain accurate results, while the latter is not entirely satisfactory either, especially if there is not appropriate information to which a fit can be made.

Chapter II reviews model potential theory and notes its approximations. Much of this chapter is directly referred to later, so serves as more than just a review.

In the ensuing chapters and Appendix II calculations are reported which go beyond this to treat the response of the electrons to the ions. This is done by determining in a non-linear, approximately self-consistent way the electron charge distribution about an atomic nucleus when immersed in an otherwise uniform electron gas, which is then exploited to obtain a description of the basic interactions within the metal. The method is based on the density functional formalism of Hohenberg and Kohn (1964) and Kohn and Sham (1965).

Chapter III deals with the energies and configurations) of dilute hydrogen and helium in aluminum and magnesium. The impurities are considered both singly and in pairs, and the host metal both as a perfect crystal and as an otherwise perfect crystal with a single vacancy present. The H and He are treated via the non-linear calculations. For the former this is necessary because the bare proton is a strong perturbation. On the other hand, the latter remains neutral and hence could presumably be treated as a weak perturbation. Benedek (1978) has in fact calculated a pseudopotential for He in Al, assuming the core states are the same as for the free atom and that they can be

represented by a simple analytic form. Although the conduction charge density is well represented near the nucleus, outside of the core region it differs, primarily in the phase of the Friedel oscillations, and the He-Al interaction differs from that obtained using the non-linear theory.

The non-linear results are used to obtain better representations of the interactions of the impurity with the electron gas and with the host ions, which are employed in computing the heats of solution and energy barriers between different sites. In addition, the interaction between pairs of impurities has been treated by making use of the density functional formalism, in which the kinetic energy functional for the electrons is approximated by the gradient expansion, and the exchange by a local expression. The energies of various configurations of the pairs are considered for hosts with and without single vacancies.

Non-linear density calculations are also the basis of the next chapter. The high density metallic state of hydrogen is studied, and the electron distributions about a proton in electron gases at densities corresponding to different pressures determined. These are subsequently employed for the phonon spectra, the electron-phonon coupling, and superconducting properties. The results are found to differ quantitatively from those of linear response, and to depend sensitively on which structure is chosen.

In Appendix II, the calculation of the interatomic

potentials introduced in chapter III is related to the model potential expression described in chapter II. In addition, the suitability of this for computing lattice vibrations is discussed, and application of the method to aluminum, for which the non-linear calculations were done at both zero and finite pressures, is described.

Except when otherwise specified, atomic units with $\hbar = e = m = 1$ are used. The unit of energy is 27.210 eV and of distance is the Bohr radius.

CHAPTER II

REVIEW OF MODEL POTENTIAL THEORY

2.1 INTRODUCTION

Since this thesis deals, to a large degree, with both model potential theory and extensions of it, it is appropriate to begin by reviewing this theory. The general case will be presented first, followed by the results obtained when a local approximation to the model potential is used.

We start by reviewing some of the basic ideas of the theory of solids and particularly of simple metals. In a solid, we are confident the electrons can be described by a many particle wave function which is a solution of a Schrödinger equation involving the kinetic energies of all the nuclei and electrons present, as well as the interactions among all these particles. Of course, directly solving this problem of about 10^{23} particles is entirely out of the question. To proceed at all, one has to make approximations.

One of these is the self-consistent field approximation. It is assumed that each electron moves not in the instantaneous field of the other electrons, but only in their average field. If one ignores the exchange forces, this approach is called the Hartree approximation; otherwise it is known as the Hartree-Fock approximation. Much work has gone into going beyond the Hartree-Fock approximation, but these many electron effects, normally

called correlation corrections, are usually small (Anderson 1966).

A second approximation often made is the adiabatic approximation (Ziman 1960) which enables the separation of the Schrödinger equation into two equations, one describing the motion of the ions and the other describing that of the electrons in the field of the ions fixed at their instantaneous positions. This is justifiable because electrons move much more quickly than the ions, so can adjust almost immediately to their locations.

Within these approximations, a major theoretical goal is finding the electronic wave functions and corresponding energies. In simple metals, which are the only ones discussed here, the electrons are divided into two groups, the valence or conduction electrons and the core electrons. The former are not localized, but can move more or less freely through the metal. The latter are very localized, essentially bound to individual nuclei. In fact, these electrons are so strongly bound that their wave functions are assumed not to differ from what they are in the free atom, and together with the nuclei form ions, normally arranged in a regular array. The simple metal can be viewed as this array of N ions immersed in a sea of NZ valence electrons, where Z is the valence of each ion. It is the valence electrons which are often of interest in metallic properties, and it is these whose properties model potential theory is designed to treat.

Since it is how they are scattered by the ions that determines the relevant behaviour of these electrons, not their detailed behaviour when they are within the ion cores, what is required is an approximate treatment which reproduces the scattering properly. This is the idea of model potential theory; within the core regions, where the electron-ion potential is strong, the potential is replaced by a weaker one; outside the core, it is left unchanged. The model potential is then determined to reproduce the electron behaviour outside the core regions, and since it is chosen to be weak everywhere, perturbation theory is used. There is a number of ways the potential can be determined (Cohen and Heine 1970), but a common procedure is to fit it, via some theory, to known experimental quantities, and then use it to calculate similar properties.

The idea of a model potential was introduced by Heine and Aberenkov (1964) and Aberenkov and Heine (1965) in the same spirit as the pseudopotential theory which had been introduced earlier (Phillips and Kleinman 1959, Kleinman and Phillips 1959, Austin, Heine and Sham 1962 and Harrison 1966). In the general formulation, several approximations were not fully investigated, and the screening was not treated in a consistent manner. Shortly after this introduction of the theory attempts were made to improve on its structure (Animalu 1965 and Animalu and Heine 1965) but it was not until the work of R.W. Shaw, Jr., and W.A. Harrison (Shaw and Harrison 1967, Shaw 1968, 1969a, 1970a, 1970b)

that the model potential theory was carefully made consistent, using a potential which is both non-local and energy dependent.

By shortly after the time of this basic reformulation, good summaries of both the pseudopotential and model potential theories existed (Harrison 1966, Heine 1970, Cohen and Heine 1970, Heine and Weaire 1970, and Shaw 1970b), and much work had been done using pseudopotentials with varying degrees of success (see for example Heine and Weaire 1970).

The development of the theory continued beyond this time with the inclusion of exchange and correlation effects among the conduction electrons (Shaw 1970a, Shyu et al 1971, Cohen and Heine 1970, Shaw and Heine 1972 and Shaw and Pynn 1969) and effective mass corrections (Shaw 1969b, Appapillai and Williams 1973 and Williams and Appapillai 1973). It was seen that exchange and correlation must be included to obtain results in agreement with experiment, but the necessity of incorporating the effective mass corrections is not so definite. In some cases it appears important to include these effects (Shaw 1969b), but for example the aluminum phonon dispersion curves can be reproduced quite accurately without them (Coulthard 1970).

In the rest of this chapter the basic formulation of the model potential theory as it had been developed up to about 1973 will be given. A full derivation will not be presented, and in particular the inclusion of exchange and correlation effects, as well as effective mass corrections, will be added in with very little discussion towards the end of the chapter.

2.2 THE PROBLEM AND THE ASSUMPTIONS

Within the self-consistent field approximation, we want to obtain the wave functions of the NZ electrons. The equation we wish to solve is

$$(T+V+V_e)|\psi_{\underline{k}}\rangle = E_{\underline{k}}|\psi_{\underline{k}}\rangle \quad (2.1)$$

The wavefunction $\langle \underline{r} | \psi_{\underline{k}} \rangle$, describes an electron with crystal momentum \underline{k} , moving in the field of the ions V and the self-consistent field V_e of the other valence electrons. T is the kinetic energy operator.

Exact solutions of this problem are still out of the question, due to the complexity of V and V_e . However if this equation were solvable for each occupied state $|\psi_{\underline{k}}\rangle$, then, for example, the electron density distribution could be constructed as a sum over occupied states.

$$n(\underline{r}) = \sum_{\underline{k}}^< |\langle \underline{r} | \psi_{\underline{k}} \rangle|^2 \quad (2.2)$$

where by $\sum_{\underline{k}}^<$ we mean the sum over all states with $|\underline{k}| \leq k_F$, the Fermi momentum for the crystal.

One way to solve (2.1) is to consider T as the unperturbed Hamiltonian and use perturbation theory. But, it can be seen immediately that this is not justified. Within each ion core $V+V_e$ is very strong becoming in fact singular right at the nucleus. It is precisely because of this that model theories are developed.

The potential is modelled in the core, but outside this region it is left as the bare ion potential, $-Z/r$. Inside the core, the model potential consists of shallow wells, which can be constructed to reproduce exactly the energy eigenvalues for each state, and which are in general functions of that state. The model equation is

$$(T+W^0+V_e)|\chi_{\underline{k}}\rangle = E_{\underline{k}}|\chi_{\underline{k}}\rangle \quad (2.3)$$

where W^0 is the model potential of all the ions, the $|\chi_{\underline{k}}\rangle$ are the model wave functions and the $E_{\underline{k}}$ are to be the same as for the true states $|\psi_{\underline{k}}\rangle$. This is an equation with a weak potential which is treated as a perturbation on the free electron system.

The model equation is quite different from the Schrödinger equation for the electrons, and it is certainly not obvious that this step does not alter the essential physics of the problem. But the model states $|\chi_{\underline{k}}\rangle$ can be made equal to the $|\psi_{\underline{k}}\rangle$ outside the core regions, and approximately related within them, thus providing the connection between the two theories. And as we have stated, the energies are to be the same.

Before proceeding further with the development of the theory, we will now briefly summarize the three basic assumptions required.

The first of these is the self-consistent approximation, already described.

The second of these is the use of perturbation theory. The whole point of developing model potential theory is to be able to use perturbation theory, but there is no easy way of knowing if the Born series converges, since computationally it is very difficult to go beyond second order in energy calculations. Operationally, if a calculated property of the metal agrees with experiment, then convergence is normally assumed. If it does not agree with experiment, then one of the questions which should be addressed in understanding the discrepancy is if indeed perturbation theory is valid. A further discussion of this is given by Williams (1973).

The third approximation is the so-called small core approximation, which is used in three ways. The first is in neglecting the variation in the core region of the potential due to the conduction electrons. The energies of the core states are shifted, but their wave functions are not altered. Secondly, in evaluating matrix elements of smooth functions over the region of a core, the spatial variation of these functions is ignored. The final and crucial way in which this assumption enters the theory is the neglect of any overlapping of the cores. This means that the theory cannot handle without modification noble and transition metals with their overlapping d-orbitals, but rather is limited to the alkali and simple polyvalent metals.

2.3 THE MODEL POTENTIAL

The Schrödinger equation (2.1) can be rewritten as

$$(T + \sum_i v_i + V_e) |\psi_{\underline{k}}\rangle = E_{\underline{k}} |\psi_{\underline{k}}\rangle \quad (2.4)$$

where each v_i is the self-consistent potential of an individual bare ion core at its location \underline{R}_i in the metal, and V_e is, as before, the self-consistent potential of the electrons. The model equation (2.3) becomes

$$(T + \sum_i w_i^\circ + V_e) |\chi_{\underline{k}}\rangle = E_{\underline{k}}^M |\chi_{\underline{k}}\rangle \quad (2.5)$$

where the w_i° are the model potentials of the individual bare ions. We shall insist later that the model and true energies be the same, $E_{\underline{k}} = E_{\underline{k}}^M$, but for now designate them separately.

In the vicinity of the j th atom, these equations become

$$(T + v_j) |\psi_{\underline{k}}\rangle = (E_{\underline{k}} - \sum_{i \neq j} v_i - V_e) |\psi_{\underline{k}}\rangle \quad (2.6)$$

$$(T + w_j^\circ) |\chi_{\underline{k}}\rangle = (E_{\underline{k}}^M - \sum_{i \neq j} v_i - V_e) |\chi_{\underline{k}}\rangle \quad (2.7)$$

where the fact that w° has been constructed so that in the core region of atom j , $w_i^\circ = v_i$ for $i \neq j$, has been used. Invoking the small core approximation, $\sum_{i \neq j} v_i + V_e$ is taken to be constant over the core region j , allowing a new energy to be defined as

$$E_{\underline{k}}' = E_{\underline{k}} - \sum_{i \neq j} v_i - V_e \quad (2.8)$$

so (2.6) and (2.7) now become

$$(T+v_j) |\psi_{\underline{k}}\rangle = E_{\underline{k}} |\psi_{\underline{k}}\rangle \quad (2.9)$$

$$(T+w_j^0) |\chi_{\underline{k}}\rangle = (E_{\underline{k}} + E_{\underline{k}}^M - E_{\underline{k}}) |\chi_{\underline{k}}\rangle \quad (2.10)$$

in this region.

Different forms can be taken for the model potential w^0 ; the widely used form discussed by Shaw illustrates the characteristic features of the different possibilities. He defines, for each value of ℓ and E of the electron state being acted upon, a well depth $A_\ell(E)$ and radius $R_\ell(E)$. His model potential for the bare ion is then

$$w^0 = -\frac{Z}{r} \Theta(r - R_\ell(E)) - \sum_{\ell} A_\ell(E) P_\ell \Theta(R_\ell(E) - r) \quad (2.11)$$

where the P_ℓ are projector operators

$$P_\ell = -\sum_m |\ell m\rangle \langle \ell m| \quad (2.12)$$

and $\Theta(r)$ is the unit step function

$$\Theta(r) = \begin{cases} 1 & r > 0 \\ 0 & r < 0 \end{cases} \quad (2.13)$$

The model and true ion potentials are shown schematically in fig. 2.1, illustrating the replacement of the true potential by a weak potential within the core region. The $A_\ell(E)$ have been observed to be very nearly linear in E , so they are taken to be

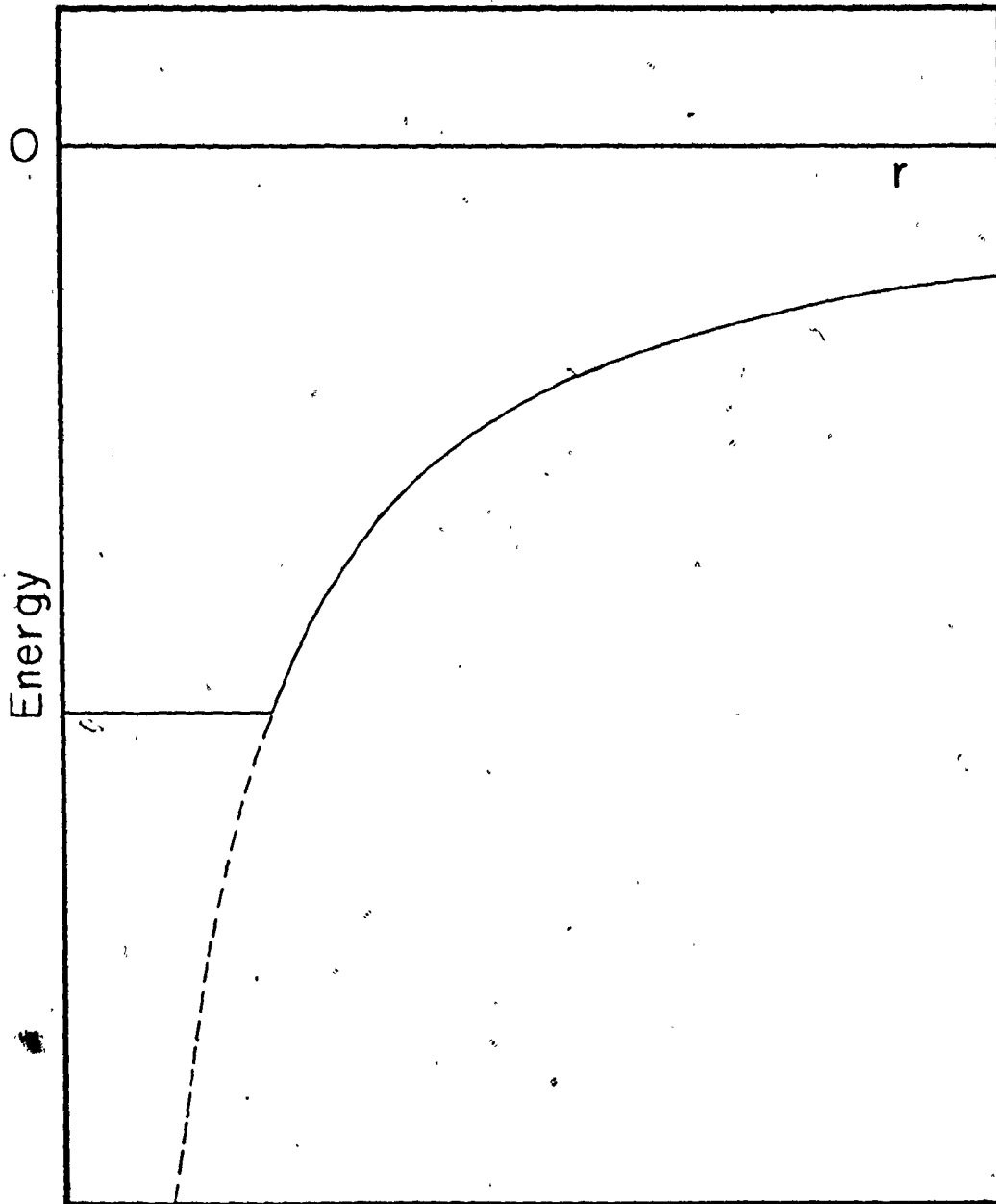


Fig. 2.1 Schematic view of model potential —
and ionic potential ---

$$A_{\ell}(E) = A_{\ell}(E_F) + (E - E_F)A'_{\ell}(E_F) \quad (2.14)$$

where $A'_{\ell}(E_F)$ is the derivative of the $A_{\ell}(E)$ with respect to E , evaluated at the Fermi energy E_F . The well depths are chosen to obtain $E_{\underline{k}} = E_{\underline{k}}^M$, so that (2.9) and (2.10) have the same eigenvalues. The parameters of the potential are determined by fitting to the energy term values of the free ion. There is some additional freedom here in that different values of the $A_{\ell}(E)$ can be chosen which give the same energies, and wavefunctions outside the core region. However each of these values of $A_{\ell}(E)$ produces a different wave function inside the core. In particular, the weakest $A_{\ell}(E)$ produces a nodeless wavefunction, and this is the value chosen. Once the $A_{\ell}(E)$ are determined, it is then necessary to use the same function for $A_{\ell}(E_{\underline{k}})$ in the metallic model equation, but at the metallic energy $E_{\underline{k}}$ which must be related to the zero of energy used in the free ion problem. Methods have been devised by Animalu and Heine (1965) for determining this relationship, but the general procedure is not very satisfactory. This is probably the biggest single problem involved in fitting a model potential to free ion properties, and extrapolating to the metallic regime.

There is still some freedom in choosing the well radii $R_{\ell}(E)$, which can be used to optimize the potential. The potential is chosen to produce the smoothest possible wave function by minimizing

$$I = \frac{\int d^3 \underline{r} |\nabla \chi_{\underline{k}}(\underline{r})|^2}{\int d^3 \underline{r} |\chi_{\underline{k}}(\underline{r})|^2} \quad (2.15)$$

with respect to the $R_{\ell}(E)$. This results in choosing

$$R_{\ell}(E) = Z/A_{\ell}(E) \quad (2.16)$$

so the model potential is continuous. The main advantage of this optimization is rapid convergence of the Fourier transform of the potential.

Once the model potential is obtained, whether in the form of Shaw or some other, the wavefunctions and energies in the metal can be calculated.

Although it is not possible to accurately construct the electron distribution within the core regions, via what is called the depletion charge density, a reasonable approximation to it can be constructed everywhere.

The total charge distribution as given by (2.2) can be expressed using the model wave functions $\chi_{\underline{k}}(\underline{r})$ and by introducing a new function $\rho_{\underline{k}}(\underline{r})$ so that

$$n(\underline{r}) = \sum_{\underline{k}} (\chi_{\underline{k}}^*(\underline{r}) \chi_{\underline{k}}(\underline{r}) + \rho_{\underline{k}}(\underline{r})) \quad (2.17)$$

where $\rho_{\underline{k}}(\underline{r})$ is non-zero only within the ion cores, since $\chi_{\underline{k}}(\underline{r}) = \psi_{\underline{k}}(\underline{r})$ outside them. The depletion charge density is defined by

$$\rho(\underline{r}) = \sum_{\underline{k}} \rho_{\underline{k}}(\underline{r}) \quad (2.18)$$

The model theory is to be thought of as producing a depletion of charge in the core regions, given by $\rho(\underline{r})$.

Knowing $\rho_{\underline{k}}(\underline{r})$ and $\chi_{\underline{k}}(\underline{r})$ would be equivalent to knowing the $\psi_{\underline{k}}(\underline{r})$, so it is hardly surprising that model potential theory does not tell us precisely the $\rho_{\underline{k}}(\underline{r})$. However, consider the total depletion charge about a single ion site of volume Ω_M , known as the depletion hole ρ .

$$\rho = \int_{\Omega_M} d^3\underline{r} (\sum_{\underline{k}} (\psi_{\underline{k}}^*(\underline{r}) \psi_{\underline{k}}(\underline{r}) - \chi_{\underline{k}}^*(\underline{r}) \chi_{\underline{k}}(\underline{r}))). \quad (2.19)$$

Although this definition of ρ clearly depends on the $\psi_{\underline{k}}(\underline{r})$, it can actually be exactly expressed solely in terms of the model parameters

$$\rho = - \int_{\Omega_M} d^3\underline{r} (\sum_{\underline{k}} \chi_{\underline{k}}^*(\underline{r}) \frac{\partial}{\partial E_{\underline{k}}} W(E_{\underline{k}}) \chi_{\underline{k}}(\underline{r})) \quad (2.20)$$

The $\rho(\underline{r})$ cannot be expressed in terms of only the model potential, but it is generally approximated by a form such as

$$\rho(\underline{r}) = \rho \sum_i \delta(\underline{r} - \underline{R}_i) \quad (2.21)$$

We now proceed to solve the model equation

$$(T+W) |\chi_{\underline{k}}\rangle = E_{\underline{k}} |\chi_{\underline{k}}\rangle \quad (2.22)$$

where $W = W^0 + V_e$, by second order perturbation theory. The zero order wave function is clearly

$$\langle \underline{r} | \underline{k} \rangle = \frac{1}{\sqrt{\Omega}} e^{i \underline{k} \cdot \underline{r}} \quad (2.23)$$

where Ω is the crystal volume. The perturbed state is

$$|\chi_{\underline{k}}\rangle = |\underline{k}\rangle + \sum_{\underline{q}} a_{\underline{q}}(\underline{k}) |\underline{k} + \underline{q}\rangle \quad (2.24)$$

with

$$a_{\underline{q}}(\underline{k}) = \frac{2 \langle \underline{k} + \underline{q} | W | \underline{k} \rangle}{k^2 - |\underline{k} + \underline{q}|^2} \quad (2.25)$$

for $\underline{q} \neq 0$. Normally in perturbation theory the $|\chi_{\underline{k}}\rangle$ are normalized so $a_0(\underline{k}) = 0$. But in this case, instead of normalizing $|\chi_{\underline{k}}\rangle$, it is required that $|\chi_{\underline{k}}\rangle = |\psi_{\underline{k}}\rangle$ outside the core regions, and this leads to

$$a_0(\underline{k}) = \frac{N}{2} \langle \underline{k} | \frac{\partial}{\partial E_{\underline{k}}} W(E_{\underline{k}}) | \underline{k} \rangle_{\Omega_M} \quad (2.26)$$

The energy to second order of the state \underline{k} is

$$E_{\underline{k}} = \frac{1}{2} k^2 + \langle \underline{k} | W | \underline{k} \rangle + 2 \sum_{\underline{q} \neq 0} \frac{\langle \underline{k} | W | \underline{k} + \underline{q} \rangle \langle \underline{k} + \underline{q} | W | \underline{k} \rangle}{k^2 - |\underline{k} + \underline{q}|^2} \quad (2.27)$$

Now writing the potential as

$$W = \sum_i w(\underline{r} - \underline{R}_i) \quad (2.28)$$

where \underline{R}_i are the ionic positions, and introducing the structure factor

$$S(\underline{q}) = \frac{1}{N} \sum_j e^{-i \underline{q} \cdot \underline{R}_j} \quad (2.29)$$

(2.27) becomes

$$E_{\underline{k}} = \frac{1}{2} k^2 + N \langle \underline{k} | w | \underline{k} \rangle + 2 \sum_{\underline{q} \neq 0} \frac{N^2 |s(\underline{q})|^2 |\langle \underline{k} | w | \underline{k} + \underline{q} \rangle|^2}{k^2 - |\underline{k} + \underline{q}|^2} \quad (2.30)$$

Using (2.17), (2.20) to first order, and (2.26), the electron distribution in the metal is given to first order by

$$n(\underline{r}) = \sum_{\underline{k}} \left(\frac{1}{\Omega} + \frac{N}{\Omega} \langle \underline{k} | \frac{\partial}{\partial E_{\underline{k}}} w(E_{\underline{k}}) | \underline{k} \rangle \right) + \frac{2}{\Omega} \sum_{\underline{q} \neq 0} a_{\underline{q}}(\underline{k}) e^{i \underline{q} \cdot \underline{r}} + \rho \sum_i \delta(\underline{r} - \underline{R}_i) \quad (2.31)$$

where (2.21) is being used for the depletion holes.

Each term in (2.31) can now be physically interpreted. The first is a uniform density which when integrated over the crystal volume compensates for the background ions. The second is another uniform term, compensating for the depletion holes which are given by the fourth term. The third term is the screening charge density. Note that this charge has no $\underline{q}=0$ component so the integrated screening density is zero. Thus we can see that the electron distribution can be conveniently pictured as a sum of two fluctuating terms superimposed on a uniform background which when integrated over the total volume exactly accounts for all the electrons present.

The non-uniform charge is clearly expressible as a Fourier sum

$$\Delta n(\underline{r}) = \sum_{\underline{q}} e^{i\underline{q} \cdot \underline{r}} n_{\underline{q}} \quad (2.32)$$

with

$$n_{\underline{q}} = \frac{2}{\Omega} \sum_{\underline{k}} a_{\underline{q}}(\underline{k}) + \frac{\rho}{\Omega_0} S(\underline{q}) \quad (2.33)$$

where Ω_0 is the volume of the unit cell

$$\Omega_0 = \Omega/N \quad (2.34)$$

It is now straightforward to illustrate explicitly the self-consistent nature of the calculation. We considered as a part of W the self-consistent potential of the electrons which must be related to the density as

$$\begin{aligned} V_e(\underline{q}) &= \frac{4\pi}{q} n_{\underline{q}} \\ &= \frac{4\pi}{q^2} \left\{ \frac{4}{\Omega} \sum_{\underline{k}} \frac{\langle \underline{k} + \underline{q} | W^\circ | \underline{k} \rangle + V_e(\underline{q})}{k^2 - |\underline{k} + \underline{q}|^2} + \frac{\rho}{\Omega_0} S(\underline{q}) \right\}. \end{aligned} \quad (2.35)$$

In (2.35) we have used $\langle \underline{k} + \underline{q} | W | \underline{k} \rangle = \langle \underline{k} + \underline{q} | W^\circ | \underline{k} \rangle + V_e(\underline{q})$, and the self-consistent nature is quite apparent. Using the \underline{k} -independence of $V_e(\underline{q})$, it is now easy to show that (2.35) is equivalent to

$$V_e(\underline{q}) = \frac{S(\underline{q})}{\epsilon(\underline{q})} \left\{ \frac{4}{\pi^2 q^2} \int d^3 \underline{k} \frac{N \langle \underline{k} + \underline{q} | W^\circ | \underline{k} \rangle}{k^2 - |\underline{k} + \underline{q}|^2} + \frac{4\pi\rho}{\Omega_0 q^2} \right\}. \quad (2.36)$$

Here we have introduced the wave vector dependent dielectric function $\epsilon(\underline{q})$, which comes from

$$P \int^< \frac{d^3 \underline{k}}{k^2 - |\underline{k} + \underline{q}|^2} = \left(\frac{\pi q}{2}\right)^2 (1 - \epsilon(q)) \quad (2.37)$$

and is given by.

$$\epsilon(q) = 1 + \frac{1}{2\pi k_F \eta} \left\{ \frac{1 - \eta^2}{2\eta} \ln \left| \frac{1 + \eta}{1 - \eta} \right| + 1 \right\} \quad (2.38)$$

where $\eta = q/2k_F$.

$V_e(\underline{q})$, and hence $n_{\underline{q}}$ have now been expressed in terms of the bare ion potential w° and the structure factor $S(\underline{q})$.

The screened form factor $w_{\underline{q}}(\underline{k})$ can now be written without the structure factor as

$$\begin{aligned} w_{\underline{q}}(\underline{k}) &= N \langle \underline{k} + \underline{q} | w | \underline{k} \rangle \\ &= N \langle \underline{k} + \underline{q} | w^\circ | \underline{k} \rangle + \frac{1}{\epsilon(q)} \left\{ \frac{4\pi\rho}{\Omega_0 q^2} + \frac{4}{\pi^2 q^2} \int^< \frac{d^3 \underline{k}' \langle \underline{k}' + \underline{q} | w^\circ | \underline{k}' \rangle}{k'^2 - |\underline{k}' + \underline{q}|^2} \right\} \quad (2.39) \end{aligned}$$

The form of the matrix elements appearing in (2.39) naturally depends on the form taken for w° . For the Shaw potential, these are detailed in his thesis (Shaw 1970b) and further transformed to expressions convenient for computation by Gilat, Rizzi and Cubiotti (1969).

2.4 TOTAL CRYSTAL ENERGY

We now have, in Hartree theory, the energy of an electron in state \underline{k} . In principle it is now straightforward to calculate the total energy of the metal, but it turns out to con-

tain very many terms which are difficult merely to keep track of. Most of these occur because of the non-locality of the potential. Because of this complexity, and because no total energy calculations using non-local potentials are reported in this thesis, only a brief outline of the total energy derivation indicating a few important points, along with a presentation of the results, will be given.

Given the electron energies $E_{\underline{k}}$, the total energy per ion is given by

$$E = \frac{1}{N} \sum_{\underline{k}} \langle E_{\underline{k}} \rangle - \frac{1}{2N} \int d^3 \underline{r} n(\underline{r}) V_e(\underline{r}) + \frac{1}{2N} \sum_{i \neq j} V_d(|\underline{R}_i - \underline{R}_j|) \quad (2.40)$$

The first term double counts the electron-electron interaction, so a term equal to this interaction must be subtracted off, accounting for the second term in (2.40). The last term is the direct ion-ion interaction. Clearly, in using this equation, we are not considering the kinetic energy of the ions, so are dealing with a rigid lattice.

Inserting the expression for $E_{\underline{k}}$, (2.40) becomes

$$E = \frac{1}{N} \sum_{\underline{k}} \left(\frac{1}{2} k^2 \right) + \sum_{\underline{k}} \langle \underline{k} | w | \underline{k} \rangle + 2N \sum_{\underline{k}} \frac{|S(\underline{q})|^2 |\langle \underline{k} + \underline{q} | w | \underline{k} \rangle|^2}{k^2 - |\underline{k} + \underline{q}|^2} - \frac{1}{2N} \int d^3 \underline{r} n(\underline{r}) V_e(\underline{r}) + \frac{1}{2N} \sum_{i \neq j} V_d(|\underline{R}_i - \underline{R}_j|) \quad (2.41)$$

By converting the sum to an integral, the first term becomes $\frac{3}{5} Z \frac{k_F^2}{2}$. The second term is the most difficult to evaluate. It involves the $q=0$ limit of the form factor for each

value of \underline{k} , as well as relating the Fermi energy to the free ion energies. The detailed form again depends on the form taken for the potential.

Equation (2.41) can be rewritten as a sum of three terms

$$E = ZE_{fe} + E_{es} + E_{bs} \quad (2.42)$$

The first is the free electron energy which depends on the total volume but not the structure of the crystal

$$ZE_{fe} = \frac{3}{5} Z \frac{k_F^2}{2} + \sum_{\underline{k}} \langle \underline{k} | w | \underline{k} \rangle \quad (2.43)$$

The electrostatic energy E_{es} and band structure energy E_{bs} each depend on both the volume and structure, and are given by

$$E_{es} = \frac{1}{2N} \int (n_u + n_d + n_{val}) (V_u + V_d + V'_{val}) d^3 \underline{r} \quad (2.44)$$

$$E_{bs} = \sum_{\underline{q} \neq 0} |S(\underline{q})|^2 F(\underline{q}) \quad (2.45)$$

The notation used in (2.44) is defined in table 2.1; in the last term of that equation, the prime on V'_{val} indicates that charge interacting with itself is to be omitted. In (2.45), $F(\underline{q})$, which is structure independent, is known as the energy-wavenumber characteristic and is given by

$$F(\underline{q}) = \frac{2\Omega_0}{(2\pi)^3} \int d^3 \underline{k} \frac{2|w_{\underline{q}}^{\circ}(\underline{k})|^2}{k^2 - |\underline{k} + \underline{q}|^2} \quad (2.46)$$

Table 2.1

Notation used in total energy calculation

<u>Quantity</u>	<u>Notation for Charge</u>	<u>Notation for Potential</u>
Valence charge Z at ion sites	n_{val}	V_{val}
Depletion hole charge	n_{d}	V_{d}
Total uniform charge	n_{u}	V_{u}

The electrostatic energy cannot be evaluated directly because of the long range nature of the forces. Sums in both \underline{r} -space and \underline{q} -space converge only very slowly. Harrison (1966) describes these calculations, which can be more readily evaluated as

$$E_{\text{es}} = \frac{2\pi(Z^*)^2}{\Omega_0} \lim_{\eta \rightarrow \infty} \left\{ \sum_{\underline{q}=0} |S(\underline{q})|^2 \frac{e^{-q^2/4\eta}}{q^2} - 2 \sqrt{\frac{\eta}{\pi}} \right\} \quad (2.47)$$

where Z^* , the effective valence is given by $Z^* = Z - \rho$, and which can be expressed as

$$E_{\text{es}} = \frac{\alpha(Z^*)^{5/3}}{2 r_s} \quad (2.48)$$

where α is a constant depending on the structure of the crystal, and r_s is the electron gas density parameter, related to the mean electron density by

$$\frac{NZ}{\Omega} = \frac{1}{\frac{4}{3} \pi r_s^3} \quad (2.49)$$

2.5 EFFECTIVE ION-ION INTERACTION

As a final consideration of the non-local Hartree theory, we wish to focus briefly on the terms contributing to the total energy of the crystal which depend on the structure of the crystal. From these terms the effective interionic potential in the metal can be developed, which is used in, for example, phonon calculations.

Returning to (2.42) through to (2.46), we see that the terms which depend on the structure are

$$E' = E_{es} + E_{bs} \quad (2.50)$$

E_{bs} can be written

$$E_{bs} = \frac{1}{2N} \sum_{i \neq j} V_{ind}(|\underline{R}_i - \underline{R}_j|) + \frac{1}{N} \sum_{q \neq 0} F(q) \quad (2.51)$$

where

$$V_{ind}(|\underline{R}_i - \underline{R}_j|) = \frac{2}{N} \sum_{q \neq 0} F(q) e^{-iq \cdot (\underline{R}_i - \underline{R}_j)} \quad (2.52)$$

is known as the indirect interaction between two ions located at \underline{R}_i and \underline{R}_j .

The part of E_{es} which depends on the structure is the interaction of each depletion hole ρ and valence charge Z located at an ion site \underline{R}_i , with all the other such charges located at ion sites \underline{R}_j .

$$E'_{es} = \sum_{i \neq j} \frac{1}{2N} V_d(|\underline{R}_i - \underline{R}_j|) \quad (2.53)$$

where

$$V_d(|\underline{R}_i - \underline{R}_j|) = (Z^*)^2 / |\underline{R}_i - \underline{R}_j| \quad (2.54)$$

The effective interaction between two ions located at \underline{R}_i and \underline{R}_j is the sum of (2.52) and (2.54):

$$V_{eff}(\underline{R}_i - \underline{R}_j) = \frac{Z^{*2}}{|\underline{R}_i - \underline{R}_j|} + \frac{2}{N} \sum_{q=0} F(q) e^{-iq \cdot (\underline{R}_i - \underline{R}_j)} \quad (2.55)$$

2.6 MANY-ELECTRON EFFECTS AND EFFECTIVE MASS CORRECTIONS

Since the theory as it has been presented so far has taken no account of exchange and correlation effects, it is a Hartree theory. In this section, following Harrison (1966, 1970) and Shaw (1970a,b) these effects are included in an approximate way.

One way in which the theory is modified is in a lowering of the energy of the uniform electron gas. Using the analytic form of Pines and Nozières (1966), a correction is added to E_{fe} (equation (2.43))

$$\Delta E_{fe} = Z \left(-\frac{.458}{r_s} - .0575 + .0155 \ln r_s \right) \quad (2.56)$$

The first term is the exchange energy, and the next two the so-called correlation energy.

There is also an important effect on terms involving the non-uniformity of the electron density. The effect of these fluctuations is to add an exchange and correlation potential V_{xc} which in linear response can be expressed as $V_{xc}(q) = \chi_q n_q$, so that the total potential felt by an electron due to the other electrons is

$$V_e(q) = \left(\frac{4\pi}{q} + \chi_q\right) n_q. \quad (2.57)$$

χ_q can be regarded as a q -dependent coupling constant relating $V_{xc}(q)$ and n_q . After defining a new function $h(q) = -\frac{q^2}{4\pi} \chi_q$, the changes in the theory can be expressed as follows. The dielectric function (2.38) becomes

$$\epsilon(q) = 1 + \frac{(1-h(q))}{2\pi k_F^3 \eta^2} \left[\frac{1-\eta^2}{2\eta} \ln \left| \frac{1+\eta}{1-\eta} \right| + 1 \right]. \quad (2.58)$$

The screened form factor (2.39) becomes

$$w_q(\underline{k}) = w_q^{\circ}(\underline{k}) + \left(\frac{1-h(q)}{\epsilon(q)}\right) \left(\frac{4\pi\rho}{\Omega_0 q^2} + \frac{4}{\pi^2 q^2}\right) \int^< \frac{d^3 \underline{k}' < \underline{k} + \underline{q} | w^{\circ} | \underline{k} \rangle}{k^2 - |\underline{k} + \underline{q}|^2} \quad (2.59)$$

and the energy-wavenumber characteristic (2.46) becomes

$$F(q) = \frac{2\Omega_0}{(2\pi)^3} \int^< d^3 \underline{k}^2 \frac{|w_q^{\circ}(\underline{k})|^2}{k^2 - |\underline{k} + \underline{q}|^2} + \frac{\Omega_0 q^2}{8\pi} \frac{(1-h(q)/\epsilon(q))}{1-h(q)} (w_q^H(\underline{k}) - w_q^{\circ}(\underline{k}))^2 \quad (2.60)$$

where $w_q^H(\underline{k})$ is the screened Hartree form factor, obtained from (2.39). $F(q)$ is still a local operator, since $w_q^H(\underline{k}) - w_q^{\circ}(\underline{k})$ is local even though each of $w_q^H(\underline{k})$ and $w_q^{\circ}(\underline{k})$ is non-local.

There is still no completely satisfactory way of calculating the function $h(q)$; in this thesis the results of Singwi et al (1970) are used,

$$h(q) = A(1 - Be^{-(q/k_F)^2}) \quad (2.61)$$

where A and B are constants which depend on the mean electron density.

Shaw has also incorporated effective mass corrections into the theory (Shaw 1969b). He defines two functions $m_E(\underline{k})$ and m_k via

$$m_E(\underline{k}) = 1 - \langle \underline{k} | \frac{\partial W}{\partial E} | \underline{k} \rangle \quad (2.62)$$

$$\frac{k^2}{2m_k} = \frac{k^2}{2} + \langle \underline{k} | W^0 | \underline{k} \rangle \quad (2.63)$$

which are well defined, with expressions for them given in that paper. Expressions for $\epsilon(q)$, $F(q)$ and $w_q(\underline{k})$, which now depend on these two new functions can also be found there. However, since these expressions are quite complicated, and are not used in this thesis, they are not reproduced here.

Appapillai and Williams (1973) have compiled a list of on the Fermi surface matrix elements and the energy-wavenumber characteristics for 33 elements, including both exchange and effective mass corrections. Cowley (1976) has found that these calculations are apparently in error, and has redone the whole fitting and extrapolation procedure for 27 elements. But the

question of how to relate the metallic energies to the free ion energies is still not completely solved. In fact, he gives three sets of model parameters for each of the elements, corresponding to three different ways of calculating this energy relationship. Taking aluminum as an example, the $\ell=0$ well depth A_0 is given as either 1.3784, 1.4319 or 1.5509 a.u. It is clear that fitting the potentials directly to metallic properties would be preferable to this fitting to free ion properties and extrapolating.

2.7 MODEL POTENTIAL THEORY IN THE LOCAL LIMIT

It is much simpler and faster computationally to use a local approximation to the model potential. This results in much simpler forms for the expressions in this chapter, which are presented in this section.

With a local potential, all the electrons, no matter what their energy E or angular momentum quantum number ℓ , feel the same potential $W(r)$. Since there is no energy dependence in W , the depletion hole is zero, as can be seen immediately from (2.20). There is correspondingly no difference between the effective valence Z^* and the true valence Z , nor a uniform charge compensating for the depletion holes. A further major simplification occurs in that all sums over \underline{k} can be done independently of sums over \underline{q} , since the matrix elements are independent of \underline{k} .

Different forms can also be chosen for the local potential. One corresponding to the Shaw form of the non-local potential, which is used in the next chapter of this thesis, is

$$w^{\circ}(r) = -A\theta(R-r) - \frac{Z}{r}\theta(r-R) \quad (2.64)$$

with form factor

$$w(q) = -\frac{4\pi}{\Omega_0 q^2} \left[A \frac{\sin qR}{q} + (Z-AR)\cos qR \right] \frac{1}{\epsilon(q)} \quad (2.65)$$

and electron distribution

$$n(\underline{r}) = n_0 + \sum_{q \neq 0} S(q) \frac{q^2}{4\pi} w(q) (1-\epsilon(q)) e^{-iq \cdot \underline{r}} \quad (2.66)$$

The total energy is again given by the sum of three terms as in (2.42), with

$$\begin{aligned} ZE_{fe} = & Z \left(\frac{1.105}{r_s^2} - \frac{.458}{r_s} - .0575 + .0155 \ln r_s \right) \\ & + \frac{2\pi}{\Omega_0} ZR^2 \left(1 - \frac{2}{3} AR \right) \end{aligned} \quad (2.67)$$

where the first term in (2.67) is the kinetic energy per ion written in terms of r_s instead of k_F ,

$$E_{es} = \frac{\alpha Z^{5/3}}{2 r_s} \quad (2.68)$$

and

$$E_{bs} = \sum_{q \neq 0} |S(q)|^2 F(q) \quad (2.69)$$

where now

$$F(q) = - \frac{\Omega_0 q^2}{8\pi} \frac{|w^\circ(q)|^2}{1-h(q)} \left(1 - \frac{1}{\epsilon(q)}\right). \quad (2.70)$$

Exchange and correlation are included in these expressions.

The last thing we are going to consider in this chapter is the effective interionic potential in Hartree theory using a local potential, which reduces to

$$V_{\text{eff}}(\underline{R}_i - \underline{R}_j) = \frac{Z^2}{|\underline{R}_i - \underline{R}_j|} + \frac{2}{N} \sum_{\underline{q} \neq 0} F(q) e^{-i\underline{q} \cdot (\underline{R}_i - \underline{R}_j)}. \quad (2.71)$$

But in this limit, $F(q)$ becomes

$$F(q) = \frac{1}{2} w(q) n_{\text{sc}}(q) \quad (2.72)$$

where $n_{\text{sc}}(q)$ is the Fourier transformed screening charge density about one ion. Hence

$$\begin{aligned} V_{\text{eff}}(R) &= \frac{Z^2}{R} + \frac{\Omega_0}{N} \sum_{\underline{q}} w(q) n_{\text{sc}}(q) e^{i\underline{q} \cdot \underline{R}} \\ &= \frac{Z^2}{R} + \int n_{\text{sc}}(\underline{R} - \underline{r}') w^\circ(\underline{r}') d^3 \underline{r}'. \end{aligned} \quad (2.73)$$

The picture for $V_{\text{eff}}(\underline{R})$ is now clear. Two identical atoms a distance R apart are allowed to overlap and the interaction energy is that of the two bare valence charges Z interacting, plus the screening cloud of one ion interacting with the other unscreened ion. Clearly this must be correct in pertur-

bation theory, but it is also clear that other effects such as changes in the electron kinetic energies, are not being considered. This point is discussed further in the next chapter, and in Appendix I.

CHAPTER III

EXTENSIONS OF THE MODEL POTENTIAL THEORY: HYDROGEN AND HELIUM IMPURITIES IN SIMPLE METALS

3.1 INTRODUCTION

Much interest has focussed recently on the problem of H and He in simple metals (see for example Bugeat et al 1976, Inglesfield and Pendry 1976, Mainwood and Stoneham 1976, Stoneham 1972a, 1972b and Vook et al 1975). In particular in a study sponsored by the American Physical Society to identify problems in radiation effects relevant to fusion energy development, Vook et al (1975) recommended study of the effects of H on the mechanical properties of alloy systems as well as of the behaviour of He in solids, including its interactions with other defects. In this chapter we consider the energies of independent, or at most pairs of, H and He in simple metals with at most isolated mono-vacancies present.

In developing the theory, a number of modifications to the model potential theory will be introduced to treat the electron-ion and interionic interactions. The first set of modifications will also be used in the next chapter, and in Appendix I the possible application of the formalism introduced for the interatomic potentials to phonon calculations will be

discussed. These modifications could be presented in a separate chapter, but it seems more appropriate to introduce them as they are needed.

Within a local model potential theory, it is straightforward to calculate the energy of a perfect simple metal. By treating a single impurity atom in a similar way, this calculation can be modified to provide the energy of the crystal when non-interacting impurities are present. The difference between these energies is an approximate heat of solution, ΔH , for the impurity in the metal. Popović et al (1976, hereafter referred to as PSCP) have done this for H in Al and Mg, and found poor agreement with experiment. They then went on to construct a new theory incorporating non-linear, approximately self-consistent screening of the proton in the electron gases, obtaining much improved results. Since then Jena and Singwi (1978) have repeated these calculations, incorporating full self-consistency, and have achieved even better agreement. We have generalized the theory of PSCP to treat an impurity of arbitrary nuclear charge Z' , and applied it to He in Al and Mg. We have also considered in some detail the behaviour of both H and He in the presence of a single vacancy, but neglecting lattice relaxation.

With further extensions of the theory, it is possible to at least partially remove the restriction to dilute impurity concentrations, by allowing for interactions between impuri-

ties. This has been done for both H-H and He-He pairs in these metals, both in the absence of and near mono-vacancies.

In the next section we start by presenting with little discussion the model potential, or linear, theory of the heat of solution for a single impurity in a simple metal. This is done primarily to provide the framework for the modifications incorporating non-linear screening which are described in the ensuing section, after which the results for a single He atom in Al and Mg are presented. The rest of the chapter is devoted to the case of pairs of impurities.

3.2 THEORY OF THE HEAT OF SOLUTION OF A SINGLE IMPURITY

In chapter 2, the energy of a perfect crystal, within a local model potential theory, was given as a sum of three terms: the free electron energy ZE_{fe} (equation 2.67), the electrostatic energy E_{es} (equation 2.68) and the band structure energy E_{bs} (equation 2.69). The local model potential $w^o(\underline{r})$ we are using (equation 2.64), form factor $w(q)$ (equation 2.65) and energy-wavenumber characteristic $F(q)$ (equation 2.70) were also listed there. The energy of the perfect crystal can be obtained from these equations, once the model potential parameters and the structure of the crystal are specified, which is now done for the host materials considered here.

Al is face centered cubic with only one atom per primitive unit cell, so

$$S(\underline{q}) = \sum_{\underline{K}_j} \delta_{\underline{q}, \underline{K}_j} \quad (3.1)$$

where the \underline{K}_j are reciprocal lattice vectors. Mg is hexagonal close packed, with two atoms per primitive unit cell. The structure factor can be expressed

$$S(\underline{q}) = S_{sh}(\underline{q}) (1 + e^{-i\underline{q} \cdot \underline{\rho}_2}) \quad (3.2)$$

where $S_{sh}(\underline{q})$ is the structure factor for the simple hexagonal lattice; within each unit cell, one atom is at the origin and the other at $\underline{\rho}_2$. $S_{sh}(\underline{q})$ is given by equation (3.1), but the \underline{K}_j refer of course to the reciprocal lattice of the simple hexagonal lattice.

The model potential parameters are taken from PSCP, where they were fitted to reproduce the equilibrium lattice parameters and binding energies of the perfect crystals; this was felt to be appropriate since our interest is in the change in energy when a few impurities are added.

The above, as well as the rest of the required data, are summarized in table 3:1.

For present purposes, consider the r_s dependence of the crystal energy to be a function of k_F . The total energy of the crystal can be written as

$$E = N(ZE_{fe}(k_F) + E_{es} + E_{bs}(k_F)) \quad (3.3)$$

When an impurity is added to the system, the addition

Table 3.1

Structure and potential parameters for Al and Mg

	Al	Mg
Structure	fcc	hcp
Ewald constant	-1.79175	-1.79166
Lattice constant (Å)	4.031	3.193
c/a	-	1.624
Valence	3	2
r_s	2.064	2.642
A	.8618	.5337
R	1.3817	1.6890

can be thought of as occurring in two stages. First, the impurity is raised from its ground state in vacuum to a nucleus of charge Z' plus Z' free electrons, and then these particles dissolved by the crystal. The heat of solution is the sum of the energies required for each of these steps:

$$\Delta H = I + \Delta H_{el-n} \quad (3.4)$$

where I is the energy required for the first step, and ΔH_{el-n} is the heat of solution for the dissociated electrons and nucleus. For H, the former is one-half the dissociation energy for the molecule plus the ionization energy of the atom, 15.86 eV, and for He it is the sum of the first and second ionization energies for the atom, 78.88 eV.

Before proceeding to the details of ΔH_{el-n} , it is appropriate to summarize the major approximations used in the theory. First, at least in the linear theory, model potentials and perturbation theory are used throughout. In the modified theory, some but not all perturbation calculations are replaced. Second, lattice relaxation is neglected. For both Al and Mg the lattice relaxation energies about a vacancy are calculated to be about -.03 eV (Popović et al 1974 and Popović and Carbotte 1974), and would not be expected to differ much from this about a light impurity. Further Mainwood and Stoneham (1976) have calculated that for H in Na, relaxation of the four host atoms

nearest the impurity leads to a lowering of the energy of only .003 eV. On the other hand, Benedek (1978) estimates that the contribution of lattice relaxation to ΔH for He in Al is about 1 eV. This is an effect which probably warrants further investigation. Finally, static impurities are assumed.

When the impurity is introduced, each term in (3.3) is modified. With the addition of Z' electrons, k_F changes, to first order in $\frac{1}{N}$, to

$$k_F' = k_F \left(1 + \frac{Z'}{3NZ}\right) \quad (3.5)$$

so that NZE_{fe} becomes

$$NZE_{fe}' = NZE_{fe}(k_F) + Z'(E_{fe}(k_F) + \frac{1}{3} \frac{\partial E_{fe}(k_F)}{\partial k_F}). \quad (3.6)$$

With the addition of the nucleus of charge Z' , NE_{es} becomes

$$NE_{es}' = \frac{N\alpha Z^{5/3}}{2 r_s} + \alpha'(\rho_n) \frac{Z^{2/3} Z'}{r_s} \quad (3.7)$$

$\alpha'(\rho_n)$ is an Ewald constant which depends not only on the structure of the host material, but also on the location of the impurity within the crystal ρ_n .

The band structure energy changes due to both the extra nucleus and extra electrons. For the hcp structure it becomes

$$\begin{aligned} NE_{bs}' &= NE_{bs}(k_F) + \frac{Z' k_F}{3Z} \sum_{\underline{K}_j \neq 0} \cos^2\left(\frac{1}{2} \underline{K}_j \cdot \underline{\rho}_2\right) w^{\circ 2}(\underline{K}_j) \frac{\partial}{\partial k_F} g(\underline{K}_j) \\ &+ \sum_{\underline{K}_j \neq 0} w^{\circ}(\underline{K}_j) w_n^{\circ}(\underline{K}_j) g(\underline{K}_j) \{ \cos(\underline{K}_j \cdot \underline{\rho}_n) + \cos \underline{K}_j \cdot (\underline{\rho}_2 - \underline{\rho}_n) \} \\ &+ \frac{1}{N} \sum_{\underline{q} \neq 0} w_n^{\circ 2}(\underline{q}) g(\underline{q}) \end{aligned} \quad (3.8)$$

where

$$g(q) = -\frac{\Omega_0 q^2}{8\pi} \frac{1}{1-h(q)} \left(1 - \frac{1}{\epsilon(q)}\right) \quad (3.9)$$

and $w_n^\circ(q)$ is the form factor of the bare impurity nucleus

$$w_n^\circ(q) = \frac{4\pi Z'}{\Omega_0 q^2} \quad (3.10)$$

For the fcc structure, E_{bs} is given by (3.8) but with $\rho_2 = 0$.

Adding together equations (3.6) to (3.8) and subtracting off the energy of the perfect crystal, an expression for ΔH_{el-n} is obtained, which can be expressed

$$\Delta H_{el-n} = \Delta H_1 + \Delta H_2 \quad (3.11)$$

$$\begin{aligned} \Delta H_1 = & Z' (E_{fe}(k_F)) + \frac{k_F}{3} \frac{\partial E_{fe}(k_F)}{\partial k_F} + \alpha'(\rho_n) \frac{Z^{2/3} Z'}{r_s} \\ & + \frac{k_F}{3Z} \sum_{\underline{K}_j \neq 0} \cos^2\left(\frac{1}{2} \underline{K}_j \cdot \underline{\rho}_2\right) w^{\circ 2}(\underline{K}_j) \frac{\partial}{\partial k_F} g(\underline{K}_j) \end{aligned} \quad (3.12)$$

$$\begin{aligned} \Delta H_2 = & \sum_{\underline{K}_j \neq 0} w^\circ(\underline{K}_j) w_n^\circ(\underline{K}_j) g(\underline{K}_j) (\cos(\underline{K}_j \cdot \underline{\rho}_n) + \cos(\underline{K}_j \cdot (\underline{\rho}_2 - \underline{\rho}_n))) \\ & + \frac{1}{N} \sum_{\underline{q} \neq 0} w_n^{\circ 2}(\underline{q}) g(\underline{q}) \end{aligned} \quad (3.13)$$

PSCP evaluated these expressions for H in Al and Mg and obtained values for ΔH of 1.99 eV and 2.89 eV respectively, compared with experimental values of .66 eV and .25 eV. They identified ΔH_2 as the cause of these discrepancies; it depends on the response of the electron gas to the presence of the pro-

ton, and since the proton is a very strong perturbation, it is essential to go beyond second order perturbation theory to treat it. On the other hand, ΔH_1 should be adequate as it is, since it does not depend on this response.

Making use of the results of chapter 2, equation (3.13) can be written

$$\Delta H_2 = \sum_{q \neq 0} S(q) w_n^{\circ}(q) n^{(1)}(q) + \frac{1}{2N} \sum_{q \neq 0} e^{iq \cdot \rho_n} w_n^{\circ}(q) n^{(1)}(q) \quad (3.14)$$

where $n^{(1)}(q)$ is the Fourier transform of the displaced electron density about the impurity nucleus, calculated to first order in $w_n^{\circ}(q)$. The first term can now be interpreted as the interaction of this screening cloud with the rest of the ions, and the second as the leading term in a perturbation series for the correlation energy of the nucleus in the electron gas. Hence an improved ΔH can be obtained by modifying ΔH_2 to

$$\Delta H_2 = \sum_{q \neq 0} S(q) w_n^{\circ}(q) n(q) + E_{\text{corr}} \quad (3.15)$$

where $n(q)$ is the Fourier transform of the true screening cloud $\Delta n(\underline{r})$ about the nucleus at ρ_n .

$$n(q) = e^{-iq \cdot \rho_n} \int_0^{\infty} 4\pi r^2 \frac{\sin qr}{qr} \Delta n(r) dr \quad (3.16)$$

and the correlation energy E_{corr} is (Fetter and Walecka 1971)

$$E_{\text{corr}} = \int_0^{Z'} \frac{dz_n}{z_n} v_{\text{int}}(z_n) \quad (3.17)$$

where $v_{\text{int}}(z_n)$, the interaction of a nucleus of charge z_n with its screening cloud is given by

$$v_{\text{int}}(z_n) = - \int d^3\underline{r} \frac{z_n}{r} \Delta n(z_n, \underline{r}) \quad (3.18)$$

where $\Delta n(z_n, \underline{r})$ is the distribution of displaced electrons about a nucleus of charge z_n , where $0 \leq z_n \leq Z'$. By evaluating $\Delta n(z_n, \underline{r})$ in a non-linear, approximately self-consistent way for sufficiently many values of z_n to carry out the calculations of equations (3.15) to (3.18), an improved ΔH_2 can be obtained.

3.3 APPROXIMATE NON-LINEAR SELF-CONSISTENT SCREENING

In the theory outlined above, an improved calculation of $\Delta n(\underline{r})$ is required. The method used is based on the density functional formalism (Hohenberg and Kohn 1964, Kohn and Sham 1965) which states that there exists a local, one body effective potential $v_{\text{eff}}(\underline{r})$ which can be used to construct the exact ground state electron density distribution through solutions of the one particle Schrödinger equation

$$\left(-\frac{1}{2} \nabla^2 + v_{\text{eff}}(\underline{r})\right) \psi_i(\underline{r}) = \epsilon_i \psi_i(\underline{r}) \quad (3.19)$$

Solving for all the states with energies less than the chemical potential μ , the density can be constructed through

$$n(\underline{r}) = \sum_{\epsilon_i < \mu} |\psi_i(\underline{r})|^2 \quad (3.20)$$

In the present case, the effective potential is, to within a constant,

$$V_{\text{eff}}(\underline{r}) = -\frac{Z}{r} + \int \frac{n(\underline{r}') d^3 r'}{|\underline{r}-\underline{r}'|} + V_{\text{xc}}(\underline{r}) \quad (3.21)$$

The first two terms constitute the self-consistent Coulomb potential of the nucleus and electron cloud. $V_{\text{xc}}(\underline{r})$ is the functional derivative of a universal exchange and correlation energy functional $E_{\text{xc}}[n(\underline{r})]$.

$$V_{\text{xc}}(\underline{r}) = \frac{\delta E_{\text{xc}}[n(\underline{r})]}{\delta n(\underline{r})} \quad (3.22)$$

Since $E_{\text{xc}}[n(\underline{r})]$ is not known exactly, neither is $V_{\text{xc}}(\underline{r})$. For a slowly varying density, it can be approximated by the exchange and correlation part of the chemical potential of a uniform electron gas, but evaluated for the local density at \underline{r} .

$$V_{\text{xc}}(\underline{r}) \approx \mu_{\text{xc}}[n(\underline{r})] \quad (3.23)$$

This approximation is used throughout the calculation. It is decreasingly valid as the nucleus is approached, but this is probably not a serious problem. First, the kinetic energy and Coulomb potential dominate the Hamiltonian in this region. Also, calculations on lithium (Whitmore 1975) indicate that the exact form of $V_{\text{xc}}(\underline{r})$ is not important in obtaining the density distributions. Third, in recent calculations of Jena and Singwi

(1978), they found that including the first gradient correction (Vashishta and Singwi 1972) actually worsened the experimental agreement for the heat of solution of H in Al and Mg. Finally, Almladh et al (1976) find the errors in $\Delta n(\underline{r})$ due to this approximation to be less than 3% for all atoms.

The form used for $\mu_{xc}[n(\underline{r})]$ is that proposed by Hedin and Lundqvist (1971) which is based on the work of Singwi et al (1970):

$$\mu_{xc}(\underline{r}) = - .02909 \left[\frac{21}{r_s(\underline{r})} + .7734 \ln \left(1 + \frac{21}{r_s(\underline{r})} \right) \right] \quad (3.24)$$

where $r_s(\underline{r})$ is the local electron gas density parameter evaluated at \underline{r} .

We approximate the screening cloud about the nucleus in the metal by that in the appropriate uniform electron gas. This makes the problem spherically symmetric so the Schrödinger equation reduces to

$$\left(-\frac{\hbar^2}{2} \frac{d^2}{dr^2} + V_{\text{eff}}(r) + \frac{\ell(\ell+1)}{r^2} - \epsilon_k \right) r R_{\ell k}(r) = 0 \quad (3.25)$$

where $R_{\ell k}(r)$ is the radial wavefunction with angular momentum labelled by ℓ and energy labelled by k . For non-localized states,

$$\epsilon_k = \frac{1}{2} k^2.$$

The boundary conditions are straightforward. Since the impurity must be fully screened, $\lim_{r \rightarrow \infty} r V_{\text{eff}}(r) = 0$. Hence the asymptotic form for the non-localized states is

$$R_{\ell k}(r) = \cos \eta_{\ell} j_{\ell}(kr) - \sin \eta_{\ell} n_{\ell}(kr) \quad (3.26)$$

where η_{ℓ} are the phase shifts, and j_{ℓ} and n_{ℓ} are spherical Bessel and Neuman functions.

Bound states can also occur; for H and He these are 1s states, with asymptotic form

$$rR_b(r) \sim e^{-k_0 r} \quad (3.27)$$

where $\epsilon_b = -\frac{1}{2} k_0^2$ is the binding energy.

After solving the Schrödinger equation for the electron states below μ , the displaced electron density $\Delta n(r)$ can be constructed from

$$\begin{aligned} \Delta n(r) &= \sum_{\epsilon_i < \mu} |\psi_i(r)|^2 - n_0 \\ &= \frac{1}{\pi^2} \int_0^{k_F} k^2 dk \sum_{\ell=0}^{\ell_{\max}} (2\ell+1) (R_{\ell k}(r)^2 - j_{\ell}(kr)^2) + 2R_b(r)^2 \end{aligned} \quad (3.28)$$

where n_0 has been expanded in terms of $j_{\ell}(kr)$. In the sum over ℓ , an exact solution is obtained by including all ℓ such that $\eta_{\ell} \neq 0$.

Equation (3.21) for $V_{\text{eff}}(\underline{r})$ can be simplified due to the spherical symmetry, and in addition is rescaled so that $\lim_{r \rightarrow \infty} rV_{\text{eff}}(r) = 0$. This is done by replacing $n(\underline{r})$ by $\Delta n(\underline{r})$ in the Coulomb potential, and taking

$$V_{\text{xc}}(\underline{r}) = \mu_{\text{xc}}[n(\underline{r})] - \mu_{\text{xc}}[n_0] \quad (3.29)$$

instead of (3.23). Hence

$$V_{\text{eff}}(r) = -\frac{Z_n}{r} + \frac{1}{r} \int_0^r 4\pi r'^2 \Delta n(r') dr' + \int_r^\infty 4\pi r' \Delta n(r') dr' + V_{\text{xc}}(r) \quad (3.30)$$

A condition on the potential which can be used advantageously is the Friedel Sum Rule (FSR). In order for the nucleus to be completely screened, exactly Z_n electrons must be displaced by it. For a potential $V_{\text{eff}}(r)$, the number of displaced electrons is given by the Friedel Sum (FS), (Kittel 1963).

$$F = \frac{2}{\pi} \sum_{\ell=0}^{\ell_{\text{max}}} (2\ell+1) \eta_{\ell}(k_F) \quad (3.31)$$

where $\eta_{\ell}(k_F)$ are the Fermi level phase shifts of the potential. The FSR requires $F = Z_n$.

In spite of the similarity between the above equations and those for a Hartree-Fock free atom calculation (Messiah 1961), they cannot be simply iterated to convergence because the number of particles is not fixed. An alternative procedure was thus derived.

The initial step is choosing a trial potential $V_{\text{tr}}(r)$ which satisfies the FSR, from which $\Delta n(r)$ is calculated through (3.25) and (3.28). From this, (3.30) is used to generate an effective potential $V_{\text{eff}}(r)$, for which the FS is calculated. In

general, $V_{\text{eff}}(r)$ will not satisfy the FSR, nor will it exhibit much self-consistency with $V_{\text{tr}}(r)$. The next step is not to use $V_{\text{eff}}(r)$, but to return to $V_{\text{tr}}(r)$ and modify it so that a different $V_{\text{eff}}(r)$ is produced, through a different $\Delta n(r)$, which hopefully more nearly satisfies both the FSR and self-consistency with $V_{\text{tr}}(r)$. These steps are repeated until a satisfactory $V_{\text{eff}}(r)$ is obtained.

For He (as for H), it was possible to use a simple parametrized form for $V_{\text{tr}}(r)$, which facilitated modifying it in a systematic way. The form chosen for $1 < Z_n \leq 2$ was

$$V_{\text{tr}}(r) = \phi_c(r) e^{-\alpha r^\beta} \quad (3.32)$$

where $\phi_c(r)$ is an approximation to the potential of the nucleus and the two bound electrons

$$\phi_c(r) = -\frac{Z_n}{r} + 2 \int \frac{|\psi_{1s}(\underline{r}')|^2 d^3 \underline{r}'}{|\underline{r} - \underline{r}'|} \quad (3.33)$$

where the core wavefunction was approximated by

$$\psi_{1s}(r) = \sqrt{\frac{\gamma^3}{\pi}} e^{-\gamma r} \quad (3.34)$$

$$\gamma = Z_n - 0.31 \quad (3.35)$$

$V_{\text{tr}}(r)$ clearly does not have any of the long-range Friedel oscillations characteristic of $V_{\text{eff}}(r)$ (see figures 3.1 and 3.2), and hence cannot be fully consistent with it. Hence a slight variation in the procedure was used in the last step. The procedure followed for the range $1 < Z_n \leq 2$ will now be

described in some detail.

To begin, an initial value of β was chosen, and then α determined so that $V_{tr}(r)$ (equation 3.32) satisfied the FSR. From this, $\Delta n(r)$ and then $V_{eff}(r)$ were calculated, and the FS on $V_{eff}(r)$ noted.

Then a different value of β was chosen, producing a new $V_{tr}(r)$ (with a different value for α), and hence a new $V_{eff}(r)$ with a new FS. The procedure was repeated a number of times with different values of β until $V_{eff}(r)$ satisfied the FSR and was approximately self-consistent for $r < 2$ a.u.. This $V_{eff}(r)$ was then used to generate a new potential which was found to satisfy approximately both the FSR and self-consistency.

The Schrödinger equation (3.25) was solved in steps of $.05 a_0$ out to $20 a_0$. The phase shifts η_l were evaluated at $r = 15$, and the asymptotic form, equation (3.26) beyond that. A 48th order Gauss integration routine was used to perform the k -integration of equation (3.28), so that (3.25) was solved for 48 positive energy states plus the bound state. The sum over l in (3.28) was terminated at $l_{max} = 6$.

As previously stated, for the heat of solution, these calculations are required for $0 < Z_n \leq 2$. For $Z_n \leq 1$, the results of PSCP were used; we have done the calculations for $Z_n = 1.25, 1.50, 1.75$ and 2.0 . The electron densities and self-consistent potentials are shown in figures 3.1 and 3.2, and the

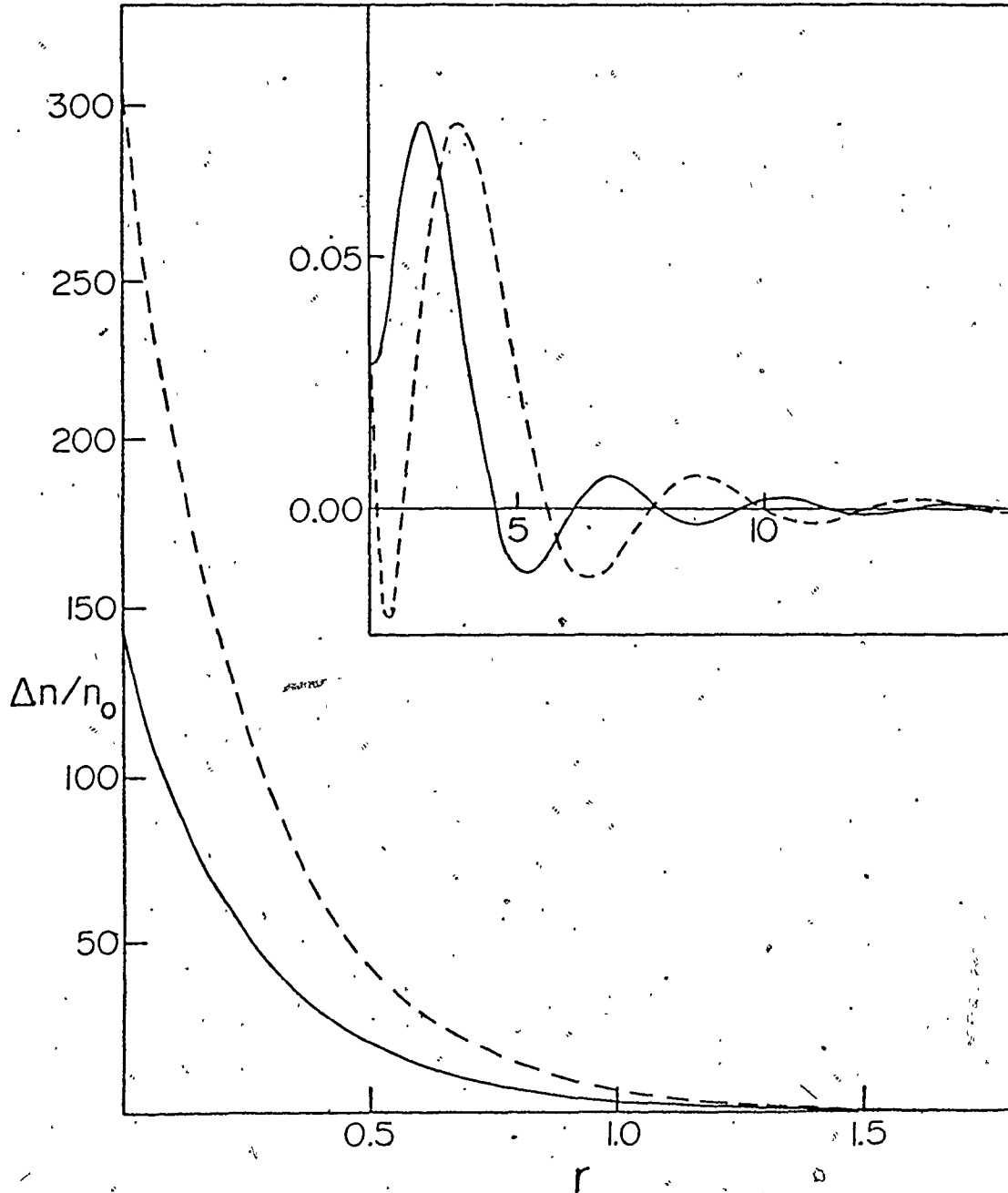


Fig. 3.1 Displaced electron density $\Delta n/n_0$ surrounding a He nucleus in uniform electron gases of density appropriate to Al (—) and to Mg (----)

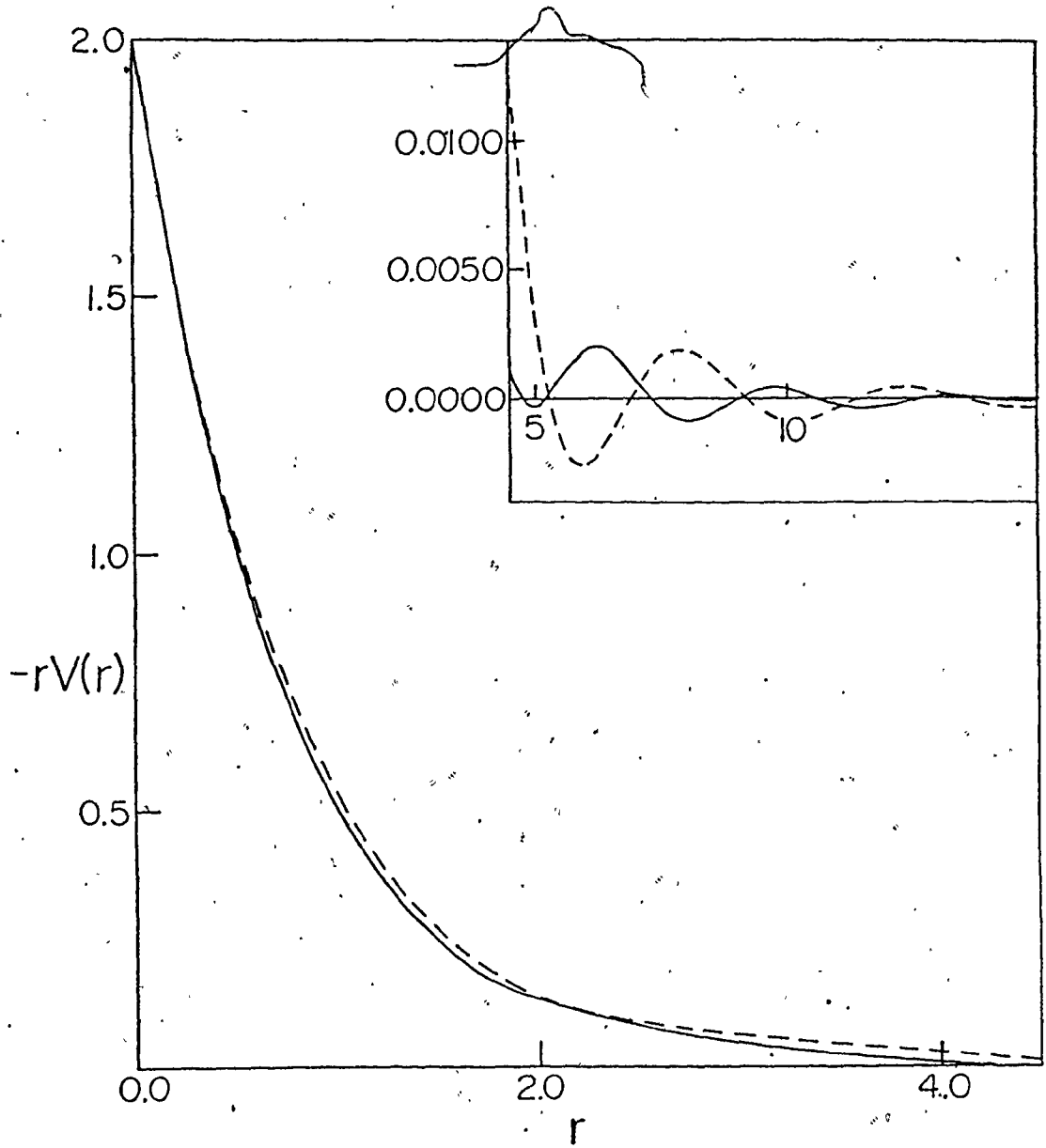


Fig. 3.2: Non-linear self-consistent potential, $-rV_{\text{eff}}(r)$, around a He nucleus in uniform electron gases of density appropriate to Al (—) and to Mg (---)

Fermi level phase shifts in table 3.2.

Table 3.2

Fermi level phase shifts for a He nucleus in uniform electron gases of mean density appropriate to Al and Mg

	η_0	η_1	η_2	η_3	η_4	η_5	η_6
Al	1.9921	.2670	.0502	.0100	.0024	.0005	.0001
Mg	2.2163	.2278	.0376	.0058	.0013	.0002	.0000

Similar non-linear self-consistent calculations are used in the next chapter on metallic H, and in Appendix I on Al under pressure. In these cases, the general procedure outlined above is used, but $V_{tr}(r)$ and manner in which it is modified are different.

3.4 ENERGIES AND EQUILIBRIUM SITES OF A SINGLE He IN Al AND Mg

In this section we present the results of the theory of the heat of solution for an isolated He atom dissolved in Al or Mg; these results apply as long as the impurity concentration is low enough that He-He interactions can be ignored.

Table 3.3 summarizes the calculations using the non-linear densities. The parameters α and β used in $V_{tr}(r)$, as well as the corresponding interaction energies for each Z_n between 1.25 and 2.0, are given along with E_{corr} for each metal.

Table 3.3.

Results of calculations of the correlation energies of the helium nucleus in the uniform electron gases of Al and Mg. Trial potential parameters and V_{int}/Z_n are given for different values of the nuclear charge Z_n , along with the correlation energies E_{corr} for each metal.

<u>Trial Potential Parameters</u>				
	Z_n	α	β	V_{int}/Z_n
Al	1.25	- .0083	2.3348	-1.629
	1.50	- .3413	1.3159	-2.135
	1.75	- .7033	1.2624	-2.709
	2.00	-1.0929	1.2233	-3.347
		$E_{\text{corr}} = -2.072$		
Mg	1.25	- .0815	1.0760	-1.596
	1.50	- .4095	1.2808	-2.117
	1.75	- .7822	1.2462	-2.721
	2.00	-1.1920	1.2043	-3.399
		$E_{\text{corr}} = -2.669$		

Table 3.4 contains the heats of solution for two different high symmetry interstitial sites. It is apparent that interstitial He will occupy the octahedral site in both metals.

Table 3.4

Summary of the calculated heats of solution of He in Al and Mg. The first two columns are the heats of solution for the octahedral (ΔH_{oct}) and tetrahedral (ΔH_{tet}) sites in each metal. The third column contains the He-vacancy binding energies, and the last column the heats of solution for substitutional He (ΔH_{sub}). All values are in eV.

	ΔH_{oct}	ΔH_{tet}	E_{B}	ΔH_{sub}
Al	4.06	5.77	3.96	.77
Mg	2.71	3.28	2.40	1.20

Binding to a vacancy has also been investigated. This is done by evaluating ΔH when the impurity is at a lattice site, and then subtracting out the interaction of the impurity with the host atom which would normally occupy that position. The binding energy E_{B} is the difference between this energy and the energy when the impurity is at the lowest energy interstitial site, in these cases the octahedral site. When these binding energies are combined with vacancy formation energies of .67 eV in Al (McKee et al 1972) and .89 eV in Mg (Bevers et al 1963), then the corresponding heats of solution for substitutional

He of .77 eV and 1.20 eV are obtained, indicating the presence of substitutional helium in both metals.

It is interesting to compare these results with those on hydrogen. The heat of solution for octahedral hydrogen was found to be lower than that for tetrahedral hydrogen in Al, and the same as that for tetrahedral hydrogen in Mg. For helium, we have found that ΔH is lower for the octahedral site in both metals, but the difference between the two sites is larger in Al than in Mg. Similarly, hydrogen-vacancy binding is expected in Al but not in Mg, whereas helium-vacancy binding is found in both metals, but with a larger binding energy in Al than in Mg.

In order to calculate the energy barriers between interstitial sites, the energy of the system as a function of the position of the impurity is required. Since the formulae for ΔH are valid for any such position ρ_n , the position dependence of the energy $E(\rho_n)$ can be investigated by focussing on the terms contributing to ΔH which depend on ρ_n . To within a constant, this energy is

$$E(\rho_n) = \alpha' (\rho_n)^{\frac{2}{3}} \frac{Z^2}{r_s} + \sum_{q \neq 0} S(q) w(q) n(q) \quad (3.36)$$

Interstitial diffusion will occur only along certain specified directions. In Al, an impurity cannot jump directly from one octahedral site to another, but must do so via an intermediate tetrahedral site. In Mg, an impurity can make a direct

octahedral-octahedral jump in the direction of the c axis, or alternatively, it can diffuse in the basal plane via a tetrahedral site. Table 3.5 presents $E(\rho_n)$ for eleven equidistant points along the straight lines described by these processes, along with the activation energies E_M . From this table, it is seen that these calculations indicate there is no barrier preventing a helium atom from diffusing from a tetrahedral site to an octahedral site, again showing that interstitial helium will locate at the octahedral site. In reality of course there is likely to be some barrier, but it is expected to be quite small.

It is difficult to obtain meaningful comparisons with experimental quantities for these calculations. The good agreement obtained by PSCP and more recently by Jena and Singwi (1978) for H in Al and Mg points to the validity of the general theory, but none of the quantities calculated here for He has been measured because ΔH and E_B are so high.

However, some indirect comparisons can be made. Because of the He-vacancy binding, energetic helium atoms injected into either of these metals should become trapped to such vacancies. Any measurements performed on such metal-helium systems, such as those of Glyde and Mayne (1965a, 1965b), should then give results relevant to the situation where the helium is trapped in this way. In these experiments helium was injected into each

Table 3.5

The energy change in eV for 11 equidistant positions of the impurity in the straight lines joining adjacent sites of high symmetry. Results are given for Al for the octahedra-tetrahedral jump and for Mg for both the octahedral-tetrahedral jump in the basal plane and the octahedral-octahedral jump in the direction of the c-axis. The heights of the energy barriers E_M are given in the last row.

	Al Oct → Tet	Mg Oct → Tet	Mg Oct → Oct
1	0.00	0.00	0.00
2	0.05	0.04	0.07
3	0.21	0.11	0.10
4	0.45	0.18	0.16
5	0.75	0.29	0.23
6	1.07	0.40	0.25
7	1.38	0.44	0.23
8	1.58	0.51	0.16
9	1.70	0.56	0.10
10	1.70	0.57	0.07
11	1.70	0.57	0.00
E_M	1.70	0.57	0.25

metal, and then the desorption spectra obtained as the temperature increased. It was concluded from these experiments that the injected helium initially binds to vacancies in each metal, and then diffuses via a vacancy mechanism with activation energies of 1.60 ± 0.07 eV in Al and 1.57 ± 0.13 eV in Mg.

The present calculations are consistent with these conclusions. We certainly have obtained vacancy binding, but the diffusion we have considered is interstitial diffusion. The following observation can be made though. If the sum of the calculated vacancy binding energies and interstitial energy barriers was less than the measured activation energies then the theory would be predicting that the trapped helium is first freed from the vacancy and then diffuses as an interstitial, in contrast to the experiments. But this is not the case for the calculations, so our results are consistent with experiment for both metals.

Recently channeling experiments have been performed (Bugeat et al 1976) on H-Al samples prepared by ion implantation, which indicate that the H sits at tetrahedral sites and that this configuration is associated with the mono-vacancies created during the implantation. Since the theory of PSCP applies only to low concentrations of impurities, and these experiments were done at high H concentrations, the two cannot be compared directly. However, because of the apparent discrepancy, it is of interest to extend the calculations to investigate more fully the

structure of H near a vacancy. We also do this for He near a vacancy, and for each impurity we consider both Al and Mg.

In table 3.6 are listed the energies of the system when the impurity lies along, first the tetrahedral-vacancy and then the octahedral-vacancy lines. We see that in each of the cases where impurity-vacancy binding has so far been predicted, the lowest energy of the system occurs when the impurity is either right at the lattice site, or very close to it in the case of He in Mg; in particular we do not find that H in Al near a vacancy will locate at a tetrahedral interstitial site.

For H near a vacancy in Mg, the situation is more complicated. While we reproduce a repulsive energy when H is right at the vacancy, we see the energy can be lowered by proximity to the vacancy, and that a minimum occurs at a position along the c-axis about 20% from the ideal tetrahedral position.

In order to understand the results of Bugeat et al (1976), we next extend the theory to allow for interactions between pairs of impurity atoms in the solid.

3.5 INTERATOMIC POTENTIALS USING NON-LINEAR SCREENING

In section 3.6 we shall describe the energies of the systems when there are two mutually interacting impurities present. An essential element of this calculation is of course the interaction energy of the pair of atoms; the technique used

Table 3.6

Energy of a single H(He) impurity in Al(Mg) for 11 equidistant positions of the impurity on the straight lines joining a vacancy site with a neighbouring interstitial site

Tetrahedral-Vacancy				Octahedral-Vacancy			
H in Al	H in Mg	He in Al	He in Mg	H in Al	H in Mg	He in Mg	He in Mg
- .23	-.07	+ .41	- .15	- .21	-.03	- .64	-.39
- .38	-.12	- .10	- .51	- .27	-.01	-.99	-.56
- .51	-.13	- .77	- .82	- .35	.01	-1.38	-.80
- .62	-.10	-1.42	-1.10	- .44	.06	-1.78	-1.01
- .71	-.06	-1.99	-1.49	- .55	.05	-2.17	-1.28
- .80	.01	-2.55	-1.58	- .68	.06	-2.53	-1.65
- .91	.03	-3.08	-2.21	- .84	.08	-2.96	-1.92
-1.04	.09	-3.43	-2.09	- .99	.10	-3.37	-2.11
-1.14	.08	-3.76	-2.68	-1.13	.10	-3.76	-2.46
-1.22	.12	-3.92	-2.27	-1.22	.11	-3.91	-2.45
-1.23	.12	-3.96	-2.40	-1.23	.12	-3.96	-2.40

for this calculation is described now.

Denote this interaction energy $E[\rho(\underline{r})]$, where $\rho(\underline{r})$ represents the total electron density about the impurity nuclei separated by a distance R . To get $E[\rho(\underline{r})]$ we use the density functional approach

$$E[\rho(\underline{r})] = \int v(\underline{r}) \rho(\underline{r}) d^3 \underline{r} + \frac{1}{2} \int \frac{\rho(\underline{r}) \rho(\underline{r}')}{|\underline{r} - \underline{r}'|} d^3 \underline{r} d^3 \underline{r}' + G[\rho(\underline{r})] + \frac{Z'^2}{R} \quad (3.37)$$

with

$$G[\rho(\underline{r})] = T[\rho(\underline{r})] + E_{xc}[\rho(\underline{r})] \quad (3.38)$$

where $T[\rho(\underline{r})]$ and $E_{xc}[\rho(\underline{r})]$ are, respectively, the kinetic energy and the exchange and correlation energy functionals. In (3.37) $v(\underline{r})$ is the potential felt by an electron at \underline{r} due to charges of Z' , one at the origin and one at \underline{R} .

$$v(\underline{r}) = - \frac{Z'}{|\underline{r}|} - \frac{Z'}{|\underline{r} - \underline{R}|} \quad (3.39)$$

The last term in (3.37) is the interaction energy of the two nuclei.

To calculate $E[\rho(\underline{r})]$ we take

$$\rho(\underline{r}) = n_0 + \Delta n(\underline{r}) + \Delta n(\underline{r} - \underline{R}) \quad (3.40)$$

with n_0 the mean electron gas density. For the kinetic energy we use the expression of Jennings (1976) and Bracket et al (1976), which was also derived by Kirzhnits (1957).

$$T = T_1 + T_2 + T_3 \quad (3.41)$$

$$T_1 = \frac{3}{10} (3\pi^2)^{2/3} \int \rho^{5/3} d^3 \underline{r} \quad (3.42)$$

$$T_2 = \frac{1}{72} \int \frac{(\nabla \rho)^2}{\rho} d^3 \underline{r} \quad (3.43)$$

$$T_3 = \frac{(3\pi^2)^{-2/3}}{540} \int \rho^{1/3} \left(\left(\frac{\nabla^2 \rho}{\rho} \right)^2 - \frac{9}{8} \left(\frac{\nabla^2 \rho}{\rho} \right) \left(\frac{\nabla \rho}{\rho} \right)^2 + \frac{1}{3} \left(\frac{\nabla \rho}{\rho} \right)^4 \right) d^3 \underline{r}. \quad (3.44)$$

For $E_{xc}[\rho(\underline{r})]$ we use

$$E_{xc}[\rho(\underline{r})] = -\frac{3}{4\pi} (3\pi^2)^{1/3} \int \rho^{4/3} d^3 \underline{r}. \quad (3.45)$$

Ma and Sahni (1977) have recently demonstrated the good convergence of these expressions for the kinetic energy for metallic electron densities, and accordingly we do not anticipate significant errors due to this approximation. On the other hand, as mentioned earlier, taking the next term for $E_{xc}[\rho(\underline{r})]$ may worsen matters.

From (3.37) must be subtracted the energy $E[\rho(\underline{r})]$ when the atoms are infinitely far apart. Since the model consists of the two atoms in an infinite electron gas, each of these values of E is divergent, so some care must be taken.

Consider first the Coulomb terms, consisting of the first, second and fourth terms in (3.37). These can be rewritten

$$E_C = E_1 + \int (-Z' \delta(\underline{r}) + \Delta n(\underline{r})) \phi_C(\underline{r}-\underline{R}) d^3 \underline{r} \quad (3.46)$$

where

$$\phi_c(\underline{r}) = \int \frac{(-Z\delta(\underline{r}') + \Delta n(\underline{r}'))}{|\underline{r} - \underline{r}'|} d^3 r' \quad (3.47)$$

and E_1 does not depend on the separation R . E_1 is in fact divergent but since it has no R dependence, can be discarded. The remaining term in (3.46), which we denote $V_c(R)$, vanishes in the limit of $R \rightarrow \infty$. According to (3.47) $\phi_c(\underline{r})$ is the Coulomb potential of the nucleus and screening electrons located at $\underline{r}=0$.

The expression for $V_c(R)$ can more conveniently be evaluated using Fourier transforms. Let $N(\underline{q})$ and $\phi_c(\underline{q})$ be the Fourier transforms of $(-Z'\delta(\underline{r}) + \Delta n(\underline{r}))$ and $\phi_c(\underline{r})$. Taking advantage of the spherical symmetry of $\Delta n(\underline{r})$, it is straightforward to show that

$$V_c(R) = \frac{1}{2\pi^2 R} \int_0^\infty q \sin qR N(q) \phi_c(q) dq \quad (3.48)$$

$$= \frac{1}{(2\pi)^3 R} \int_0^\infty q^3 \sin qR (\phi_c(q))^2 dq \quad (3.49)$$

since

$$N(q) = \frac{q^2}{4\pi} \phi_c(q). \quad (3.50)$$

In its present form, (3.49) is a difficult integral to evaluate; for large q , $\phi_c(q)$ is given by

$$\phi_c(q) = -\frac{4\pi Z'}{q^2} \quad (3.51)$$

so the asymptotic form of the integrand is proportional to

$\sin qR/q$. This means the integral converges only very slowly, and the integration must be carried out to large q . However, an alternative approach is available. Suppose there exists a Q such that for $q \geq Q$, $\phi_c(q)$ is given by (3.51). Then (3.49) can be rewritten

$$V_c(R) = \frac{Z^2}{R} + \frac{1}{(2\pi)^3 R} \int_0^Q q^3 \sin qR (\phi_c(q)^2 - (\frac{4\pi Z'}{q^2})^2) dq \quad (3.52)$$

This integral need be carried out only to where the difference $(\phi_c(q)^2 - (4\pi Z'/q^2)^2)$ is negligible, not out to where $(\phi_c(q))^2$ itself is negligible. For H-H and He-He interactions, $Q = 20 a_0^{-1}$ was found to be large enough.

The other contribution to $E[\rho(\underline{r})]$, $G[\rho(\underline{r})]$, was approached differently, all integrations being done in \underline{r} -space. The contributions T_2 and T_3 can be evaluated directly, since very far from both nuclei all derivatives of ρ vanish and ρ itself becomes n_0 . However T_1 and E_{xc} diverge if the integration is done over all space. Both these terms are of the form

$$I = \alpha \int_{\Omega} \rho(\underline{r})^\beta d^3 \underline{r} \quad (3.53)$$

$$= \alpha \int_{\Omega} (n_0 + \Delta n(\underline{r}) + \Delta n(\underline{r}-\underline{R}))^\beta d^3 \underline{r} \quad (3.54)$$

where Ω is all space. Clearly I is infinite due to the n_0 in the integrand. This divergence can be removed by taking instead

$$I' = \alpha \int_{\Omega} ((n_0 + \Delta n(\underline{r}) + \Delta n(\underline{r}-\underline{R}))^\beta - n_0^\beta) d^3 \underline{r} \quad (3.55)$$

and, practically, the integral must be done over a large enough volume Ω that $(\frac{\Delta n(\underline{r}) + \Delta n(\underline{r}-\underline{R})}{n_0})$ makes a negligible contribution to I' outside Ω . This in fact requires Ω to be a very large volume. The problem can be solved by conceptually viewing Ω as made up of two regions, $\Omega = \Omega_1 + \Omega_2$. Ω_1 is the region close to the nuclei, and all points in Ω_2 are far from both nuclei in the sense that

$$\left| \frac{\Delta n(\underline{r}) + \Delta n(\underline{r}-\underline{R})}{n_0} \right| \ll 1 \quad (3.56)$$

for all \underline{r} in Ω_2 . In this region we can then make the following expansion

$$[\rho(\underline{r})]^\beta = n_0^\beta \left(1 + \frac{\Delta n(\underline{r}) + \Delta n(\underline{r}-\underline{R})}{n_0} \right)^\beta \quad (3.57)$$

$$\approx n_0^\beta \left(1 + \beta \frac{(\Delta n(\underline{r}) + \Delta n(\underline{r}-\underline{R}))}{n_0} + o\left(\frac{\Delta n}{n_0}\right)^2 \right) \quad (3.58)$$

Using this expansion, and the fact that within the total volume Ω each charge cloud must contain exactly Z' electrons, (3.55) can be rewritten

$$I' = \alpha \int_{\Omega_1} ([\rho(\underline{r})]^\beta - n_0^\beta - \beta n_0^{\beta-1} (\Delta n(\underline{r}) + \Delta n(\underline{r}-\underline{R}))) d^3 \underline{r} + 2\alpha \beta n_0^{\beta-1} Z' \quad (3.59)$$

The volume Ω_1 need contain only those points where

$\left(\frac{\Delta n(\underline{r}) + \Delta n(\underline{r}-\underline{R})}{n_0}\right)^2$ makes a non-negligible contribution to I' , and is in practice much smaller than Ω .

In order for the potential to vanish in the limit of infinite separation, the limiting value of $G[\rho(\underline{r})]$ is found and subtracted off the calculation for each value of R .

The $\Delta n(\underline{r})$ used in calculating $G[\rho(\underline{r})]$ was that of the non-linear screening calculations described in section 3.3. The derivatives were calculated by using a fifth order Bessel interpolation. To perform the integral over the volume Ω_1 , the cylindrical and mirror symmetries were utilized to reduce it to a two-dimensional integral over a plane. For this, the plane was divided into rectangles of various sizes, over each of which a two dimensional Gauss integration (48th order in each direction) was performed. The volume Ω_1 and the rectangles were chosen to achieve three figure accuracy in the interatomic potentials.

The procedure described here is quite different from the method for calculating interatomic potentials described in the preceding chapter. The relationship between the two approaches is discussed in Appendix I.

3.6 ENERGIES AND EQUILIBRIUM SITES OF PAIRS OF H AND He IN Al AND Mg

With a procedure for treating interactions between atoms, we can now proceed with a discussion of the energies of various configurations of pairs of mutually interacting H or He in both perfect crystals, and in otherwise perfect crystals with a single mono-vacancy. In addition to the impurity-impurity interaction, all that is needed is the energy dependent terms

which contribute to ΔH , given by equation (3.36). The general procedure followed is the calculation of the energy of the two interacting atoms at the various configurations, relative to the energy when they are each at well separated octahedral sites in the perfect crystal.

Consider first the perfect crystal: no vacancy. We have extended the calculations of PSCP to include two H at neighbouring interstitial sites. We find that for two H at octahedral sites colinear with a host atom at the corner of the unit cell, the H-H interaction is slightly repulsive, while it is slightly attractive ($\sim .01$ eV) if they are at tetrahedral sites colinear with the host atom. Other configurations of the H atoms in the lattice were investigated, but in no case was the H-H interaction sufficiently attractive to lower the energy of these configurations to below the energy of octahedral H. The situation is not so clear for H in Mg where PSCP find that for a single impurity they cannot differentiate between octahedral and tetrahedral sites (both configurations having the same energy to within the accuracy of the calculation). This ambiguity remains when two H are considered.

For helium in Al (and Mg), we find again that the octahedral site is favoured for the case of a pair of He at adjoining interstitial sites so that in all cases considered, the impurity-impurity interaction does not lead to octahedral-tetrahedral conversion.

Next, consider pairs of H(He) in the vicinity of a vacancy. For the cases of H or He in Al, and He in Mg, the first possibility considered consisted of one impurity trapped at the vacancy, with the second at an adjoining interstitial site. In table 3.7 we give the energy of such a configuration, as the second H(He) moves along the tetrahedral-vacancy or octahedral-vacancy line in ten equal steps. For H in Al, the lowest energy (1.64 eV) is obtained when it is about 20% away from the tetrahedral site. In both Al and Mg, the He will sit along the octahedral-vacancy line, displaced by about 40%, thereby lowering the energy by 5.58 and 3.56 eV respectively.

There are other configurations of two H(He) near a vacancy which are energetically more favourable than those considered so far. As for the case of a perfect lattice, a number of geometries was considered; results for those which were found to have the lowest energies are reported here. Consider a dumb-bell arrangement of two H(He) in Al each placed equidistant from the vacancy along the line joining the two octahedral sites $(0, 0, \frac{1}{2})$ and $(0, 0, -\frac{1}{2})$, or the two tetrahedral sites $(\frac{1}{4}, \frac{1}{4}, \frac{1}{4})$ and $(-\frac{1}{4}, -\frac{1}{4}, -\frac{1}{4})$. (These are the lines discussed at the beginning of this section, now with a vacancy at the cube corner.) In table 3.8 we enter the energy as both impurities move into the vacancy in ten equal steps. As the impurities are relaxed towards the vacancy the energy is lowered reaching

Table 3.7.

Energy of a pair of H(He) impurities in Al(Mg) with one H(He) at the vacancy and the other moving from a neighbouring interstitial site towards the origin in 10 equidistant steps. The energy is relative to having both H(He) at well separated lowest energy sites in the perfect lattice. Columns 1 to 3 give results for the tetrahedral case while 4 to 6 apply to the octahedral case. The last row is the minimum energy for the column.

Tetrahedral						Octahedral					
H in Al	H in Mg	He in Al	He in Mg	H in Al	H in Mg	He in Al	He in Mg	H in Al	H in Mg	He in Al	He in Mg
-1.44		-3.30	-2.41	-1.42		-4.48	-2.72				
-1.57		-3.76	-2.77	-1.48		-4.73	-2.85				
-1.64		-4.36	-3.08	-1.54		-5.06	-3.07				
-1.59		-4.86	-3.34	-1.57		-5.38	-3.28				
-1.37		-4.87	-3.43	-1.51		-5.58	-3.51				
-.89		-3.99	-2.75	-1.23		-5.12	-3.43				
.37		-.25	-.06	-.50		-3.11	-2.17				
2.54		6.56	4.35	2.03		4.95	4.27				
12.		38.	32.	8.		26.	20.				
25.		80.	70.	16.		60.	60.				
--		--	--	--		--	--				
-1.64		-4.91	-3.46	-1.49		-5.58	-3.56				

Table 3.8

Energy of two H(He) impurities in Al(Mg) each on a line joining opposing tetrahedral (octahedral) sites with the origin in 10 equidistant steps. The energy is relative to both H(He) being at well separated lowest energy sites in the perfect lattice. Columns 1 to 4 (5 to 8) apply to the tetrahedral (octahedral) case. The last row is the minimum energy for the column.

Tetrahedral				Octahedral			
H in Al	H in Mg	He in Al	He in Mg	H in Al	H in Mg	He in Al	He in Mg (oct-tet)
-.46	-.15	.84	-.30	-.41	-.11	-1.27	-.52
-.78	-.20	-.21	-1.03	-.54	-.13	-1.96	-1.01
-1.02	-.40	-1.57	-1.67	-.70	-.11	-2.74	-1.59
-1.21	-.10	-2.86	-2.19	-.88	-.02	-3.58	-2.07
-1.39	-.05	-3.90	-2.92	-1.09	.00	-4.36	-2.66
-1.59	.04	-4.87	-3.03	-1.35	.04	-4.94	-3.04
-1.72	.13	-5.78	-4.28	-1.64	.08	-5.64	-3.96
-1.51	.60	-5.79	-3.72	-1.70	.46	-6.19	-3.86
.23	2.13	-.74	-.80	-.68	1.74	-3.71	-1.77
12.	13.	38.	32.	8.	11.	26.	27.
-	--	--	--	--	--	--	--
-1.73	-.42	-6.04	-4.33	-1.72	-.13	-6.23	-4.10

a minimum of ~ 1.73 eV in both octahedral and tetrahedral cases. This is a lower energy configuration than the one previously discussed for which the relevant energy was 1.64 eV. For He in Al the octahedral direction is favoured with energy 6.23 eV and position $\sim 35\%$ away out from the origin. This energy is to be compared with 5.58 eV for the substitutional-interstitial configuration.

For Mg which is hcp we discuss two possibilities. In the first the H(He) sit at tetrahedral sites along the c-axis, one above and one below the central atom. The other configuration which we will refer to as octahedral has one H(He) at the closest octahedral position to the origin with the second H(He) at the high symmetry position closest to the line through the first H(He) and the origin, which is tetrahedral. From the tables we see that for both H and He in Mg the tetrahedral configuration is preferred. For H the energy is .42 eV and the dumb-bell is rather extended with best position about 20% off the tetrahedral site towards the vacancy. For He, on the other hand, the energy is 4.10 eV [to be compared with 3.56 eV for the substitutional-interstitial case previously described], but with the He closer to the vacancy: 40% of the way from the origin to the tetrahedral site.

In conclusion, we have found that quite different energies and configurations are obtained when pairs of impurities are

involved. The results suggest, in particular, that H in Al will indeed associate itself with a vacancy, and may be found in tetrahedral sites, but well off the ideal interstitial site.

CHAPTER IV

APPLICATION TO SUPERCONDUCTIVITY: METALLIC HYDROGEN

4.1 INTRODUCTION

Since Ashcroft (1968) first suggested that metallic hydrogen might be a high temperature superconductor, much theoretical work has been done on this material. Because the metal is a very high density state, corresponding to $r_s < 1.6$, pressures on the order of megabars are required to obtain it (Beck and Strauss 1975 and Nagara et al 1976), and hence it has been observed in only a few cases (Grigor'ev et al 1972, Vereshchagin et al 1975). Nevertheless, it has been the object of much interest.

In order to see the relevance of the work reported here, let us review briefly recent developments relevant to the superconductivity of metallic H. In Ashcroft's original paper, he considered the BCS expression (Bardeen, Cooper and Schrieffer 1957) for the transition temperature T_c . After making estimates of the parameters entering that equation appropriate for H, he suggested T_c would be high.

Schneider and Stoll (1971) went beyond this to an approximate solution of the Eliashberg gap equations for an assumed hcp structure. Using an earlier calculation of the lattice vibrations done in the adiabatic, harmonic approximation

(HA) (Schneider 1969) they obtained a T_c of about 70° to 200° , depending on the density.

Face-centered cubic H was studied quite extensively by Caron (1974) in the range of densities specified by $.1 \leq r_s \leq 1.5$. The potentials used by him were based on linear response theory, using a dielectric function (Caron 1972) which is a variant of the one developed by Singwi et al (1970). For calculating the lattice vibrations the interatomic potential was approximated by a series of Gaussians, and the phonons calculated using the self-consistent harmonic approximation (SCHA). For increasing values of r_s , he found that at certain points within the Brillouin zone the transverse modes softened, until at $r_s \approx 1.5$ some frequencies dropped to zero, indicating an instability to shearing. This dynamic instability in turn indicates a phase change to a different structure. Caron pointed out that this mode softening is very sensitive to the electron screening.

Using these phonons and the linear response potentials he went on to solve the Eliashberg gap equations, assuming a spherical Fermi surface, and a plane wave description of the electrons for the electron-phonon matrix elements (EPME's). The T_c 's he obtained depended strongly on density, being 140° at $r_s = 1.5$, dropping to 1° at $r_s = .5$, and 0° at $r_s = .1$.

Beck and Strauss (1975) considered in some detail the dynamics of the metal and the associated instabilities, for r_s ranging from .6 to 1.5. They again used a dielectric function to

describe the response of the electrons to the protons, but calculated the phonons in the HA, the SCHA, and also by including a third order contribution to the dynamical matrix. They found that using the SCHA reduces the number of imaginary frequencies, compared to using only the HA, thus improving stability. However they found that including the third order term had the opposite effect. Although this term had little effect on most frequencies, at those points where the modes are soft, and hence the frequencies small, the effect can be important. In particular, in some cases where the SCHA predicts small but real frequencies, and hence no instabilities, including the third term causes them to become imaginary. They found instabilities for the fcc structure to occur for $r_s \geq 1.0$; they also considered the body-centered cubic structure which they found to be unstable for all $.6 \leq r_s \leq 1.5$. They remark further that the quantitative features of the instabilities depend on the dielectric function used, i.e. on the screening.

Papaconstantopoulos and Klein (1977) and Switendick (1976) approached the problem in similar ways. They used one version of the approximate T_c formula of McMillan (1968), and hence needed only the mass enhancement factor λ , Coulomb parameter μ^* and maximum phonon frequency, from which they obtained an approximate average of the squares of the phonon frequencies. For the electronic contribution to λ , they used a theory of Gaspari and Gyorffy (1972), which although it avoids the prob-

lem of using plane waves in the EPME's, does neglect important screening effects, (Gupta and Sinha 1976). For the phonon frequencies, they used the results of Caron, and obtained T_c 's of about 250° .

A one augmented plane wave calculation was done for both fcc and body-centered cubic structures, at r_s values of 1.29 and 1.64 by Gupta and Sinha (1976), using approximate crystal potentials. The EPME's were then calculated using these wavefunctions, and the McMillan equation used for T_c . The highest value obtained was only $.08^\circ$. Although a one APW calculation using an approximate potential can certainly be criticized, it is probably true that using plane waves to calculate the EPME's introduces significant errors into the calculation of T_c .

Finally we point out that band structure calculations: (Harris et al 1973, Switendick 1976 and Papaconstantopoulos and Klein 1977) indicate the Fermi surface is nearly spherical, and the Fermi surface density of states very nearly that of the free electron case.

The work described in the rest of this chapter differs from previous work mainly in the choice of the potential, i.e. the screening. As done by Caron, we employ the SCHA for the phonons, a spherical Fermi surface, and plane waves for the EPME's. However, the calculations differ in that instead of linear response being used, non-linear self-consistent calculations are used to generate the electron-proton and proton-proton potentials.

The Eliashberg gap equations are solved for T_c and for its functional derivatives with respect to the effective phonon distribution $\alpha^2F(\omega)$ and Coulomb parameter μ^* . We consider both fcc and bcc structures, and also employ the approximate formulae of McMillan and of Leavens (1973).

In the rest of this chapter, we first exhibit the formalism for the calculation of T_c and its functional derivatives. Following this the screening calculations are briefly discussed, and then the phonons. Finally the results for the superconductivity are presented.

4.2 ELIASHBERG GAP EQUATIONS AND FUNCTIONAL DERIVATIVES

In the calculations of the superconducting properties of hydrogen which are reported here, the procedure used involves the solution of the Eliashberg gap equations using a spherical Fermi surface and plane wave description of the electron states. In this section we present the formalism for this case, along with the expressions for certain functional derivatives of T_c . The development here is taken from Daams (1977) and Daams and Carbotte (1978), who follow Bergmann and Rainer (1973), Rainer and Bergmann (1974) and Leavens (1974). At the end of this section approximate formulae for T_c are exhibited.

The Eliashberg gap equations are the central result of the strong coupling theory of superconductivity. They are a set of non-linear, integral equations which require as input

only normal state properties of the metal. These equations are derived from considering the electron self energies, which when evaluated at the discrete set of points on the imaginary axis $i\omega_n = i\pi k_B T(2n-1)$, contain the information on the thermodynamics of the system. The ω_n are the Matsubara frequencies, k_B the Boltzmann constant, and T the temperature. Within the approximations outlined above, these gap equations are

$$\tilde{\Delta}(n) = \pi k_B T \sum_m \frac{(\lambda(m-n) - \mu^*) \tilde{\Delta}(m)}{\sqrt{\tilde{\omega}(m)^2 + \tilde{\Delta}(m)^2}} \quad (4.1)$$

$$\tilde{\omega}(n) = \omega_n + \pi k_B T \sum_m \frac{\lambda(m-n) \tilde{\omega}(m)}{\sqrt{\tilde{\omega}(m)^2 + \tilde{\Delta}(m)^2}} \quad (4.2)$$

$\tilde{\Delta}(n)$ is the generalization of the BCS gap evaluated at $i\omega_n$. In practice, the sum over m is truncated when the corresponding Matsubara frequency ω_m reaches a cut-off frequency ω_c , usually taken to be at least five times the maximum phonon frequency.

The necessary normal state information is contained in the quantities $\lambda(m-n)$ and μ^* . The first of these is given by

$$\lambda(l) = 2 \int \frac{\omega d\omega \alpha^2 F(\omega)}{\omega^2 + (2\pi l k_B T)^2} \quad (4.3)$$

where $\alpha^2 F(\omega)$ is the average over all electron states \underline{k} and \underline{k}' on the Fermi surface, of the phonon density of states $F(\underline{k}-\underline{k}', \omega)$ weighted by the effectiveness of these phonons for causing

electron transitions between the states \underline{k} and \underline{k}' . It can be expressed (Leavens 1970)

$$\alpha^2 F(\omega) = N(0) \int \frac{d\Omega_{\underline{k}}}{4\pi} \frac{d\Omega_{\underline{k}'}}{4\pi} \sum_{\lambda} |g_{\underline{k}\underline{k}',\lambda}|^2 \delta(\omega - \omega_{\lambda}(\underline{k} - \underline{k}')) \quad (4.4)$$

where $N(0)$ is the electron density of states at the Fermi surface, $d\Omega_{\underline{k}}$ is an element of solid angle on the Fermi surface at \underline{k} , $\omega_{\lambda}(\underline{k} - \underline{k}')$ is the phonon frequency corresponding to wave vector $\underline{k} - \underline{k}'$ and branch λ , and $g_{\underline{k}\underline{k}',\lambda}$ is the electron-phonon coupling constant, which in the plane wave approximation is

$$g_{\underline{k}\underline{k}',\lambda} = \frac{-iq \cdot \underline{\epsilon}_{\lambda}(q) w_{\underline{q}}(k_F)}{\sqrt{2MN} \omega_{\lambda}(q)} \quad (4.5)$$

where $\underline{q} = \underline{k} - \underline{k}'$, $\underline{\epsilon}_{\lambda}(q)$ is the polarization vector corresponding to $\omega_{\lambda}(q)$, $w_{\underline{q}}(k_F)$ is the form factor for scattering on the Fermi surface (equation 2.59, or 2.65 for a local potential), M is the ionic mass and N the number of ions in the metal.

The other normal metal quantity required is the Coulomb parameter μ^*

$$\mu^* = \frac{N(0)V_C}{1 + N(0)V_C \ln\left(\frac{E_F}{\omega_C}\right)} \quad (4.6)$$

where V_C is the Fermi surface average of the Coulomb repulsion between electrons. The cutoff frequency ω_C is the one used as the upper limit of the sums over the Matsubara frequencies.

The non-linear equations (4.1) and (4.2) have non-trivial solutions only for $T \leq T_C$. At T_C they can be made

linear by neglecting the terms which are of order $\tilde{\Delta}(m)^2$; after a pair breaking parameter ρ is introduced for convenience, they become (Bergmann and Rainer 1973)

$$\tilde{\Delta}(n) = \pi k_B T \sum_m (\lambda(m-n) - \mu^*) \frac{\tilde{\Delta}(m)}{|\tilde{\omega}(m)| + \rho} \quad (4.7)$$

$$\tilde{\omega}(n) = \omega_n + \pi k_B T \sum_m \lambda(m-n) \text{sgn}(\omega_m) \quad (4.8)$$

At a temperature T , the parameter $\rho(T)$ can be defined as the largest ρ for which (4.7) has a non-trivial solution. The transition temperature T_c can be obtained by solving $\rho(T_c) = 0$.

In addition to knowing T_c for a given $\alpha^2 F(\omega)$ and μ^* , it is often of interest to know quantitatively how T_c would change with changes in the normal state properties; this question can be formulated in terms of the functional derivatives of T_c with respect to these properties. To evaluate these, define a new function

$$\bar{\Delta}(n) = \frac{\tilde{\Delta}(n)}{|\tilde{\omega}(n)| + \rho} \quad (4.9)$$

With this substitution, equation (4.7) becomes

$$\rho \bar{\Delta}(n) = \pi k_B T \sum_m (\lambda(m-n) - \mu^* - \frac{\delta_{mn} |\tilde{\omega}(m)|}{\pi k_B T}) \bar{\Delta}(m) \quad (4.10)$$

This equation is an eigenvalue equation with kernel

$$K_{nm} = \pi k_B T (\lambda(m-n) - \mu^* - \frac{\delta_{nm} |\tilde{\omega}(m)|}{\pi k_B T}). \quad (4.11)$$

Changes in $\alpha^2 F(\omega)$ or μ^* manifest themselves as changes in this kernel; to first order a change in K_{nm} causes a change in the transition temperature of

$$\delta T_C = - \left(\frac{\partial \rho}{\partial T} \right)_{T_C}^{-1} \left(\sum_{m,n} \bar{\Delta}(m) \delta K_{mn} \bar{\Delta}(n) \right) / \left(\sum_n \bar{\Delta}(n)^2 \right) \quad (4.12)$$

with

$$\left(\frac{\partial \rho}{\partial T} \right)_{T_C} = \left(\sum_{m,n} \bar{\Delta}(m) \left(\frac{\partial K_{mn}}{\partial T} \right)_{T_C} \bar{\Delta}(n) \right) / \left(\sum_n \bar{\Delta}(n)^2 \right) \quad (4.13)$$

and

$$\left(\frac{\partial K_{nm}}{\partial T} \right)_{T_C} = \pi k_B T_C \left(\left(\frac{\partial \lambda(n-m)}{\partial T} \right)_{T_C} - \delta_{nm} \sum_{\ell} \left(\frac{\partial \lambda(n-\ell)}{\partial T} \right)_{T_C} \operatorname{sgn}(\omega_{\ell} \omega_n) \right). \quad (4.14)$$

To calculate the influence of changes in $\alpha^2 F(\omega)$ on T_C , let $\delta \alpha^2 F(\omega)$ be a delta function of infinitesimal height ε centered at frequency ω . This leads to a change

$$\delta T_C = \varepsilon \left(\frac{\partial \rho}{\partial T} \right)_{T_C}^{-1} \left(\pi k_B T_C \right) \left(\frac{\sum_{m,n} \frac{2\omega}{\omega^2 + \omega_{n-m}^2} (\bar{\Delta}(m) \bar{\Delta}(n) - \bar{\Delta}(n)^2 \operatorname{sgn}(\omega_n \omega_m))}{\sum_n \bar{\Delta}(n)^2} \right). \quad (4.15)$$

This derivative exhibits the effectiveness of the different parts of $\alpha^2 F(\omega)$ for enhancing T_C .

If μ^* changes by an infinitesimal ε then T_C changes by

$$\delta T_c = \epsilon \left(\frac{\partial \rho}{\partial T} \right)_{T_c}^{-1} (\pi k_B T_c) \frac{\sum_{m,n} \bar{\Delta}(m) \bar{\Delta}(n)}{\sum_n \bar{\Delta}(n)^2} \quad (4.16)$$

These two equations are the functional derivatives reported later.

Before ending this section, two approximate solutions to the gap equations are recorded. The first, due to McMillan (1968) has as its most useful form (Dynes 1972)

$$k_B T_c^M = \frac{\langle \omega \rangle}{1.20} \exp\{-1.04(1+\lambda)/(\lambda - \mu^*(1+0.62\lambda))\} \quad (4.17)$$

where λ is the mass enhancement factor, (equation (4.3) with $l=0$), and $\langle \omega \rangle$ is the average phonon frequency defined by

$$\langle \omega \rangle = \frac{2 \int_0^\infty d\omega \alpha^2 F(\omega)}{\lambda} \quad (4.18)$$

The second, which is due to Leavens (1973) consists of a pair of simple, coupled equations

$$k_B T_c^L = 1.134 \omega_0 \exp\{-(1+\lambda+\bar{\lambda}(T_c))/(\lambda - \mu^*)\} \quad (4.19)$$

$$\bar{\lambda}(T_c) = 2 \int_0^{\omega_0} \frac{d\omega \alpha^2 F(\omega)}{\omega} \ln \left(\frac{\omega + \omega_0}{\omega + k_B T_c / 1.134} \right) \quad (4.20)$$

where ω_0 is the maximum phonon frequency.

Since $\alpha^2 F(\omega)$ is known in our case, Leavens' formula is virtually no more difficult to use than McMillan's, but, as

will become apparent in section 4.5, is more accurate.

4.3 NON-LINEAR SCREENING CALCULATIONS AND POTENTIALS

The calculations of PSCP referred to in chapter III certainly indicate that for $r_s \approx 2$, linear response is inadequate for calculating the screened electron-proton potential. On the other hand, for the limiting case of $r_s \rightarrow 0$, linear response should be exact (since the Hamiltonian for the system is dominated by the kinetic energy); the densities corresponding to the presumed metallic state of hydrogen are between these limits.

The electron-proton potential used in this chapter was calculated following almost exactly the procedure described in section 3.3. The only non-trivial difference is that the following form for the trial potential was used.

$$V_{tr}(r) = -\frac{1}{r} \left\{ \frac{e^{-\alpha r}}{1 + \beta r + (\beta^2 + (\alpha + \beta)^2) r^2 / 2} \right\} \quad (4.21)$$

The calculations were performed for r_s values of .6, .8, 1.0, 1.2, and 1.4. The Schrödinger equation was solved in steps of $.05 a_0$ for $r_s \geq 1.0$, and $.0125 a_0$ for smaller r_s . It was found that going out to $10 a_0$ was far enough, with the phase shifts calculated at $5 a_0$. The sums over l , in equation (3.28) were terminated at $l_{max} = 7$.

Since the phonons calculated in the next section are all real only for $r_s \leq 1.0$, and hence the superconducting properties calculated only for these densities, the results of the potential calculations are presented for only these densities.

Table 4.1 contains the parameters and phase shifts for the trial potentials, and fig. 4.1 illustrates the displaced densities as a function of r/a_0 for each r_s . Since the electron-proton potential in \underline{r} -space is not used in calculating $\alpha^2 F(\omega)$, but rather its form factor for the range $0 \leq q \leq 2k_F$, this is shown in fig. 4.2.

The proton-proton potential is given by the Coulomb interaction of one proton with the other proton and its associated screening cloud. The potentials so obtained are plotted in fig. 4.3 as a function of r/r_s . On the same plot, the first 15 neighbour shells of the fcc lattice are shown. It can be seen from this figure that relative to the neighbours, the phase of the oscillations in the potential is nearly the same for each density.

We compare briefly with linear response. Of the three densities considered in detail here, that corresponding to $r_s = 1.0$ is of the most interest since it would require the least pressure to attain. Linear response calculations were done for this density using the Singwi dielectric function described in chapter II. The differences are illustrated in figs. 4.4 and 4.5.

Linear response underestimates the displaced charge at the nucleus by a factor of about 2.5, and differs substantially from non-linear response throughout the region $0 \leq r \leq 2 a_0$. The oscillations are also different. The first few differ in amplitude as well as phase; for larger distances the amplitude agrees although the phase remains different.

Table 4.1
Parameters and Phase Shifts of H Potentials

r_s	α	β	η_0	η_1	η_2	η_3	η_4	η_5	η_6	η_7
0.6	1.0440	.5211	.4518	.1445	.0578	.0257	.0123	.0062	.0032	.0018
0.8	1.0736	.2273	.5874	.1572	.0541	.0209	.0087	.0038	.0018	.0008
1.0	1.0359	.1175	.7241	.1616	.0488	.0167	.0062	.0024	.0010	.0004

R

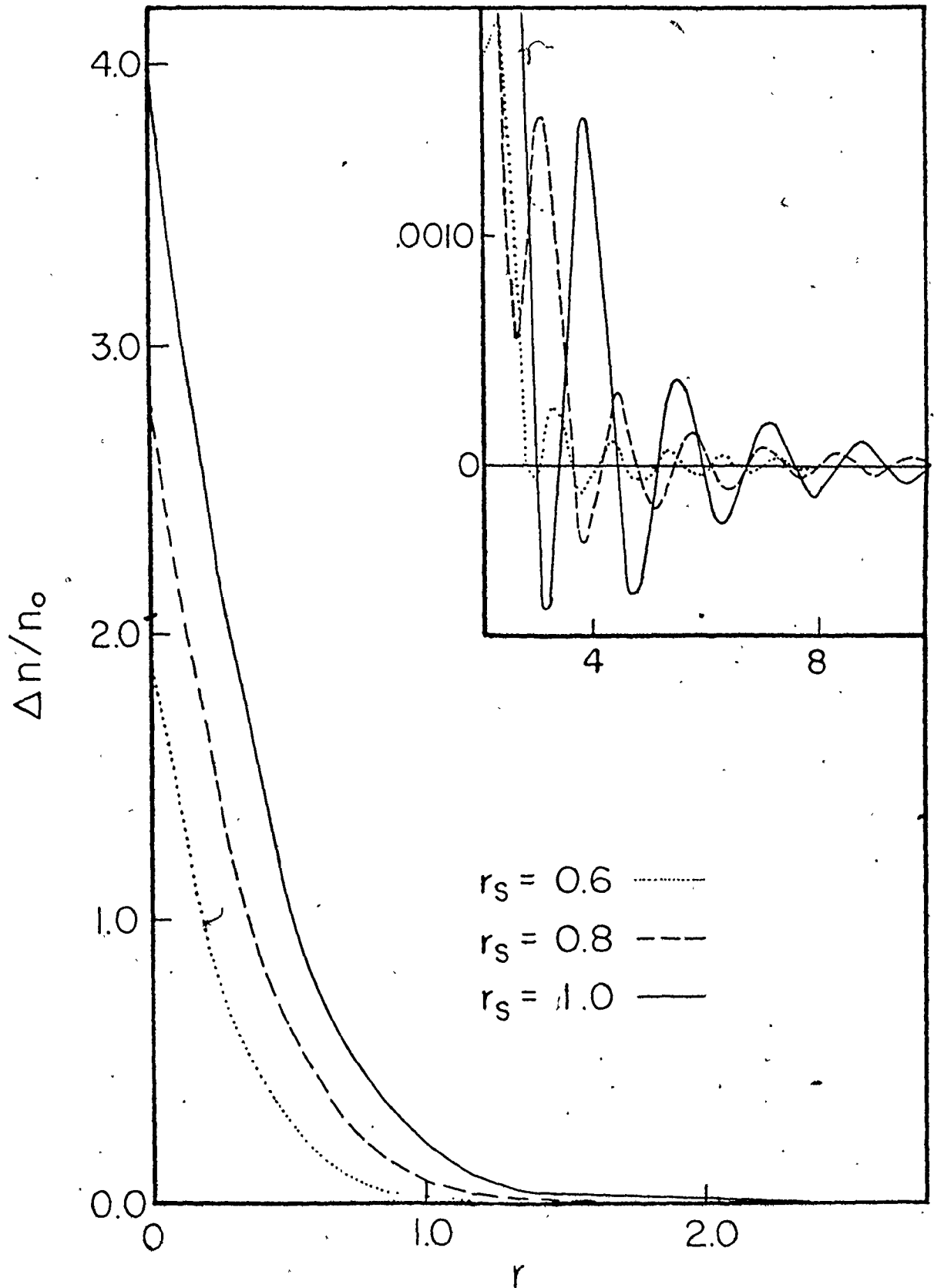
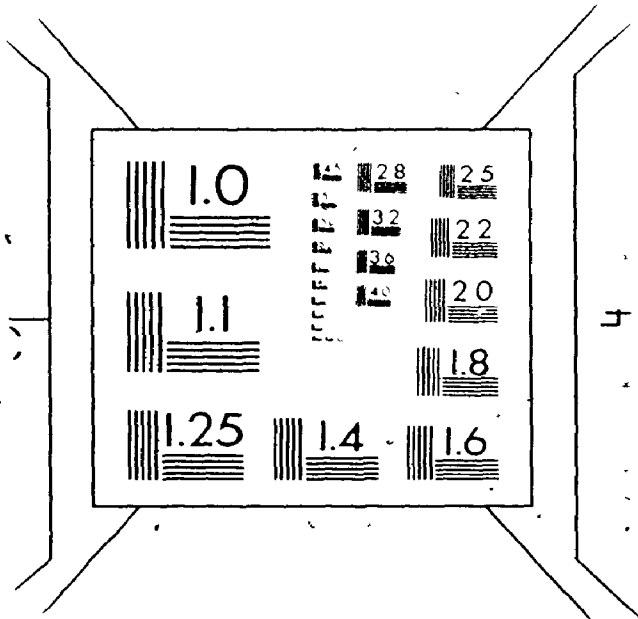


Fig. 4.1: Displaced electron density $\Delta n/n_0$ surrounding a proton in the electron gas.

2

OF / DE

2



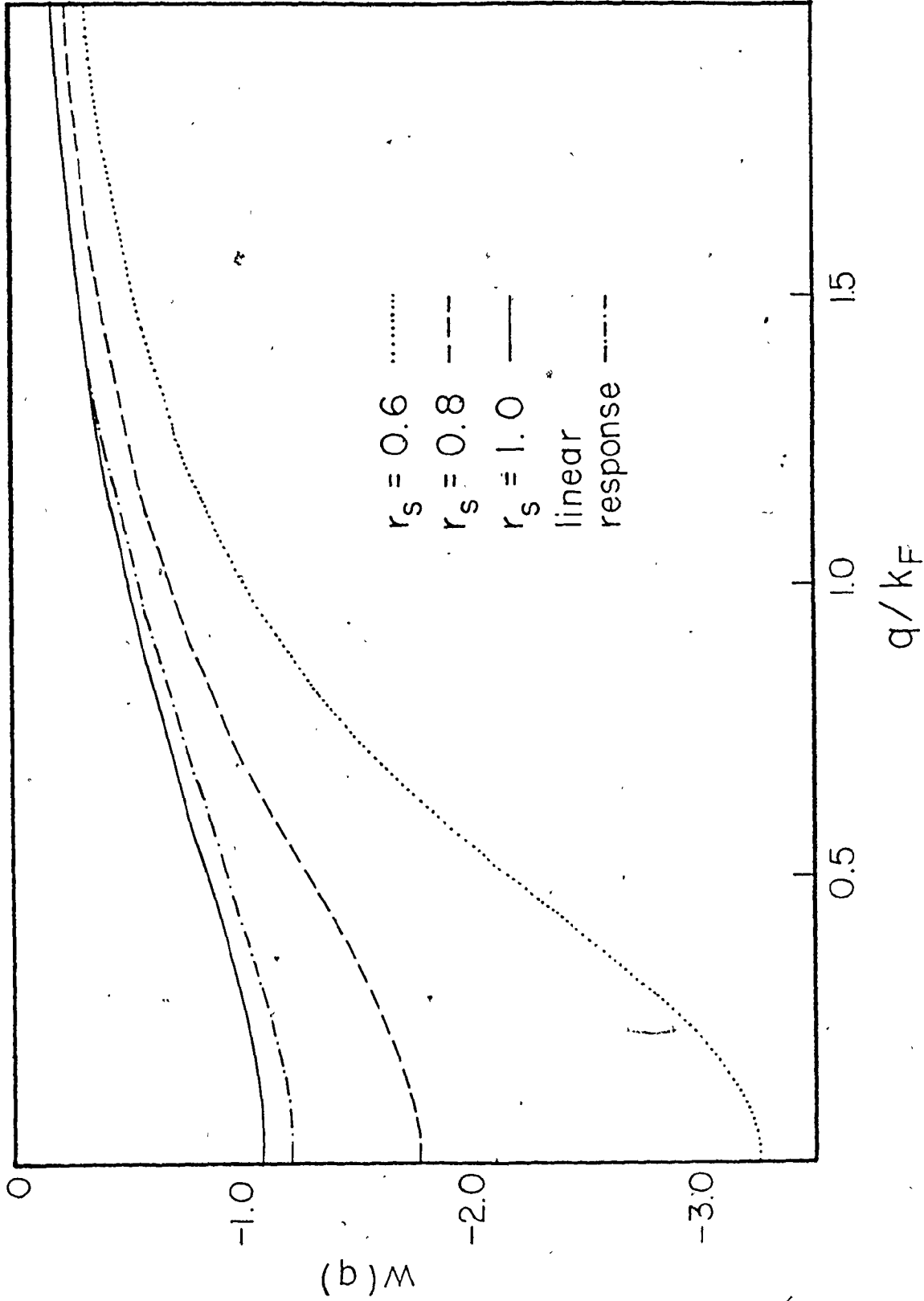


Fig. 4.2: Screened electron-proton form factors. The linear response form factor is for $r_s = 1.0$.

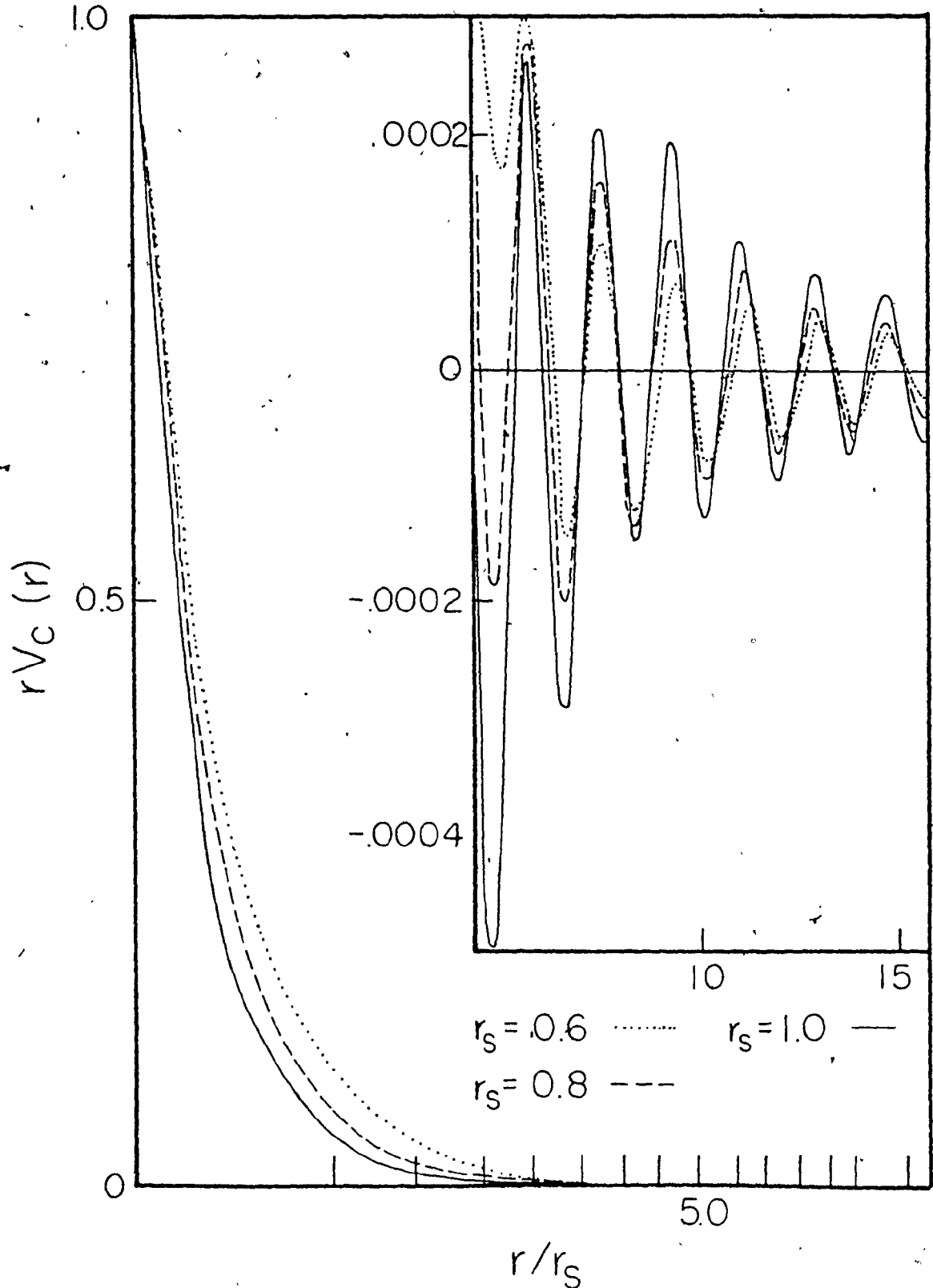


Fig. 4.3: Screened proton-proton potentials. The vertical lines mark the distances to the neighbours of the fcc structure.

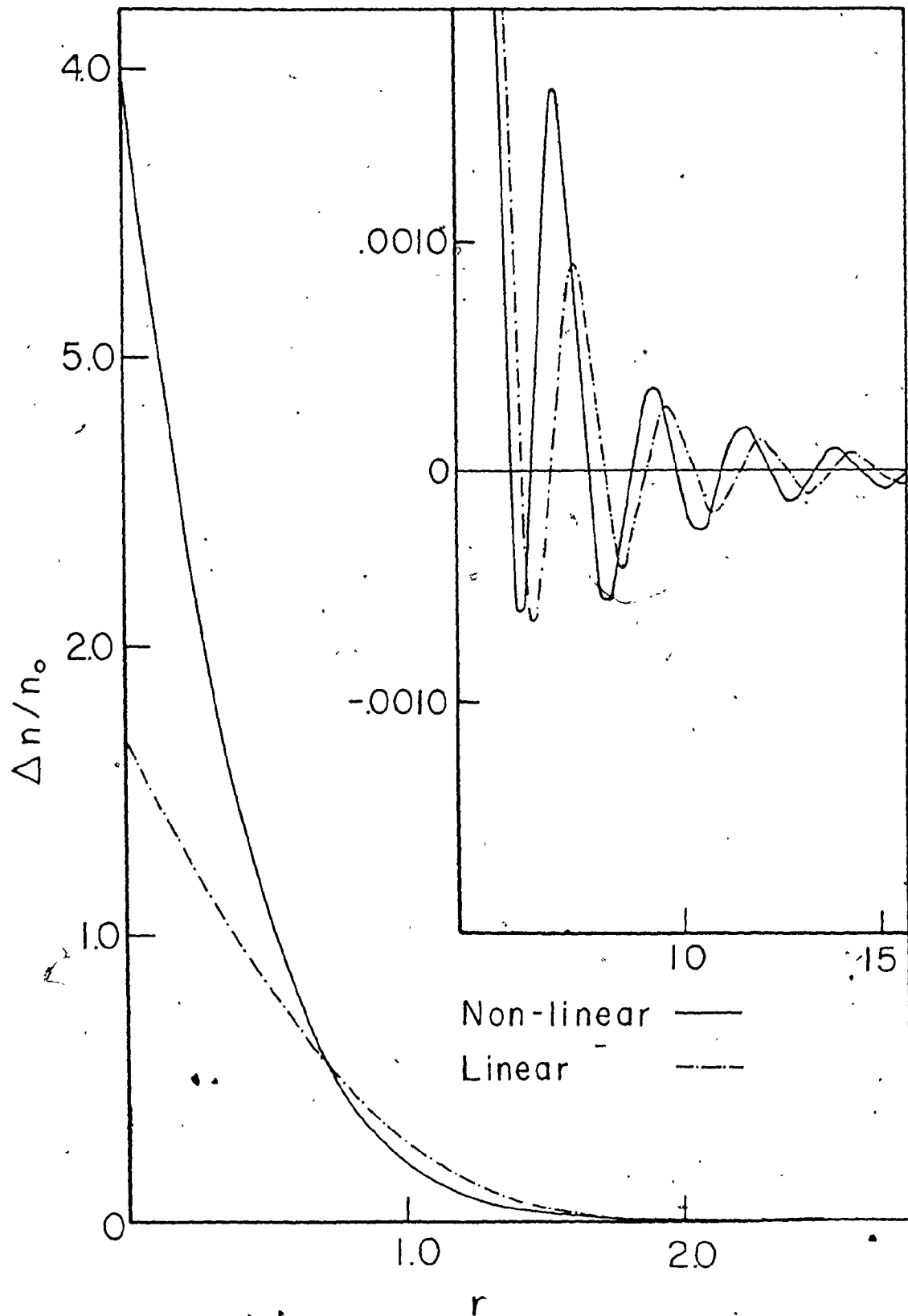


Fig. 4.4: Displaced electron density for $r_s = 4.0$, using non-linear and linear calculations.

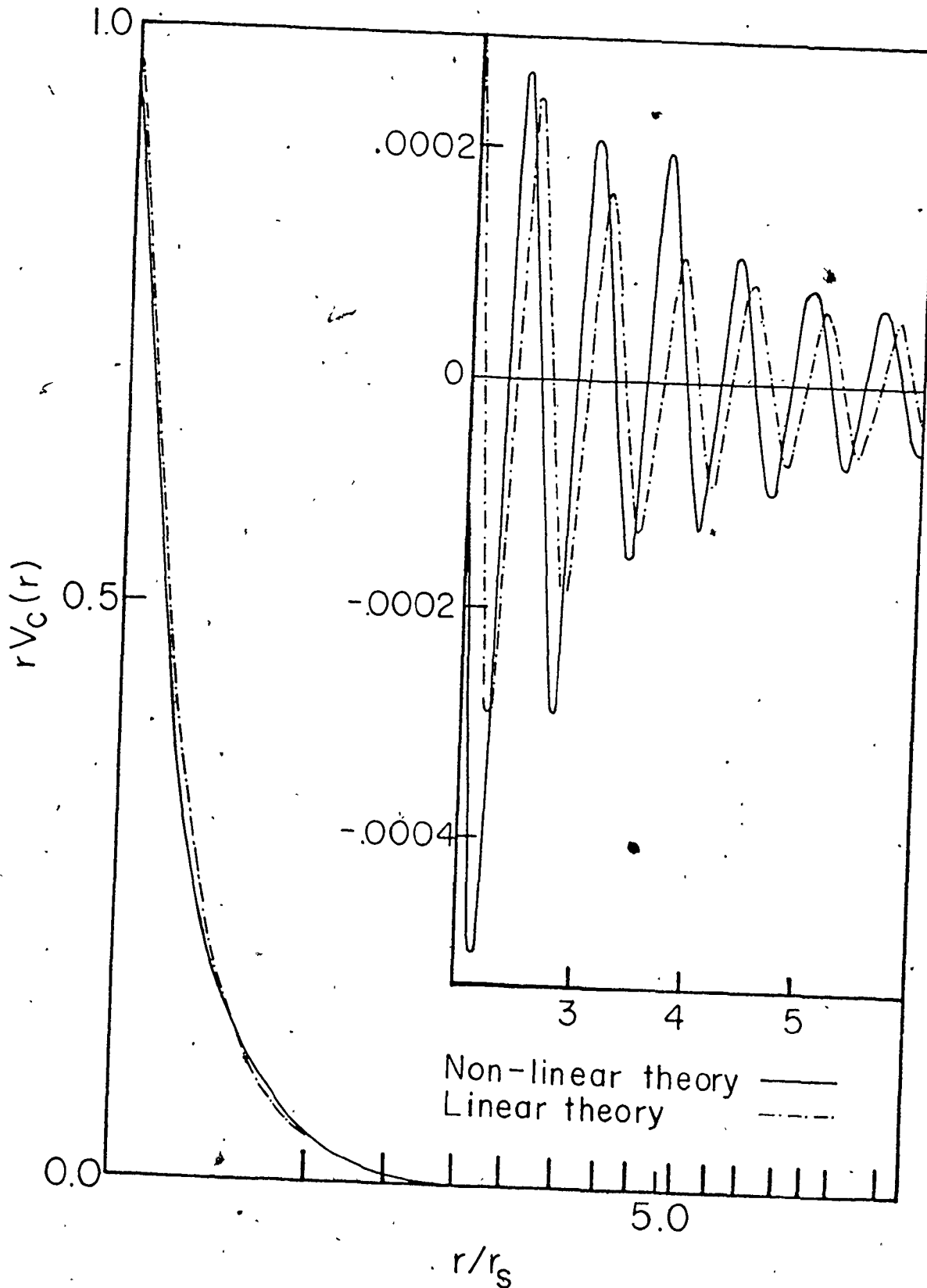


Fig. 4.5: Screened proton-proton potentials for $r_s = 1.0$, using non-linear and linear theory.

The differences in the potential reflect those in the density, so are not discussed further.

The behaviour at large r can be understood from the general linear response theory. Following Harrison (1966) it is easy to show that if a bare potential is local and has no singularities, then the asymptotic form of the density is, in linear response,

$$\Delta n(r) = - \frac{3w(2k_F)}{k_F^2 \epsilon(2k_F)} \frac{\cos 2k_F r}{r^3} \quad (4.22)$$

These are oscillations with zero phase and amplitude determined by $w(2k_F)$. In fig. 4.2 the linear response form factor for this density is also included, where it can be seen that $w(2k_F)$ is the same as for the non-linear potential. This explains the agreement of the amplitudes, although linear response cannot reproduce the phase correctly, which is .98 for $r_s = 1.0$, and .82 and .60 for r_s equal to .8 and .6 respectively.

Although there are in the literature no other non-linear calculations for H in the density range reported here, there are some for the range $1.0 \leq r_s \leq 6.0$. In addition to the Mg and Al densities considered by PSCP, Almbladh et al (1976) have applied both the method used here and another procedure in which the self-consistency equations were iterated to convergence for this range. They report that the two methods agree well for $1 \leq r_s \leq 3$.

Zaremba et al (1977) also obtained an interaction procedure, which they too applied to the range $1 \leq r_s \leq 6$. We can make one comparison of our results with those published by both these authors, and that is the displaced electron charge density at the proton for $r_s = 1.0$. For $\Delta n(0)/n_0$, we obtain 4.11, Almbladh et al 4.16, and Zaremba et al 4.13.

Finally, we mention again the calculations of Jena and Singwi (1978), who repeated the calculations of H in Al and Mg, but using a procedure which converged automatically. This was achieved by choosing for $V_{\text{eff}}(r)$ not equation (3.30), but rather

$$V_{\text{eff}}(r) = -\frac{e^{-k_{\text{TF}}r}}{r} + \int \frac{e^{-k_{\text{TF}}|\underline{r}-\underline{r}'|}}{|\underline{r}-\underline{r}'|} \Delta n(\underline{r}') - k_{\text{TF}}^2 V_{\text{tr}}(r) + (1+k_{\text{TF}}^2) V_{\text{xc}}(r). \quad (4.23)$$

with k_{TF} the Thomas-Fermi screening parameter.

This is equivalent to (3.30) if $V_{\text{eff}}(r) = V_{\text{tr}}(r)$, and has the advantage that the Coulomb tail which would normally exist if the FSR were not satisfied is automatically truncated.

4.4 SELF-CONSISTENT PHONONS IN HYDROGEN

The discussion of section 4.1 clearly indicates the need to go beyond the HA to calculate the phonons in H. If the present aim were to investigate the stability of the metal it would also be necessary to go beyond the SCHA. However, since our primary interest is in T_c , the SCHA should be adequate at

those densities for which it predicts no instabilities.

In the SCHA, the phonon frequencies and polarization vectors are given by the eigenvalue equation (Cowley and Shukla 1974)

$$\omega_{\lambda}^2(\underline{k}) \varepsilon_{\lambda}^{\alpha}(\underline{k}) = \sum_{\beta} D_{\alpha\beta}(\underline{k}) \varepsilon_{\lambda}^{\beta}(\underline{k}) \quad (4.24)$$

where $\varepsilon_{\lambda}^{\alpha}(\underline{k})$ is the α component of the polarization vector $\underline{\varepsilon}_{\lambda}(\underline{k})$, and the dynamical matrix is

$$D_{\alpha\beta}(\underline{k}) = \frac{1}{M} \sum_{\ell} (1 - \cos(\underline{k} \cdot \underline{R}_{\ell})) \langle \phi_{\alpha\beta}(\underline{R}_{\ell}) \rangle \quad (4.25)$$

The force constant matrix is given by a thermal average

$$\langle \phi_{\alpha\beta}(\underline{R}_{\ell}) \rangle = \frac{1}{(8\pi^3 \det \lambda_{\ell})^{1/2}} \int d^3 \underline{u} \exp\left(-\frac{1}{2} \sum_{\gamma\delta} u_{\gamma} (\lambda_{\ell}^{-1})_{\gamma\delta} u_{\delta}\right) \phi_{\alpha\beta}(\underline{R}_{\ell} + \underline{u}) \quad (4.26)$$

where \underline{u}_{ℓ} is the vector describing the displacement of atom ℓ from its equilibrium position \underline{R}_{ℓ} ; and $\phi_{\alpha\beta}(\underline{R}_{\ell} + \underline{u}_{\ell})$ the tensor derivative of the interatomic potential evaluated at $\underline{R}_{\ell} + \underline{u}_{\ell}$.

The λ_{ℓ} are given by

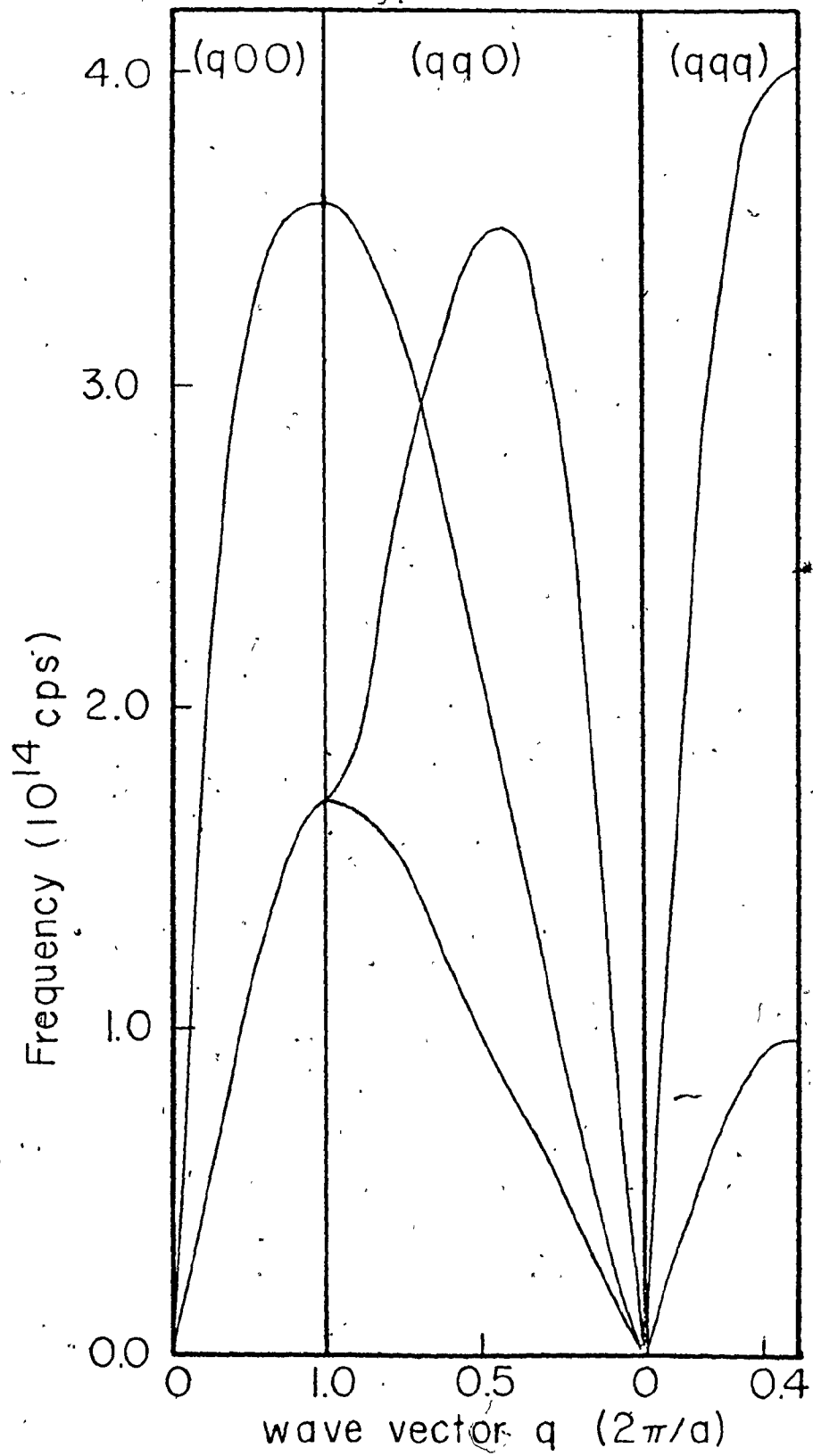
$$(\lambda_{\ell})_{\alpha\beta} = \frac{1}{MN} \sum_{\underline{k}, \lambda} (1 - \cos \underline{k} \cdot \underline{R}_{\ell}) \varepsilon_{\lambda}^{*\alpha}(\underline{k}) \varepsilon_{\lambda}^{\beta}(\underline{k}) \coth\left(\frac{1}{2} \beta \hbar \omega_{\lambda}(\underline{k})\right) / \omega_{\lambda}(\underline{k}) \quad (4.27)$$

The $\langle \phi_{\alpha\beta}(\underline{R}_{\ell}) \rangle$ which play the same role as the $\phi_{\alpha\beta}(\underline{R}_{\ell})$ in the HA, are the tensor derivatives of the potential averaged over the phonon states generated by that potential, and $\beta = 1/k_B T$.

These phonon calculations have been done at zero temperature for both the fcc and bcc structures for the five densities listed in section 4.3. Repeating the calculations at higher temperatures had no significant effect on $\alpha^2 F(\omega)$ or T_c , so only the $T=0$ results are reported. Except for the fcc structure at $r_s = 0.6$, the HA always gave at least some imaginary frequencies. Converged solutions with no imaginary frequencies were obtained for both structures for r_s of .6, .8 and 1.0. These dispersion curves comprise figures 4.6 to 4.11, and the converged force constants are Appendix II. For comparison, the dispersion curves for $r_s = 1.2$, fcc structure are shown in fig. 4.12, with the imaginary frequencies represented by zeros.

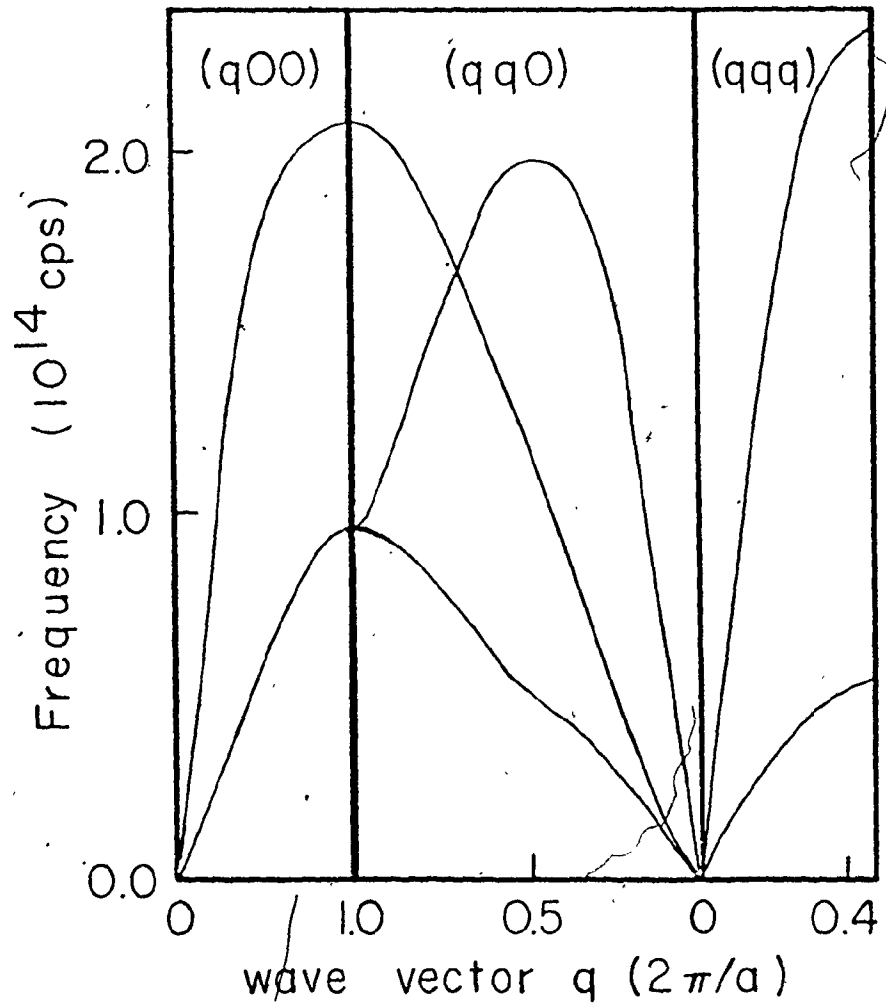
These calculations included interactions extending over 30(35) neighbouring shells for the fcc (bcc) structures, corresponding to about 3.5(4.5) lattice constants. Except for the Kohn anomalies, the frequencies were converged with respect to the number of shells to within one percent.

In order to obtain this same convergence at these points, a large number of shells of neighbours would need to be included. This would imply knowledge of the pair potential for separations of many lattice constants, with many protons in between. Numerically this long range nature of the potential can be treated by working in q -space as Caron did. He obtained small wiggles in his dispersion curves occurring over a very small range of q . But this implies knowledge of the potential



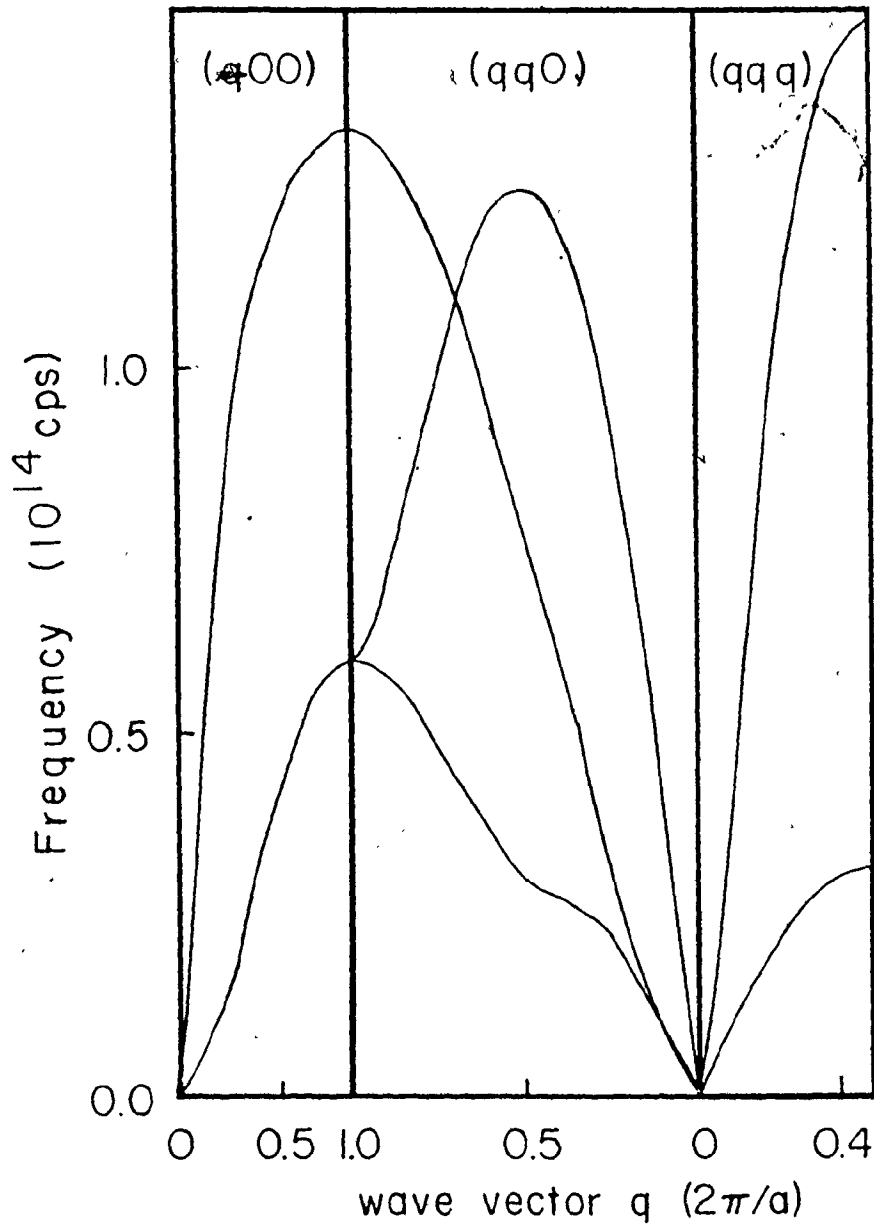
Phonon dispersion curves for fcc H,
 $r_s = 0.6$

Fig. 4.6



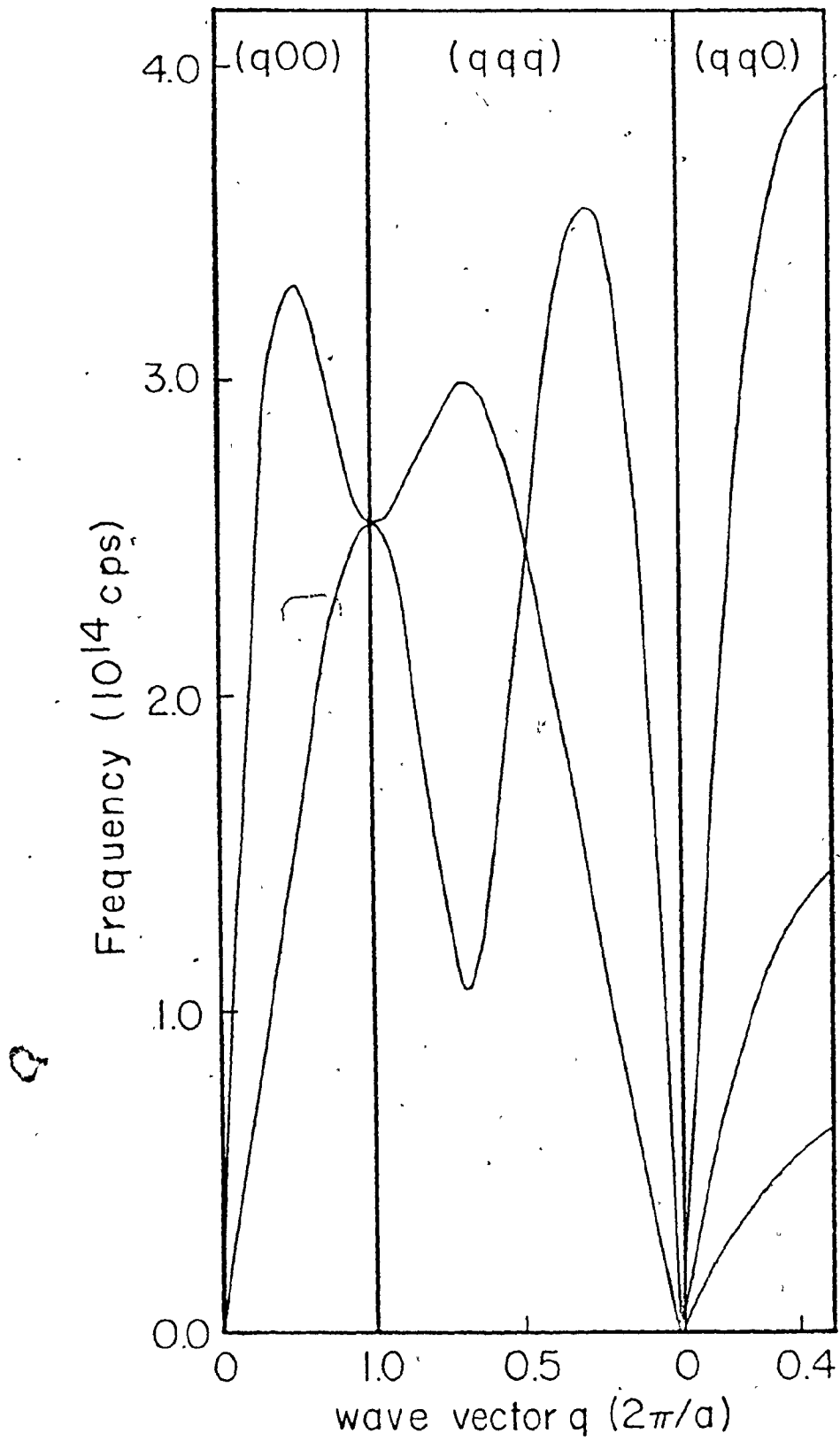
Phonon dispersion curves for fcc H,
 $r_s = 0.8$

Fig. 4.7



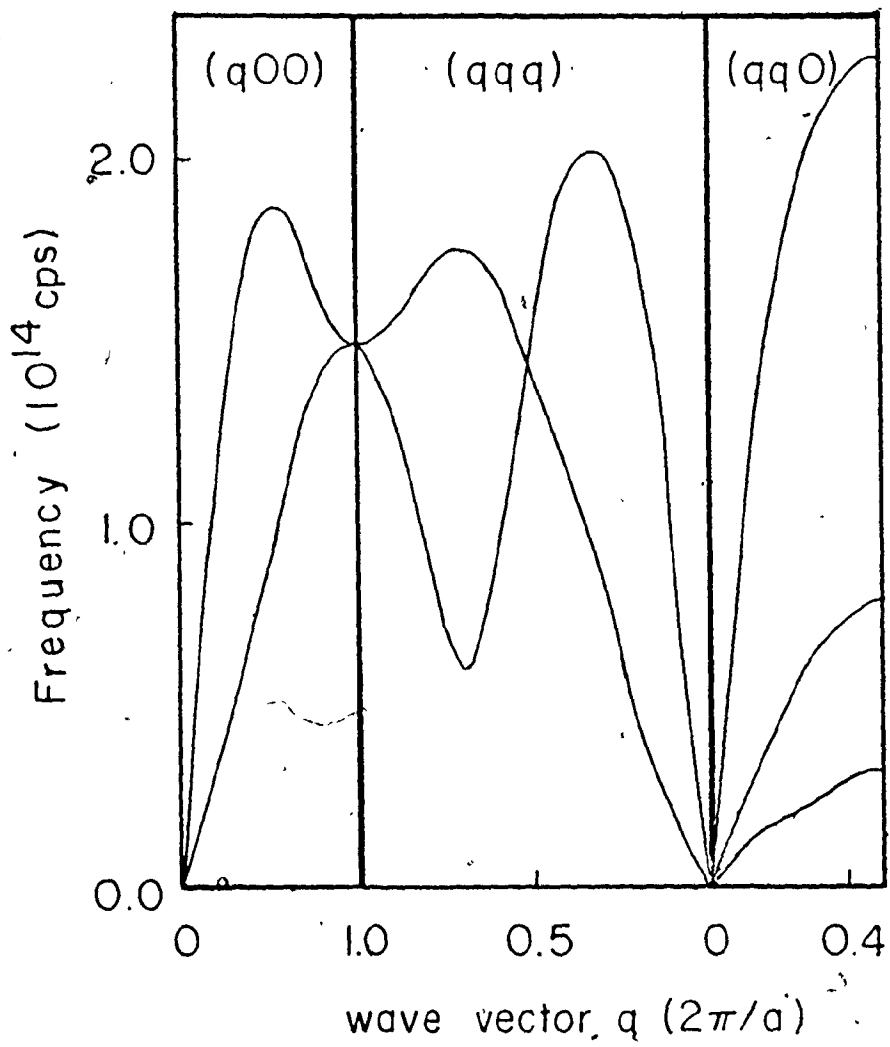
Phonon dispersion curves for fcc H,
 $r_s = 1.0$

Fig. 4.8



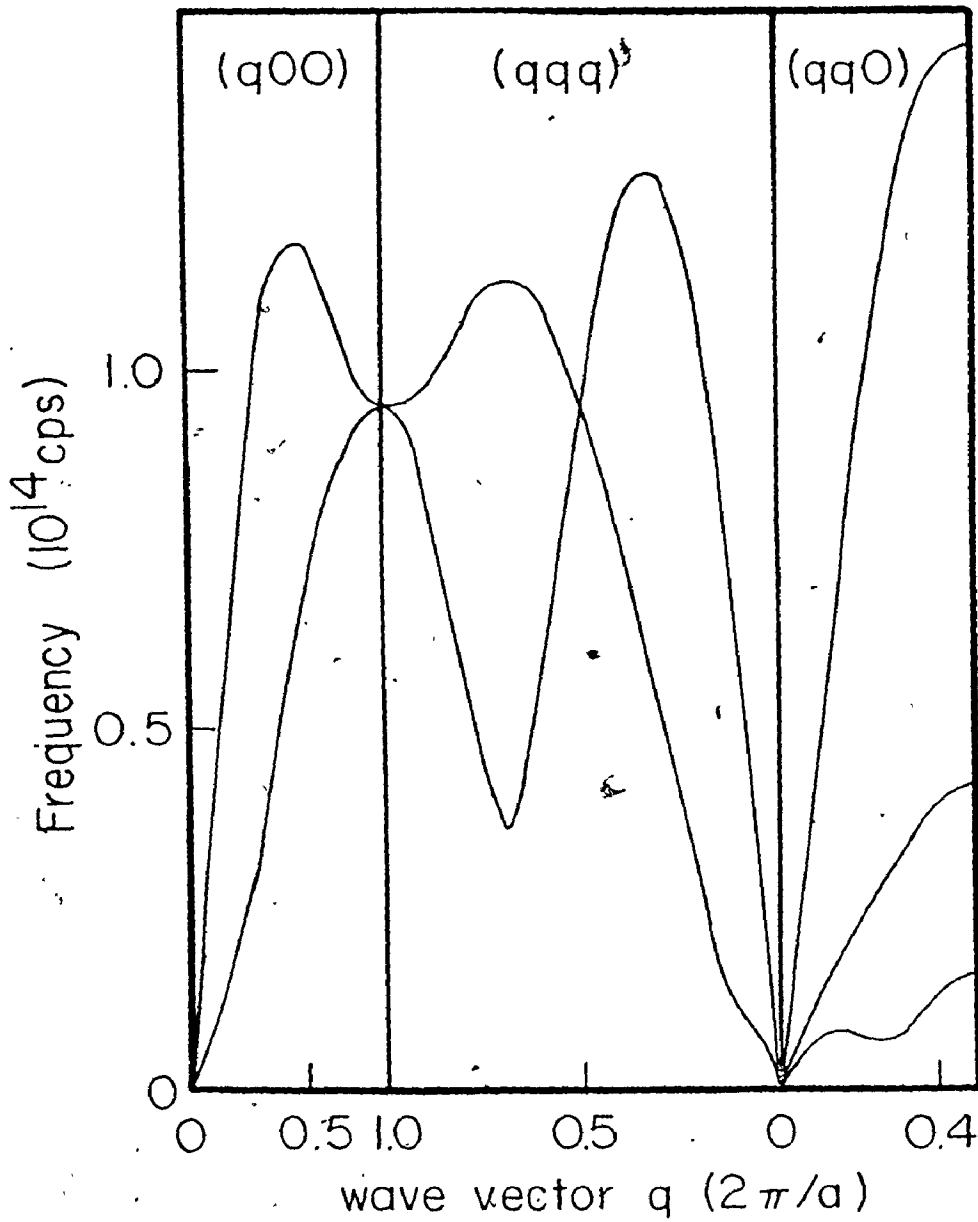
Phonon dispersion curves for bcc H,
 $r_s = 0.6$

Fig. 4.9



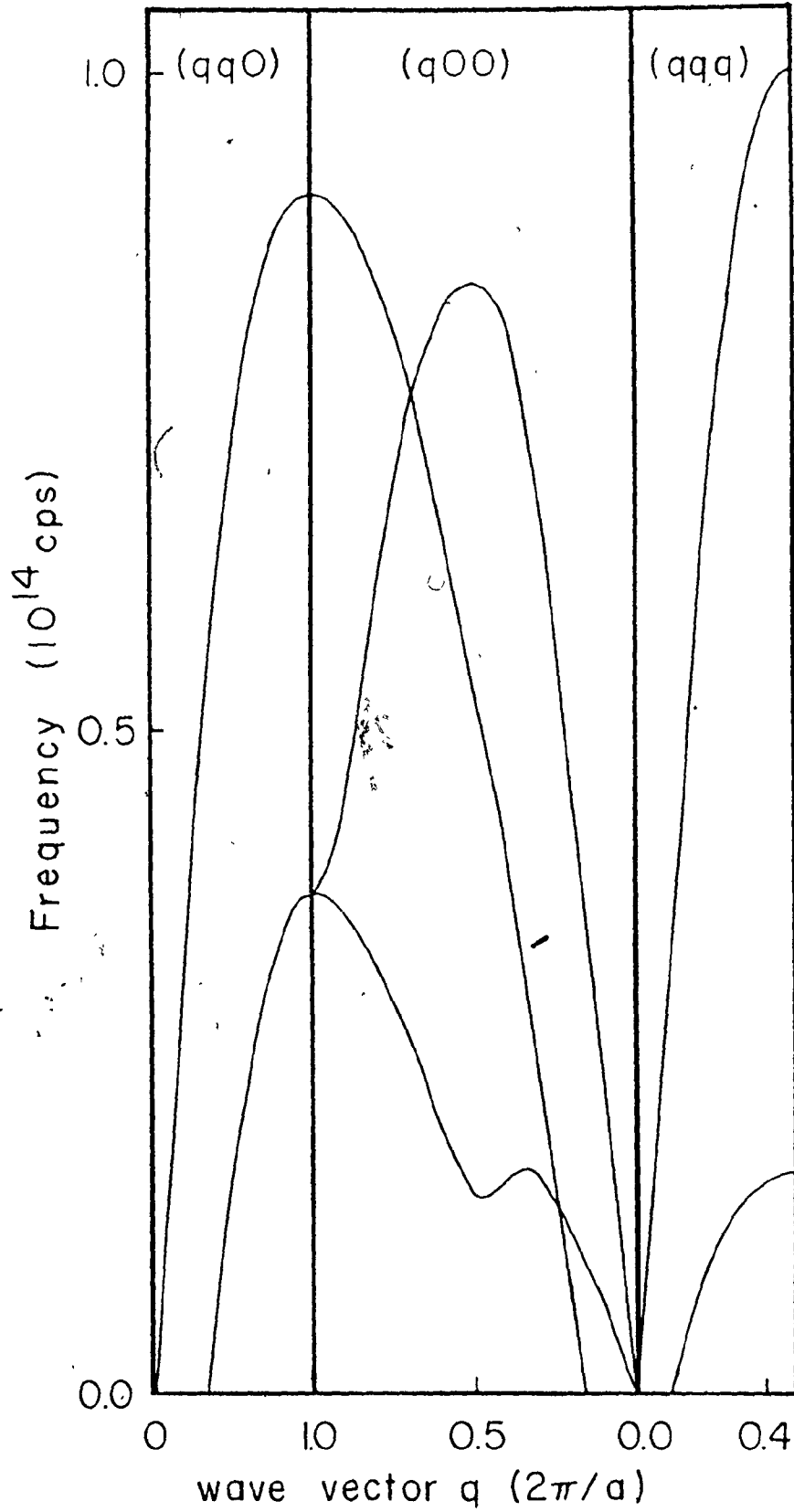
Phonon dispersion curves for bcc H,
 $r_s=0.8$

Fig. 4.10



Phonon dispersion curves for bcc H,
 $r_s = 1.0$

Fig. 4.11



Phonon dispersion curves for fcc H,
 $r_s = 1.2$

for separations of many lattice constants, so the detailed structure of these anomalies is probably not significant.

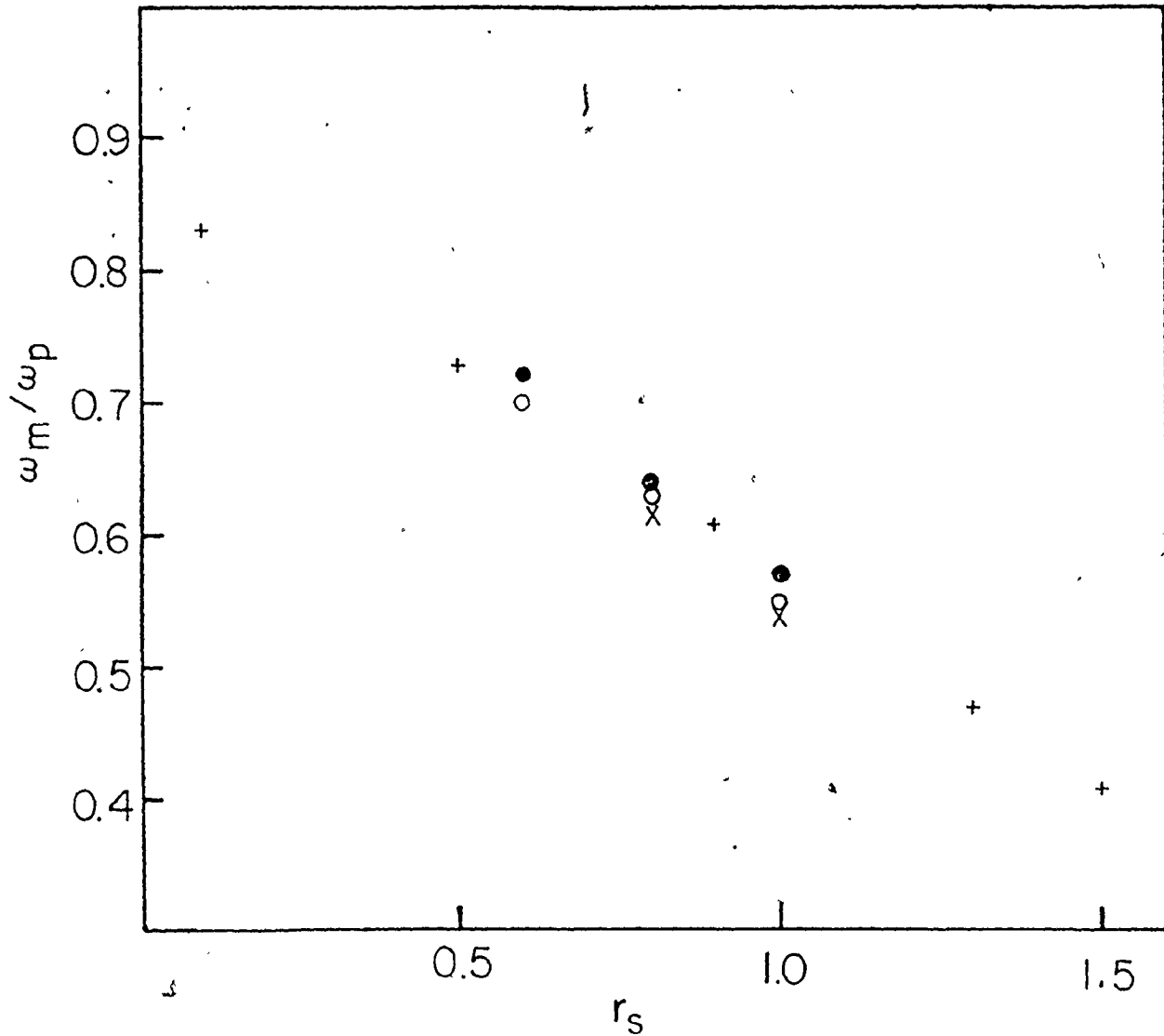
The number of shells we have used produces good convergence at all frequencies, except for partially smoothing out the small wiggles; in addition, going to 39 shells for $r_s = 1.2$ did not alter the occurrence of imaginary frequencies, so the conclusions regarding at what densities the structures are unstable should not be changed by including more neighbours. Hence it appears reasonable to use the number of neighbours reported here.

The most striking difference between these results and those of Caron is the density at which the fcc structure is predicted to be unstable. Our results are more in agreement with Beck and Strauss for fcc H, although not for bcc which they predict to be unstable for all $r_s \geq 0.6$.

Another comparison which can be made with previous work is the maximum phonon frequencies ω_m obtained. Since the calculations have been done at different densities, this comparison is facilitated by considering instead ω_m/ω_p , where ω_p is the plasma frequency of the bare protons. Figure 4.13 illustrates the similarity of the results.

4.5 TRANSITION TEMPERATURES AND FUNCTIONAL DERIVATIVES

Figures 4.14 to 4.19 are the functions $\alpha^2 F(\omega)$ for the three densities and two structures for which no instabilities were found. Table 4.2 displays the superconductivity data for



Maximum Phonon Frequencies as Fractions of the Plasma Frequency

Present Work fcc	●
Present Work bcc	○
Caron (1974)	+
Beck and Strass (1975)	x

Fig. 4.13

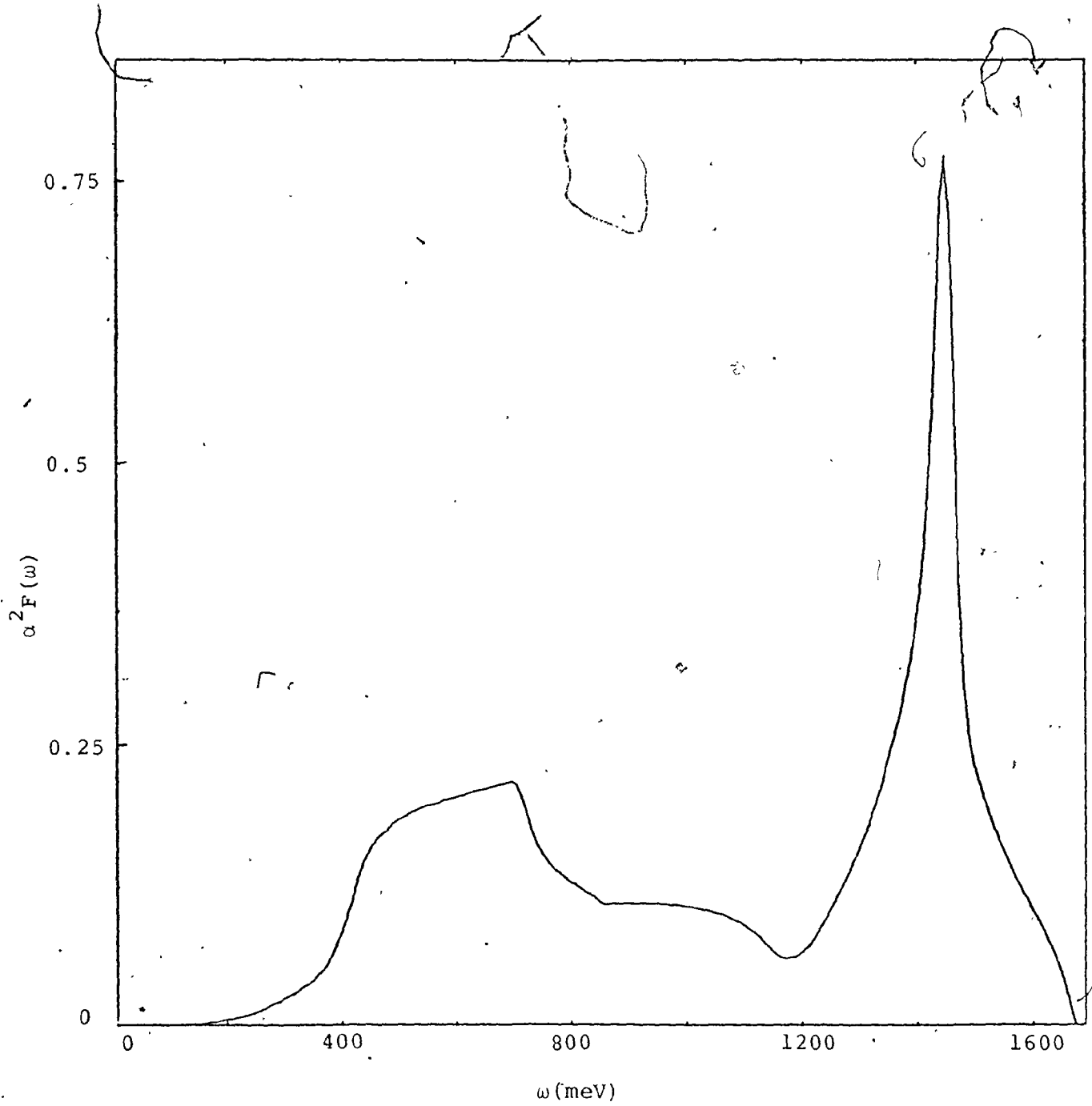


Fig. 4.14: $\alpha^2 F(\omega)$ for fcc H, $r_s = 0.6$

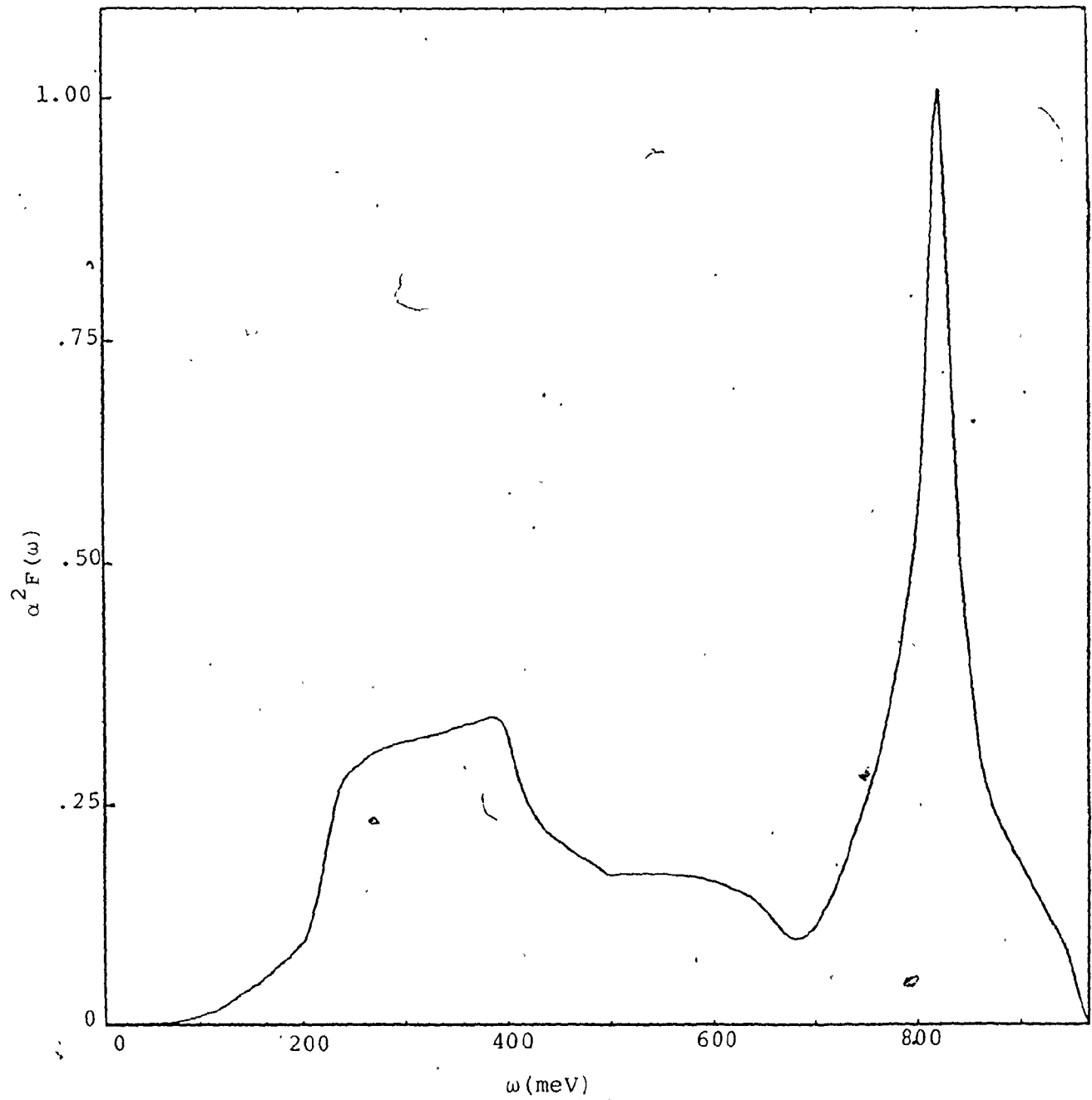


Fig. 4.15: $\alpha^2 F(\omega)$ for fcc H, $r_s = 0.8$

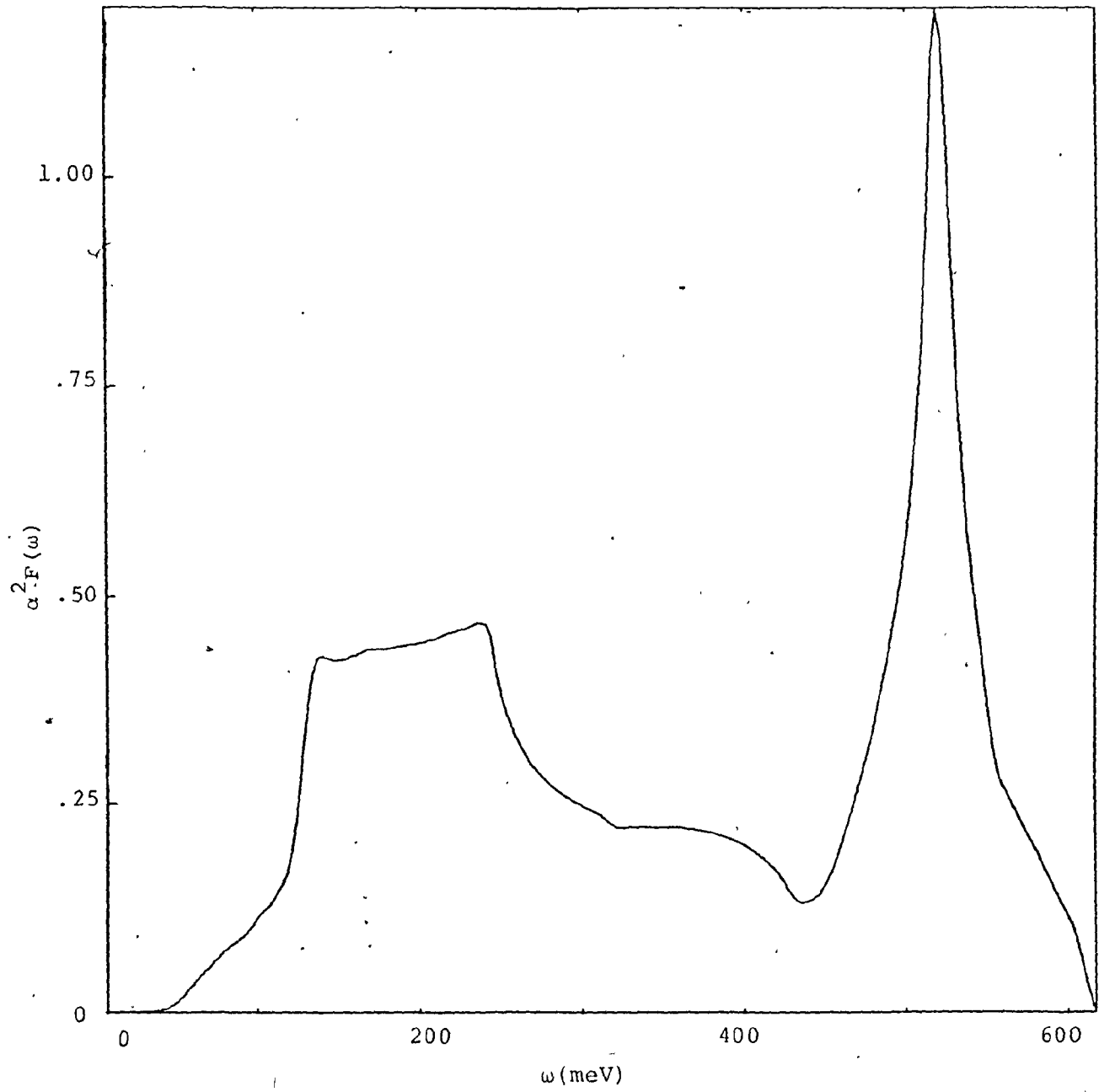


Fig. 4.16: $\alpha^2 F(\omega)$ for fcc H, $r_s = 1.0$.

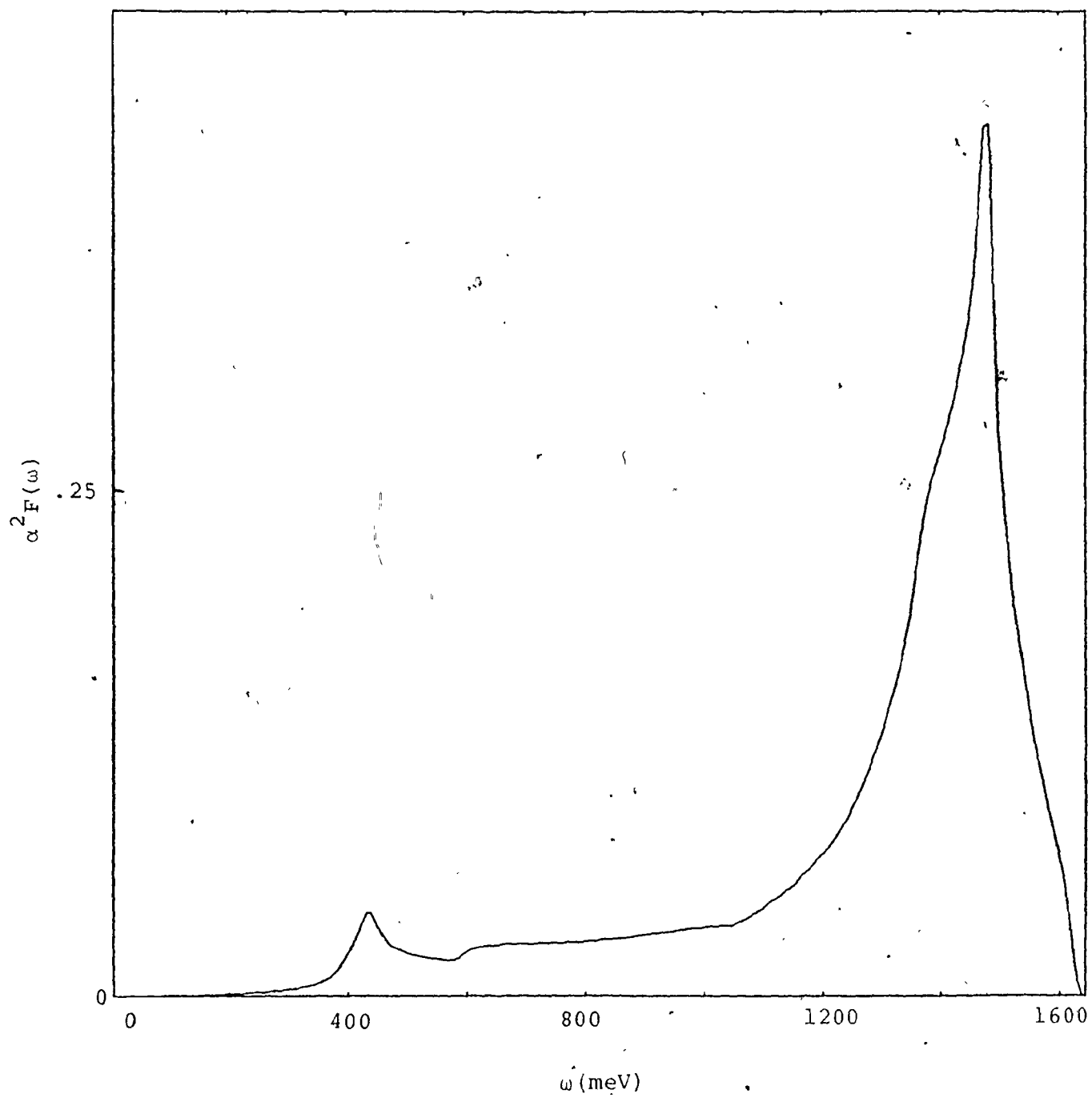


Fig. 4.1.7: $\alpha^2 F(\omega)$ bcc H, $r_s = 0.6$

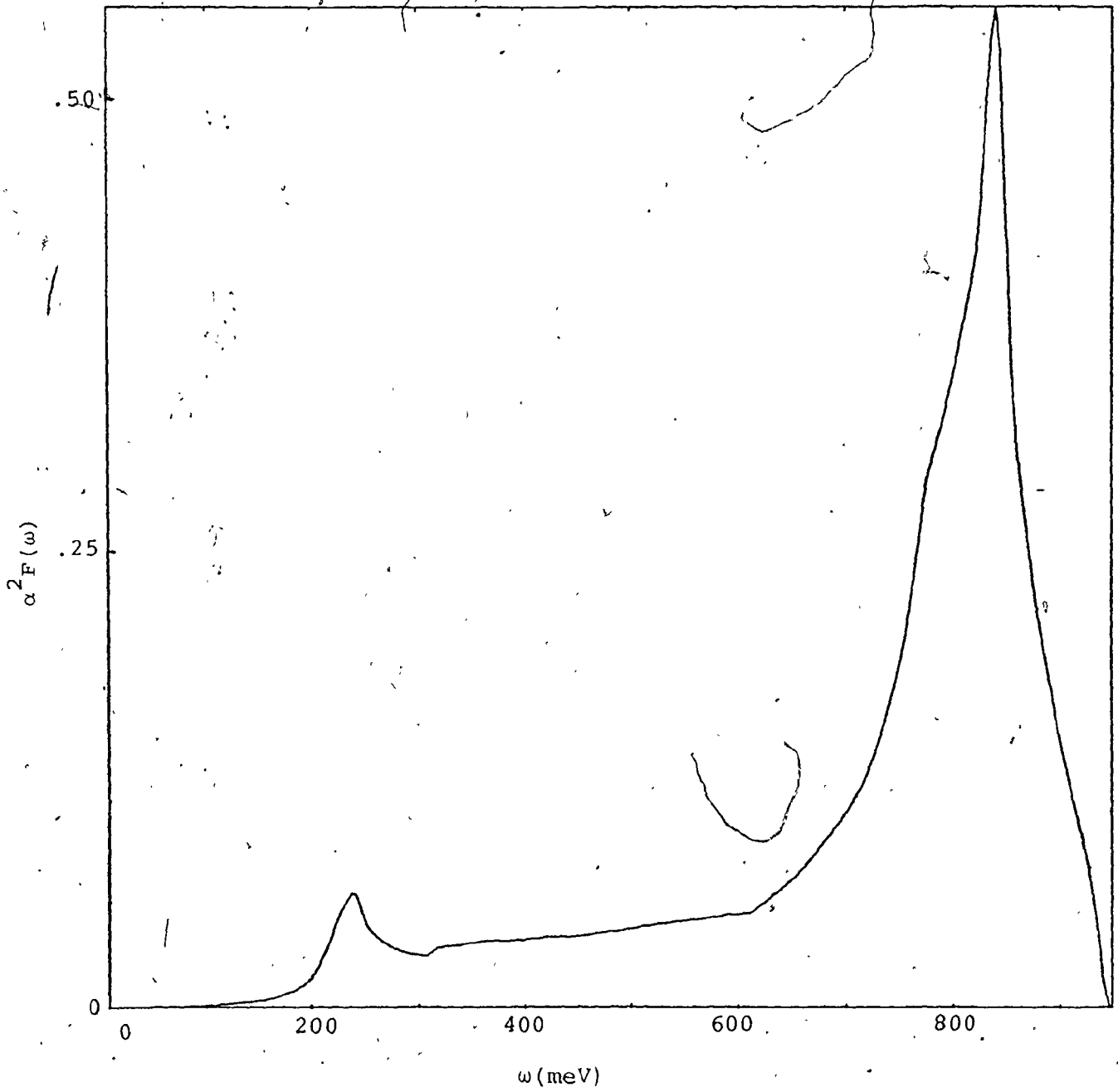


Fig. 4.18: $\alpha^2 F(\omega)$ for bcc H, $r_s = 0.8$

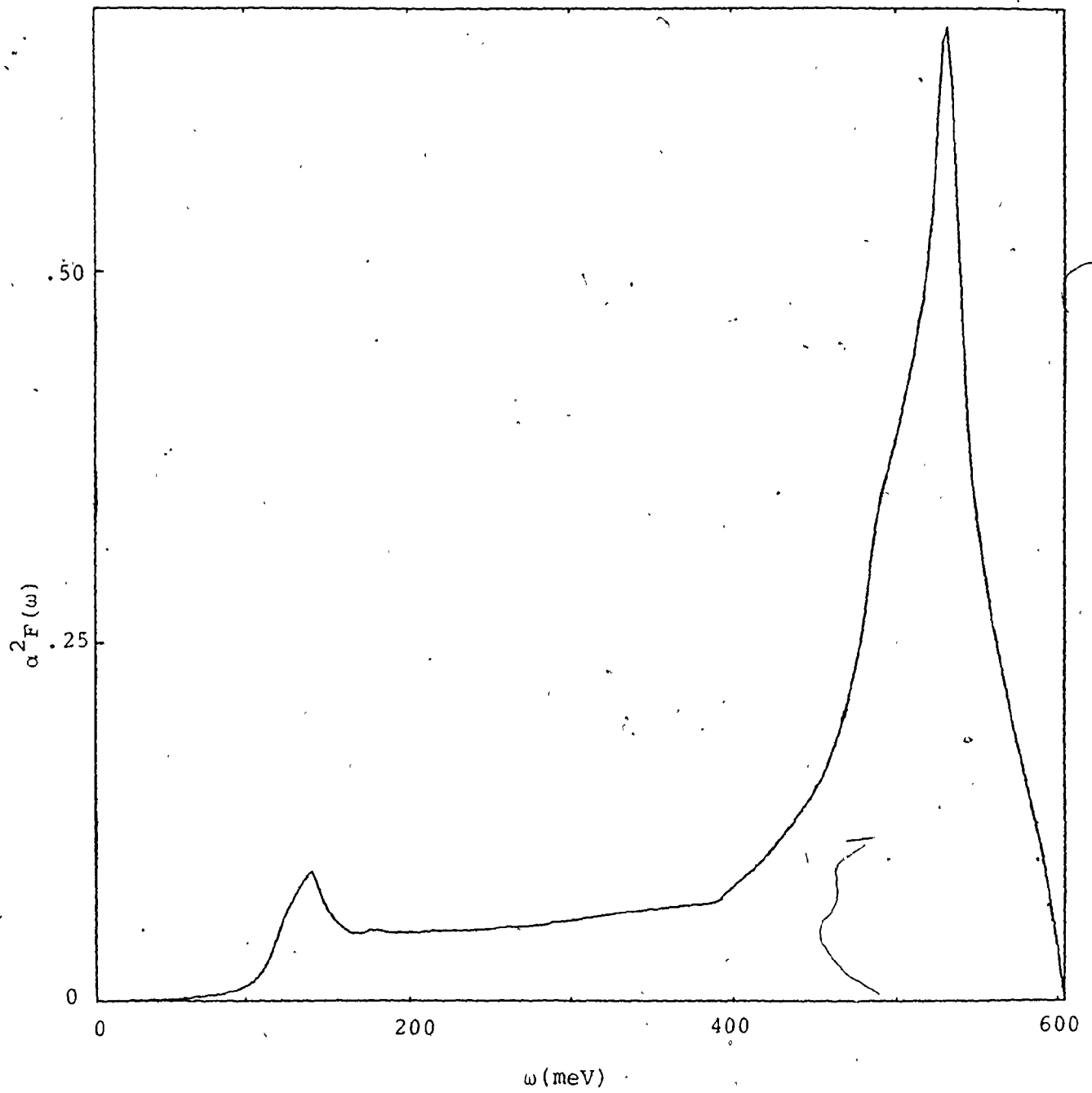


Fig. 4.19: $\alpha^2 F(\omega)$ for bcc H, $r_s = 1.0$

the fcc structure which we describe first.

The calculation of μ^* is subject to a large uncertainty and is usually obtained independently of the calculated electron-ion potential. We have calculated it using both the linear response and the non-linear response potentials; the two values agreed to within a few percent. Nonetheless we have determined T_c for the calculated μ^* as well as for μ^* 30% smaller and 30% larger. T_c is reported for each density first for the expected μ^* , and then, in brackets, for the other two values. The occurrence of high T_c is seen to be independent of the uncertainty in this parameter.

Also in that table are the mass enhancement factor λ , the area of $\alpha^2 F(\omega)$ A , average frequency $\langle \omega \rangle$, as well as $\frac{\partial T_c}{\partial \Omega}$ and $\frac{\partial T_c}{\partial \mu}$. T_c^L and T_c^M are the transition temperatures calculated using the approximate formulas described in section 4.2. McMillan's formula overestimates T_c by about 40%, whereas Leavens' gives a much better result, agreeing to within 10% of the T_c 's resulting from the solutions of the gap equations.

The functional derivatives $\delta T_c / \delta \alpha^2 F(\omega)$ are shown in fig. 4.20. The three curves all have the characteristic maxima at $\omega \approx 7 k_B T_c$. Some comments can now be made regarding the uncertainty in the Kohn anomalies at low frequency. For $r_s = 1.0$, which is our primary interest, the instabilities are expected to occur in the region $\omega \lesssim 40$ meV, which is $\omega \lesssim 1.3 k_B T_c$. From figs. 4.16 and 4.20 we see first that $\alpha^2 F(\omega)$ is small in this

Table 4.2

Superconductivity of fcc H. T_C was calculated using cutoff frequencies of at least ten times the maximum phonon frequency. T_C^L and T_C^M were obtained using the approximate formulas of McMillan (1968) and Leavens (1973)

r_s	.6	.8	1.0
$N(0)V_C$.130	.157	.182
λ	.5096	.8073	1.2631
A (meV)	222.2	189.8	172.3
$\langle\omega\rangle$ (meV)	1059	584.0	354.3
T_C ($^{\circ}$ K)	147 (182,114)	243 (281,214)	280 (306,260)
$\frac{\partial T_C}{\partial \rho}$.5334	.3907	.2831
$\frac{\partial T_C}{\partial \mu^*}$ (meV)	-115.5	-76.87	-41.11
T_C^L ($^{\circ}$ K)	162	268	310
T_C^M ($^{\circ}$ K)	204	339	390
T_C^L/T_C	1.10	1.10	1.11
T_C^M/T_C	1.39	1.40	1.39

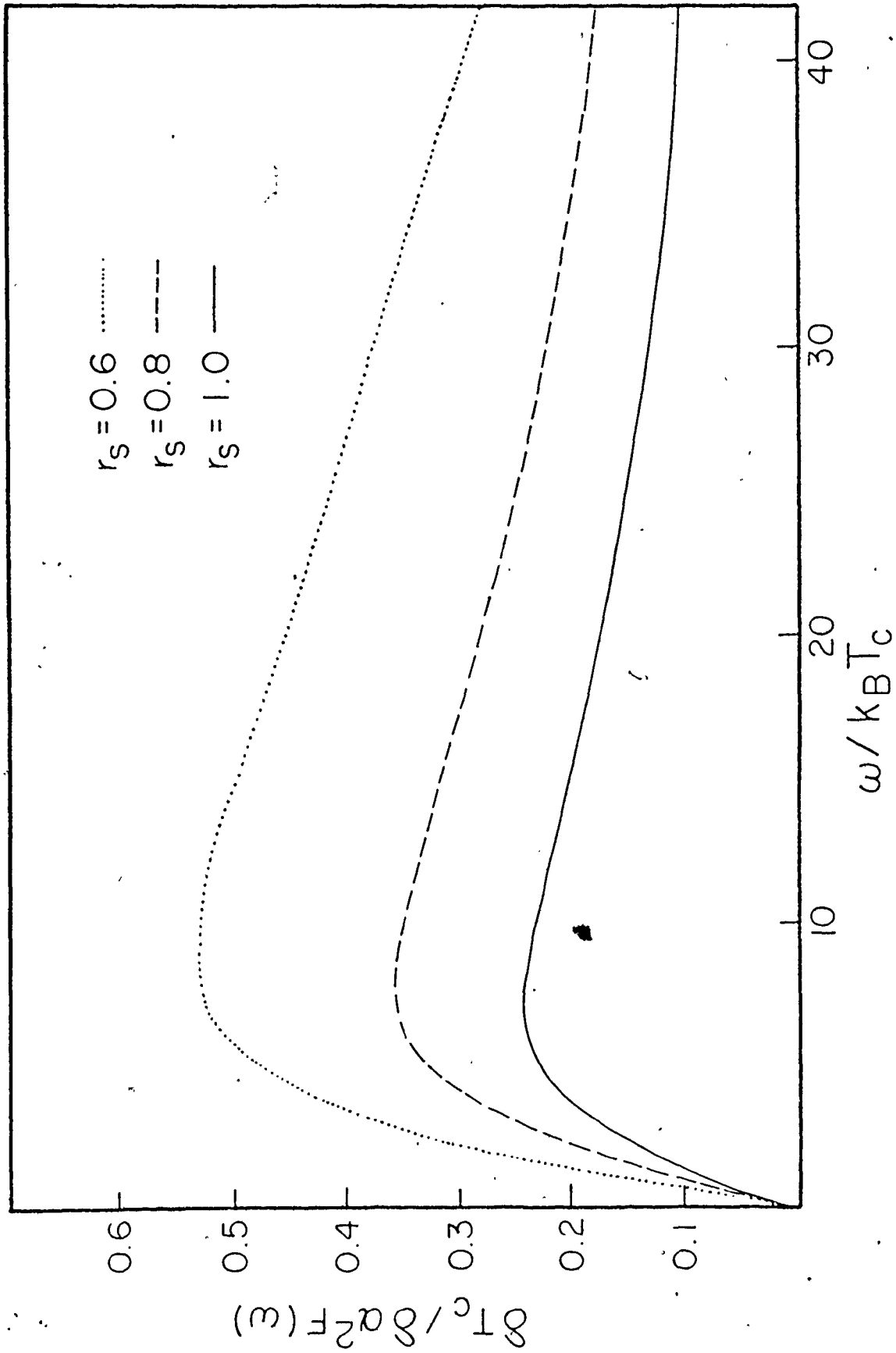


Fig. 4.20: $\delta T_c / \delta \alpha^2 F(\omega)$ for fcc H.

region, and second that these are not important frequencies for determining T_c , so small inaccuracies should not be important. For $r_s = .6$ and $.8$, the uncertainties occur in the regions $\omega \leq 100$ meV and $\omega \leq 50$ meV, where $\alpha^2 F(\omega)$ is so small that even large relative errors would make little difference to the function as a whole.

For the bcc structure, solutions to the gap equations were not obtained because of the low T_c . The number of Matsubara frequencies required in the sums is proportional to the highest phonon frequency divided by the temperature, and in this case too many were needed.

Therefore the approximate formulae were used, giving the much lower values of T_c listed in table 4.3. These formulae should be sufficiently accurate that at least the order of magnitude is correct, and are probably at least as accurate as for the fcc case. This is because for this structure λ is small, indicating a weak coupling superconductor to which McMillan's and Leavens' equations should both apply, and because the two formulae agree quite well with each other.

In conclusion we have found that using a non-linear procedure to calculate the potentials has resulted in a higher T_c for fcc hydrogen than that obtained by Caron, but that the transition temperature depends strongly on the structure assumed.

Table 4.3

Superconductivity of bcc H. Only T_C^M and T_C^L were obtained due to the low T_C

r_s	.6	.8	1.0
$N(0)V_C$.130	.157	.182
λ	.1840	.2584	.3546
A (meV)	106.2	82.62	68.72
$\langle \omega \rangle$ (meV)	1284	725.0	452.8
T_C^L ($^{\circ}K$)	.03	1.3	8.8
T_C^M ($^{\circ}K$)	.02	1.2	10

CHAPTER V

SUMMARY AND CONCLUSIONS

Non-linear, approximately self-consistent calculations of the electron distributions about hydrogen and helium in electron gases of various metallic densities have been performed. This constitutes an extension of model potential theory in that the response of the electrons is treated not just to second order with the atom represented by an approximate, weak perturbation.

For dilute hydrogen and helium in aluminum and magnesium, a theory of the heat of solution of single H atoms in simple metals has been generalized and applied to He. It was deduced that this impurity occupies the octahedral sites in a pure crystal for both materials, but that if there is a vacancy present, it will bind to it. Motivated by experiments of Bugeat et al (1976), pairs of both H and He impurities were then considered, both in the pure crystal and when a single vacancy is present. The impurity-impurity interaction was treated by using an expression based on the density functional formalism, in which the kinetic energy of the electrons was calculated using the gradient expansion, and the exchange by a local approximation. It was found that pairs of impurities occupy the same interstitial sites in the perfect solid as isolated ones, but the situation is different when a vacancy

is present. In particular, H in Al is expected to occupy tetrahedral sites bracketing the defect but relaxed towards it from the ideal interstitial sites. He pairs remain in relaxed octahedral sites, while for both impurities in Mg, the relaxed tetrahedral sites are favoured.

For metallic hydrogen the effect of using non-linear potentials was seen to be important even though the density of the electron gas is high. The potentials differ from what is obtained using linear response theory, especially at distances where the Friedel oscillations are dominant. This results in both the fcc and bcc structures being dynamically unstable, within the self-consistent harmonic approximation, for $r_s > 1.2$. This contrasts with linear theory which indicates the fcc structure to be stable up to $r_s \approx 1.5$.

The superconducting transition temperature T_c was found to be highest for the fcc structure at $r_s = 1.0$, for which it is about 280°K, declining to about 150° for $r_s = 0.6$. These are higher temperatures than those obtained in linear theory. Although the exact value of T_c depends on the Coulomb parameter μ^* , its being high does not. It does however depend on the structure assumed, being less than 10°K for bcc H.

For the fcc case the approximate formula of McMillan and Leavens were used to estimate T_c , along with solutions of the Eliashberg gap equations. For all three densities it was found that McMillan's equation overestimated T_c by about 40%,

whereas Leavens' equation predicted T_c to be about 10% larger than that obtained by the full calculation. This discrepancy occurs even for the highest pressure considered, with $\lambda = .5$. For the bcc case only the approximate formulae were used due to the low value of T_c , and they were in reasonable agreement with each other.

The functional derivatives of T_c with respect to μ^* and $\alpha^2 F(\omega)$ were calculated for the fcc structure, and found to exhibit the same type of behaviour found for lower temperature superconductors.

APPENDIX I

INTERATOMIC POTENTIALS FROM THE DENSITY FUNCTIONAL FORMALISM

In section 3.5, a procedure for calculating interatomic potentials was described which is different from the approach usually taken in model potential theory (Shaw 1970b) as described in chapter II of this thesis. The purpose of this appendix is twofold; first the differences and similarities between the two methods are pointed out, and second, the applicability of the alternative procedure to the calculation of phonons in simple metals will be discussed.

AI.1 RELATIONSHIP BETWEEN INTERATOMIC POTENTIALS CALCULATED USING MODEL POTENTIALS AND USING THE DENSITY FUNCTIONAL FORMALISM

Our interest is in understanding physically the relationship between the two approaches. For this reason, we shall neglect in this discussion complicating exchange and correlation effects, and consider the bare electron-ion potential $w^{\circ}(\underline{r})$ to be local. Following the procedure of chapter II, if we consider the unperturbed state of the metal to be a collection of ions in a uniform electron gas of density n_0 , then through second order perturbation theory we derive for the effective interatomic potential for ions of valence Z' separated by a distance R (see section 2.7)

$$V(R) = \frac{Z'^2}{R} + \int \Delta n(\underline{r}) w^{\circ}(\underline{r}-\underline{R}) d^3 \underline{r} \quad (\text{A.1})$$

where $\Delta n(\underline{r})$ is the screening charge density about an ion, and $w^{\circ}(\underline{r})$ is the bare potential of a single ion. Equation (A.1) has the physical interpretation of one bare ion interacting via the Coulomb potential with one screened ion a distance R away.

The expression used in section 3.5 for the interatomic potential can be written (again neglecting exchange and correlation)

$$V(R) = T[\rho(\underline{r})] - Z'e\phi_c(R) + \int \Delta(\underline{r})\phi_c(\underline{r}-\underline{R})d^3\underline{r} - T_0 \quad (\text{A.2})$$

where $T[\rho(\underline{r})]$ is the kinetic energy of the system of electrons with distribution given by

$$\rho(\underline{r}) = \Delta n(\underline{r}) + \Delta n(\underline{r}-\underline{R}) + n_0 \quad (\text{A.3})$$

where $\Delta n(\underline{r})$ is the same as in (A.1) except it is not now calculated only in perturbation theory, and $\phi_c(\underline{r})$ is the Coulomb potential of the screened ion. T_0 is included to make $V(R)$ finite and vanish as $R \rightarrow \infty$.

Equation (A.2) has the physical interpretation of changes in the kinetic energy with changes in R , plus the Coulomb interaction of two fully screened ions. Hence this expression differs from (A.1) by the inclusion of changes in kinetic energy, plus the interaction of one screened ion with the screening cloud associated with the other ion.

Since (A.1) follows from a calculation of the total energy of the crystal (see section (2.5), to understand the difference between these expressions, it is sufficient to consider the corresponding equations for the energy.

When calculated in second order perturbation theory, the total energy of the conduction electrons in the metal can be written

$$E = E_{fe} + \int n_0 W(\underline{r}) d^3 \underline{r} + \frac{1}{2} \int \Delta N(\underline{r}) W^{\circ}(\underline{r}) d^3 \underline{r} \quad (\text{A.4})$$

which is the kinetic energy of the uniform electron gas plus the interaction of this uniform distribution with the potential of all the screened ions $W(\underline{r})$, plus one-half the interaction energy of all the screening charge density $\Delta N(\underline{r})$ with all the bare ions $W^{\circ}(\underline{r})$.

In contrast to this, from a non-perturbation point of view the energy for this system is given by

$$E = T + \int n_0 W(\underline{r}) d^3 \underline{r} + \int \Delta N(\underline{r}) W^{\circ}(\underline{r}) d^3 \underline{r} + \frac{1}{2} \int \Delta N(\underline{r}) W'(\underline{r}) d^3 \underline{r} \quad (\text{A.5})$$

which is the kinetic energy of the non-uniform electron gas plus the interaction of the uniform distribution with the screened ions plus the interaction of $\Delta N(\underline{r})$ with the bare ions, plus the interaction of the charge density with itself, through its potential $W'(\underline{r})$. The difference between the two expressions can then be written

$$T - E_{fe} + \frac{1}{2} \int \Delta N(\underline{r}) W^{\circ}(\underline{r}) d^3 \underline{r} + \frac{1}{2} \int \Delta N(\underline{r}) W'(\underline{r}) d^3 \underline{r} \quad (\text{A.6})$$

If this difference were to vanish, then the two approaches would be the same. This in fact does occur if all calculations are done in second order perturbation theory. Although the algebra to show this is somewhat tedious, the basic ideas are simple. Consider first a general quantum system governed by Hamiltonian $H = T+V$, where T is the unperturbed Hamiltonian having normalized eigenstates $|\phi_{\underline{k}}^{\circ}\rangle$. Two exact expressions for

the energies $E_{\underline{k}}$ of the corresponding perturbed eigenstates $|\psi_{\underline{k}}\rangle$ of H are (Park 1974)

$$E_{\underline{k}} = \langle \phi_{\underline{k}}^{\circ} | T | \phi_{\underline{k}}^{\circ} \rangle + \frac{\langle \phi_{\underline{k}}^{\circ} | V | \psi_{\underline{k}} \rangle}{\langle \phi_{\underline{k}}^{\circ} | \psi_{\underline{k}} \rangle} \quad (\text{A.7})$$

and

$$E_{\underline{k}} = \langle \psi_{\underline{k}} | T+V | \psi_{\underline{k}} \rangle \quad (\text{A.8})$$

If each of (A.7) and (A.8) is expanded in a perturbation series for the energy, and the terms identified physically as was done for equations (A.1) and (A.5), then the vanishing of (A.6), at least up to second order, is established. This means that within second order perturbation theory, which is what is generally used in model potential theory, the change in the kinetic energy of the electrons is exactly cancelled by the sum of one-half of the interaction energy of the displaced electrons with the bare ions, plus the energy of the mutual interaction of all the displaced electrons.

AI.2 APPLICABILITY TO PHONON SPECTRA

In chapter II of this thesis, the model potential formalism for interionic potentials, which are appropriate for determining the lattice vibrations in simple metals, was presented, and in chapter IV calculations of the phonons in metallic hydrogen were reported. An alternative approach would be to make use of non-linear self-consistent calculations of the electron density $\Delta n(\underline{r})$, and calculate the interionic potentials through the density functional formalism, as in

section 3.5.

One anticipated advantage of (A.2) over (A.1), or (3.37) over (2.55) if exchange and correlation are included, is that it provides a means of going beyond second order perturbation theory, without losing the advantages of retaining two-body forces. In fact, if $\rho(\underline{r})$ and the energy functionals T and E_{xc} were known exactly, then for only two ions in an otherwise uniform electron gas, this procedure would provide an exact potential. With the $\rho(\underline{r})$ constructed from the non-linear densities $\Delta n(\underline{r})$ as described, and the energy functionals used here, this is expected to give accurate potentials, unless quantum mechanical effects which are not adequately treated by the expressions used for T and E_{xc} are important.

Another expected advantage follows from including the core electrons in the description of $\rho(\underline{r})$. This means that the small core approximation described in section 2.2 is avoided for calculating the interionic potential.

This procedure was carried through for aluminum. In collaboration with F. Magaña approximate non-linear calculations of the electron distributions, similar to those described in chapters III and IV, about an Al ion in its own electron gas were carried out. In fact, since the goal was the calculation of the phonon spectra and superconducting transition temperatures T_c for Al under pressure, the calculations were performed for six values of r_s corresponding to volume changes ranging from +2% to -9.5%.

The computer programme used to calculate the contribution of the kinetic and exchange energies was modified somewhat from the form described in section 3.5; the major changes were that for the two dimensional integrals over each rectangle a 96th order Gauss integral was performed in each direction, and special care was needed near the nuclei due to the divergence in the kinetic energy density (the integrand of T_3 , equation 3.44).

The integrals for T and E_{xc} were evaluated with an accuracy of about $\pm 5 \times 10^{-6}$ a.u.. The convergence of the gradient expansion (equations 3.41 to 3.44) was also checked. For separations corresponding to nearest neighbour distances, about $5 a_0$, the contribution of T_2 to $V(R)$ was about one-tenth that of T_1 , and the contribution of T_3 down by a further factor of ten. In the region of the eighth nearest neighbours, about $15 a_0$, the contributions of T_2 and T_3 were about equal, approximately twenty times smaller than that of T_1 . The contribution to $V(R)$ of E_{xc} was generally about three times smaller than that of T .

In view of the above comments and the possible advantages of this method, it was anticipated that the potentials calculated this way would generate phonons in at least reasonable agreement with experiment. For this calculation, the first and second derivatives of the interatomic potential at the neighbours are required, so the potential was evaluated at five points bracketing each neighbour distance. The values

of the contributions to $V(R)$ of the kinetic energy, exchange energy, and also the Coulomb term for each point are listed in table A.1. It is apparent that the kinetic energy contribution to $V(R)$ is a significant part.

The phonons generated were in fact not good. This is believed to be due to using the gradient expansion of T . The Friedel oscillations in $\Delta n(\underline{r})$ lead to corresponding oscillations in $V(R)$, and in particular in the contribution from the kinetic energy. However, these oscillations, which are quantum mechanical in origin are not well reproduced by using the gradient expansion for T . In fact, use of this expansion leads to oscillations in T which are out of phase with the true oscillations. When this is combined with the Coulomb term which has oscillations with the correct phase, the resulting potential is inaccurate. Since this will affect $V(R)$ for all values of R sufficiently large that the oscillations make a significant contribution to the potential or its first and second derivatives, the potential is not adequate for work on lattice vibrations.

The method in principle should work; the problem appears to be in the evaluation of $T[\rho(\underline{r})]$. With a kinetic energy functional which properly treats quantum effects, in particular the Friedel oscillations, it is expected that useful interionic potentials could be obtained using this method.

As a final point, we note that because the calculations

Table A.1

Contributions to the interatomic potential. The potential is evaluated at the five points which are integral multiples of .02 lattice constants nearest each neighbour distance

Neighbour ($\times \frac{a}{2}$)	T	E_{xc}	$T+E_{xc}$	Coulomb
(110)	.028246	-.009550	.018696	-.013207
	.026206	-.008357	.017849	-.013608
	.025131	-.007443	.017688	-.014725
	.024628	-.006739	.017889	-.016178
	.024373	-.006186	.018187	-.017655
(200)	.012296	-.002660	.009636	-.012497
	.010719	-.002378	.008341	-.010900
	.009202	-.002106	.007096	-.009347
	.007773	-.001843	.005930	-.007878
	.006469	-.001595	.004874	-.006531
(211)	.001234	-.000366	.000868	-.001104
	.000821	-.000253	.000568	-.000707
	.000440	-.000150	.000289	-.000356
	.000091	-.000060	.000031	-.000046
	-.000224	.000020	-.000204	.000227
(220)	-.001119	.000249	-.000870	.000982
	-.001138	.000263	-.000875	.000999
	-.001104	.000266	-.000839	.000973
	-.001026	.000261	-.000765	.000909
	-.000912	.000248	-.000664	.000813
(310)	-.000175	.000154	-.000021	.000186
	-.000068	.000138	.000070	.000093
	.000010	.000125	.000135	.000026
	.000055	.000116	.000171	-.000013
	.000068	.000110	.000178	-.000024
(222)	-.000045	.000115	.000070	.000083
	-.000116	.000125	.000009	.000146
	-.000184	.000126	-.000058	.000211
	-.000251	.000133	-.000118	.000272
	-.000307	.000138	-.000169	.000323

Neighbour ($\times \frac{a}{2}$)	T	E_{xc}	$T+E_{xc}$	Coulomb
(321)	-.000367	.000142	-.000225	.000374
	-.000345	.000138	-.000207	.000351
	-.000306	.000134	-.000172	.000311
	-.000252	.000124	-.000127	.000256
	-.000187	.000119	-.000068	.000191
(411)	.000015	.000095	.000110	-.000016
	.000069	.000087	.000156	-.000072
	.000108	.000083	.000191	-.000115
	.000132	.000079	.000211	-.000142
	.000138	.000077	.000215	-.000152

described in chapter III are for smaller separations, these difficulties should not affect them.

APPENDIX II

ATOMIC FORCE CONSTANTS FOR METALLIC HYDROGEN

FCC

RS = 0.50

T = 0

NEIGHBOUR			ϕ_{xx}	ϕ_{yy}	ϕ_{zz}
			ϕ_{yz}	ϕ_{xz}	ϕ_{xy}
1	1	0	.4952E+05 -.2812E-09	.4952E+05 -.2971E-09	.4931E+05 -.3975E+06
2	0	0	.3454E+06 .7613E-12	-.7231E+05 -.5877E-10	-.7233E+05 -.9886E-13
2	1	1	.6155E+05 .2168E+05	-.1364E+04 .4198E+05	-.1364E+04 .4198E+05
2	2	0	-.2427E+05 -.5879E-11	-.2427E+05 -.5599E-11	-.3255E+04 .3353E+05
3	1	0	-.3322E+05 -.2628E-11	-.2953E+03 -.4337E-11	-.3442E+04 .1122E+05
2	2	2	.3182E+04 .4365E+04	.3132E+04 .4366E+04	.3182E+04 .4366E+04
3	2	±	.1292E+04 .4314E+03	.2138E+03 .6471E+03	-.4332E+03 .1294E+04
4	0	0	-.2592E+04 -.6619E-15	-.4747E+03 -.2459E-12	-.4747E+03 -.3906E-11
3	3	0	-.1872E+04 -.2929E-12	-.1372E+04 -.2931E-12	-.2511E+03 .2123E+04
4	1	1	.3492E+04 .2340E+03	-.1734E+02 .9359E+03	-.1734E+02 .9359E+03
4	2	0	-.2142E+04 -.1654E-12	.4934E+03 -.2045E-12	-.5620E+02 .1099E+04
3	3	2	.4341E+02 .2113E+02	-.4341E+02 .2113E+02	.2594E+02 .3151E+02
4	2	2	-.9484E+03 -.2312E+03	-.2547E+03 -.4624E+03	-.2547E+03 -.4624E+03
4	3	1	-.5548E+03 -.1986E+03	-.4015E+03 -.1446E+03	-.1123E+03 -.4343E+03
5	1	0	-.9710E+03 .1475E-13	-.1114E+03 .3765E-13	-.7546E+02 -.1796E+03
5	2	1	.1196E+04 .9893E+02	.1432E+03 .2471E+03	-.3405E+01 .4942E+03
4	4	0	-.7378E+03 -.7457E-13	.7378E+03 -.6793E-13	.1193E+01 .7366E+03

4	3	3	.3224E+03 .1621E+03	.1963E+03 .2162E+03	.1963E+03 .2162E+03
5	3	0	.4339E+03 -.1504E-13	.1960E+03 -.2572E-13	.3405E+02 .2699E+03
4	4	2	-.1458E+03 -.9125E+02	-.1457E+03 -.9125E+02	-.3423E+01 -.1825E+03
5	0	0	-.3703E+03 .5955E-13	.3649E+02 .2406E-13	.3649E+02 .3083E-12
5	3	2	-.6382E+03 -.1571E+03	-.2193E+03 -.2618E+03	-.3844E+02 -.3927E+03
6	1	1	-.9223E+03 -.2637E+02	-.9832E+01 -.1564E+03	-.9832E+01 -.1564E+03
6	2	0	-.8375E+03 .1572E-13	-.1116E+03 .4077E-13	-.9657E+01 -.2759E+03
5	4	1	-.2439E+03 -.3485E+02	-.1555E+03 -.4356E+02	-.3485E+02 -.1742E+03
6	2	2	.2193E+03 .2733E+02	.6226E+00 .6226E+02	.6226E+00 .6226E+02
6	3	1	.5681E+03 .4729E+02	.1291E+03 .9577E+02	.1395E+01 .2873E+03
4	4	4	.2605E+03 .2582E+03	.2605E+03 .2582E+03	.2605E+03 .2582E+03
5	4	3	.2480E+03 .1117E+03	.1642E+03 .1395E+03	.3911E+02 .1861E+03
5	5	0	-.2482E+03 -.1116E-13	-.2482E+03 -.1759E-13	.1544E+02 .2328E+03

ATOMIC FORCE CONSTANTS FOR METALLIC HYDROGEN

FCC

RS = .85

T = 0

NEIGHBOUR			ϕ_{xx}	ϕ_{yy}	ϕ_{zz}
			ϕ_{yz}	ϕ_{xz}	ϕ_{xy}
1	1	0	.1728E+06 -.1104E-09	-.1728E+06 -.9666E-10	-.1233E+06 .2963E+06
2	0	0	.1220E+05 .1463E-12	-.1762E+05 -.2544E-10	-.1762E+05 -.2676E-10
2	1	1	.1220E+05 .4334E+04	-.7038E+03 .8667E+04	-.7033E+03 .3667E+04
2	2	0	.6636E+04 -.1334E-11	-.6636E+04 -.1474E-11	-.2121E+04 .8797E+04
3	1	0	.8266E+04 -.3591E-12	-.4410E+03 -.1037E-11	-.5366E+03 .2934E+04
2	2	2	.2789E+03 .3434E+03	.2789E+03 .3434E+03	.2789E+03 .3434E+03
3	2	1	-.9205E+03 -.1791E+03	-.4728E+03 -.2686E+03	-.2042E+03 -.5372E+03
4	0	0	.5037E+03 -.2942E-15	-.1431E+03 -.1006E-12	-.1431E+03 -.6800E-12
3	3	0	.9127E+03 -.9555E-13	-.9127E+03 -.1110E-12	-.5321E+02 .9709E+03
4	1	1	.1644E+04 .1964E+03	.4817E+02 .4255E+03	.4817E+02 .4255E+03
4	2	0	.9241E+03 -.4445E-13	.2531E+03 -.8286E-13	.2943E+02 .4473E+03
3	3	2	-.1165E+03 -.1087E+03	-.1165E+03 -.1087E+03	-.2611E+02 -.1631E+03
4	2	2	-.7288E+03 -.1845E+03	-.1752E+03 -.3691E+03	-.1752E+03 -.3691E+03
4	3	1	-.4530E+03 -.7935E+02	-.2679E+03 -.1058E+03	-.5623E+02 -.3174E+03
5	1	0	-.6881E+03 .8162E-14	-.5599E+02 .4537E-13	-.2964E+02 -.1317E+03
5	2	1	.6432E+03 .5305E+02	.8616E+02 .1326E+03	.6562E+01 .2653E+03
4	4	0	.3817E+03 -.3362E-13	.3817E+03 -.3306E-13	.6755E+01 .3749E+03

4	3	3	.1328E+03 .6220E+02	.5446E+02 .3294E+02	.8446E+02 .3294E+02
5	3	0	.1951E+03 -.8165E-14	.3448E+02 -.1555E-13	.2227E+02 .1037E+03
4	4	2	-.1231E+03 -.7186E+02	-.1230E+03 -.7186E+02	-.1524E+02 -.1437E+03
6	0	0	-.3113E+03 .8603E-13	.2864E+02 .9499E-14	.2064E+02 .3023E-12
5	3	2	-.3855E+03 -.9427E+02	-.1340E+03 -.1571E+03	-.5544E+02 -.2357E+03
6	1	1	-.5569E+03 -.1567E+02	-.3273E+01 -.9405E+02	-.3273E+01 -.9405E+02
6	2	0	-.4518E+03 .9129E-14	-.5672E+02 .2941E-13	-.7335E+01 -.1482E+03
5	4	1	-.1518E+03 -.1381E+02	-.7074E+02 -.1727E+02	-.1895E+02 -.5906E+02
6	2	2	.1715E+03 .2155E+02	.6276E+01 .6194E+02	.6275E+01 .6194E+02
6	3	1	.3352E+03 .2849E+02	.7887E+02 .5697E+02	.2907E+01 .1709E+03
4	4	4	.1409E+03 .1380E+03	.1409E+03 .1380E+03	.1409E+03 .1380E+03
5	4	3	.1139E+03 .5011E+02	.7630E+02 .6264E+02	.4708E+02 .3352E+02
5	5	0	-.1142E+03 -.1152E-13	-.1142E+03 -.8604E-14	.9520E+01 .1347E+03

ATOMIC FORCE CONSTANTS FOR METALLIC HYDROGEN

FCC

R0=1.00

T= 0

NEIGHBOUR			ϕ_{xx}	ϕ_{yy}	ϕ_{zz}
			ϕ_{yz}	ϕ_{xz}	ϕ_{xy}
1	1	0	.7296E+05 -.4175E-10	.7296E+05 -.4380E-10	-.4785E+05 .1207E+06
2	0	0	.3742E+05 .4757E-13	-.5227E+04 -.9197E-11	-.5227E+04 -.1045E-09
2	1	1	.2086E+04 .8951E+03	-.5995E+03 .1791E+04	-.5995E+03 .1791E+04
2	2	0	-.2686E+04 -.6591E-12	-.2686E+04 -.5244E-12	-.6804E+03 .3367E+04
3	1	0	.3281E+04 -.1755E-12	.3251E+03 -.5682E-12	-.4356E+02 .1107E+04
2	2	2	-.1649E+03 -.2414E+03	-.1649E+03 -.2414E+03	-.1649E+03 -.2414E+03
3	2	1	-.8714E+03 -.1875E+03	-.4019E+03 -.2814E+03	-.1204E+03 -.5630E+03
4	0	0	.2291E+03 -.4539E-15	-.6373E+02 -.8622E-13	-.6373E+02 -.4245E-12
3	3	0	-.5590E+03 -.7462E-13	.5590E+03 -.7460E-13	-.1461E+02 .5737E+03
4	1	1	.9876E+03 .6264E+02	.4798E+02 .2506E+03	.4798E+02 .2506E+03
4	2	0	.4762E+03 -.2039E-13	-.1447E+03 -.4533E-13	.3439E+02 .2208E+03
3	3	2	-.1273E+03 -.1096E+03	-.1273E+03 -.1096E+03	-.3606E+02 -.1643E+03
4	2	2	-.5057E+03 -.1286E+03	-.1199E+03 .2572E+03	-.1199E+03 -.2572E+03
4	3	1	-.2792E+03 -.4906E+02	-.1645E+03 -.6543E+02	-.3358E+02 -.1964E+03
5	1	0	-.4259E+03 .4643E-14	-.3354E+02 .3009E-13	-.1719E+02 -.8173E+02
5	2	1	.4221E+03 .3449E+02	.6103E+02 .6621E+02	.9300E+01 .1724E+03
4	4	0	.2301E+03 -.2697E-13	.2301E+03 -.1330E-13	.7706E+01 .2224E+03

4	3	3	.6079E+02 .2493E+02	.4594E+02 .3327E+02	.4094E+02 .3327E+02
5	3	0	.8546E+02 -4.526E-14	.4105E+02 -.289E-14	.1614E+02 .4156E+02
4	4	2	-.9716E+02 -.5538E+02	-.9716E+02 -.5538E+02	-.1414E+02 -.1107E+03
6	0	0	-.2367E+03 .4630E-16	.1366E+02 .2108E-13	.1366E+02 .1976E-12
5	3	2	-.2535E+03 -.6188E+02	-.8648E+02 -.1031E+03	-.3691E+02 -.1547E+03
5	1	1	-.3678E+03 -.1034E+02	-.5997E+01 -.6202E+02	-.5997E+01 -.6202E+02
6	2	0	-.2711E+03 .818E-14	-.3452E+02 .1434E-13	-.4960E+01 -.8970E+02
5	4	1	-.4387E+02 -.5493E+01	-.3145E+02 -.6877E+01	-.1083E+02 -.2754E+02
6	2	2	.1336E+03 .1574E+02	.7775E+01 .4719E+02	.7775E+01 .4719E+02
6	3	1	.2209E+03 .1662E+02	.5328E+02 .3725E+02	.3623E+01 .1117E+03
4	4	4	.8526E+02 .8195E+02	.8526E+02 .8195E+02	.8526E+02 .8195E+02
5	4	3	.5774E+02 .2434E+02	.3947E+02 .3443E+02	.2524E+02 .4059E+02
5	5	0	.5740E+02 -.5159E-14	.5740E+02 -.2207E-14	.7077E+01 .5032E+02

ATOMIC FORCE CONSTANTS FOR METALLIC HYDROGEN

BCC

RS = .60

T = 0

NEIGHBOUR			ϕ_{xx}	ϕ_{yy}	ϕ_{zz}
			ϕ_{yz}	ϕ_{xz}	ϕ_{xy}
1	1	1	.2593E+06 .6578E+06	.2593E+06 .6578E+06	.2593E+06 .6578E+06
2	0	0	-.9342E+06 -.1128E-11	-.2447E+06 -.3337E-19	-.2447E+06 -.3642E-08
2	2	0	.6952E+05 -.3013E-11	.6950E+05 -.2921E-10	-.3670E+05 .1362E+06
3	1	1	.5791E+05 .6030E+04	-.6749E+04 .2425E+05	-.6749E+04 .2425E+05
2	2	2	.1356E+05 .2477E+05	.1356E+05 .2477E+05	.1356E+05 .2477E+05
4	0	0	.3293E+05 .3339E-13	-.3310E+04 -.4312E-11	-.3310E+04 -.5181E-10
3	3	1	.5157E+04 .2119E+04	.5157E+04 .2119E+04	-.5029E+03 .6366E+04
4	2	0	-.6013E+04 -.4741E-12	.7998E+03 -.7696E-12	-.9359E+03 .3471E+04
4	2	2	.1597E+04 .4121E+03	-.1592E+03 .8242E+03	-.1302E+03 .8242E+03
3	3	3	.9399E+03 .1308E+04	.9399E+03 .1308E+04	.9399E+03 .1308E+04
5	1	1	.3232E+04 .1439E+03	-.2232E+03 .7176E+03	-.2232E+03 .7176E+03
4	4	0	-.1221E+04 -.1597E-12	-.1221E+04 -.1603E-12	-.4631E+02 .1266E+04
5	3	1	.3604E+02 .3355E+01	.2136E+02 .5551E+01	.1129E+02 .1684E+02
4	4	2	-.2684E+03 -.1376E+03	-.2684E+03 -.1376E+03	-.5248E+02 -.2749E+03
6	0	0	-.5952E+03 -.1655E-19	.5568E+01 .7666E-13	.5568E+01 .4194E-12
6	2	0	-.1286E+04 .2351E-13	-.1852E+03 .6331E-13	-.5736E+02 -.3835E+03
5	3	3	-.2024E+03 -.4104E+02	-.1289E+03 -.6426E+02	-.1289E+03 -.6426E+02

6	2	2	•1250E+03 •2341E+02	•5235E+02 •7033E+02	•6295E+02 •7033E+02
4	4	4	•4711E+03 •5145E+03	•4711E+03 •5145E+03	•4711E+03 •5145E+03
5	5	1	•6992E+03 •1391E+03	•6992E+03 •1391E+03	•3160E+02 •6992E+03
7	1	1	•1359E+04 •2756E+02	•3125E+02 •1936E+03	•3125E+02 •1936E+03
6	4	0	•3442E+03 •5513E-13	•3844E+03 •6068E-13	•1643E+02 •5519E+03
6	4	2	•1259E+01 •8833E+01	•2588E+02 •1327E+02	•3403E+02 •2647E+02
5	5	3	•3208E+03 •2503E+03	•3208E+03 •2503E+03	•9875E+02 •3477E+03
7	3	1	•6496E+03 •4144E+02	•9783E+02 •9638E+02	•1231E+02 •2391E+03
8	0	0	•8554E+03 •5930E-17	•1293E+02 •5098E-13	•1293E+02 •6436E-12
7	3	3	•2399E+03 •3923E+02	•6574E+02 •9149E+02	•6574E+02 •9149E+02
6	4	4	•6880E+02 •1018E+02	•4619E+02 •2723E+02	•4619E+02 •2723E+02
8	2	0	•1009E+03 •1480E-14	•3239E+02 •8323E-14	•2782E+02 •1827E+02
6	6	0	•2948E+03 •1865E-13	•2948E+03 •2576E-13	•1923E+02 •3140E+03
8	2	2	•5357E+03 •3467E+02	•1551E+02 •1387E+03	•1551E+02 •1387E+03
5	5	5	•2637E+03 •2677E+03	•2637E+03 •2677E+03	•2637E+03 •2677E+03
7	5	1	•5159E+03 •5306E+02	•2612E+03 •7428E+02	•6561E+01 •3714E+03
6	6	2	•3690E+03 •1223E+03	•3661E+03 •1223E+03	•4194E+02 •3663E+03
8	4	0	•3151E+03 •5483E-14	•9133E+02 •2240E-13	•1674E+02 •1492E+03

ATOMIC FORCE CONSTANTS FOR METALLIC HYDROGEN

BCC

A = RS = 0.0

T = 0

NEIGHBOUR			ϕ_{xx}	ϕ_{yy}	ϕ_{zz}
			ϕ_{yz}	ϕ_{xz}	ϕ_{xy}
1	1	1	.7889E+05 .2172E+06	.7889E+05 .2172E+06	.7889E+05 .2172E+06
2	0	0	-.8129E+05 -.3833E+02	-.7199E+05 -.7435E+01	-.7199E+05 -.1153E+08
2	2	0	-.1639E+05 -.5586E+01	-.1689E+05 -.6169E+01	-.5201E+04 .2511E+05
3	1	1	.1267E+05 .1705E+04	-.1659E+04 .5382E+04	-.1659E+04 .5382E+04
2	2	2	.3456E+04 .5183E+04	.3466E+04 .5183E+04	.3466E+04 .6088E+04
4	0	0	.8836E+04 .3952E+05	-.5071E+03 -.1083E+01	-.5071E+03 -.1337E+01
3	3	1	.4839E+03 .1837E+03	.4839E+03 .1837E+03	-.8841E+01 .5537E+03
4	2	0	-.2870E+03 .2358E+03	-.1185E+03 .1929E+03	.6264E+02 -.1119E+03
4	2	2	-.3637E+03 -.5484E+02	-.2513E+03 -.1092E+03	-.2513E+03 -.1092E+03
3	3	3	.4157E+03 .5249E+03	.4157E+03 .5249E+03	.4157E+03 .5249E+03
5	1	1	.1296E+04 .5609E+02	-.5106E+02 .2805E+03	-.5106E+02 .2805E+03
4	4	0	-.5268E+03 -.8721E+03	-.5268E+03 -.8243E+03	.3282E+02 .4946E+03
5	3	1	-.2496E+03 -.3531E+02	-.6125E+02 -.5388E+02	.3281E+02 -.1769E+03
4	4	2	-.3003E+03 -.1886E+03	-.3003E+03 -.1886E+03	-.4781E+02 -.3369E+03
6	0	0	-.7199E+03 -.2733E+05	.3617E+02 .2129E+03	.3617E+02 .8103E+02
6	2	0	-.3557E+03 .2275E+03	-.1093E+03 .7956E+03	-.1624E+02 -.2305E+03
5	3	3	-.1544E+03 -.4193E+02	-.8034E+02 -.6975E+02	-.5134E+02 -.6975E+02

6	2	2	.2632E+02 .7395E+01	- .3136E+02 .2227E+02	- .1125E+02 .2227E+02
4	4	4	.2582E+03 .2749E+03	.2582E+03 .2749E+03	.2582E+03 .2749E+03
5	5	1	.3558E+03 .5671E+02	.3558E+03 .6975E+02	.2488E+02 .3489E+03
7	1	1	.6858E+03 .1346E+02	.2165E+02 .9701E+02	.2165E+02 .9701E+02
6	4	0	.4119E+03 -.1952E-13	-.1959E+03 -.2417E-13	.1411E+02 .2692E+03
6	4	2	-.5514E+02 -.1958E+02	-.1637E+02 -.2925E+02	-.1202E+02 -.9344E+02
5	5	3	-.2670E+03 -.1323E+03	-.2874E+03 -.1323E+03	-.6589E+02 -.2225E+03
7	3	1	-.4145E+03 -.2621E+02	-.6519E+02 -.6114E+02	-.4709E+01 -.1635E+03
8	0	0	-.4493E+03 -.6507E-16	-.5946E+01 .3803E-13	-.5346E+01 .3703E-12
7	3	3	-.9352E+02 -.1302E+02	-.2924E+02 -.3221E+02	-.2924E+02 -.3221E+02
6	4	4	-.5385E+01 .4593E+01	-.1123E+02 .6924E+01	-.1123E+02 .6924E+01
6	2	0	.1933E+01 .1616E-14	-.1460E+02 .5439E-14	-.1574E+02 .4421E+01
5	6	0	.1342E+03 -.1310E-13	-.1842E+03 -.1584E-13	-.9391E+01 .1936E+03
8	2	2	.3322E+03 .2134E+02	.1200E+02 .8538E+02	.1200E+02 .8538E+02
5	5	5	.1481E+03 .1486E+03	.1481E+03 .1486E+03	.1481E+03 .1486E+03
7	5	1	.2869E+03 .2934E+02	.1461E+03 .4116E+02	.5292E+01 .2053E+03
6	6	2	.1988E+03 .6551E+02	.1936E+03 .6551E+02	.2412E+02 .1966E+03
6	4	0	.1333E+03 -.1719E-14	-.4071E+02 -.2237E-14	.9956E+01 .6151E+02

ATOMIC FORCE CONSTANTS FOR METALLIC HYDROGEN

ECC

RS=1.10

T= 0

NEIGHBOR			ϕ_{xx}	ϕ_{yy}	ϕ_{zz}
			ϕ_{yz}	ϕ_{xz}	ϕ_{xy}
1	1	1	.3452E+05 .6603E+05	.3452E+05 .6603E+05	.3452E+05 .6603E+05
2	0	0	-.1336E+05 -.3372E-13	-.2696E+05 -.1566E-11	-.2696E+05 -.5103E-09
2	2	0	.4407E+04 -.1537E+11	.4407E+04 -.1590E-11	-.2231E+04 .6639E+04
3	1	1	.3415E+04 .5024E+03	-.6134E+03 .1509E+04	-.6134E+03 .1509E+04
2	2	2	.1273E+04 .2135E+04	.1273E+04 .2135E+04	.1273E+04 .2135E+04
4	0	0	.3407E+04 -.7972E-15	-.3807E+02 -.3781E-12	-.3807E+02 -.6641E-11
3	3	1	-.2296E+03 -.1013E+03	-.2296E+03 -.1113E+03	.4324E+02 -.3323E+03
4	2	0	-.9345E+03 .4183E-13	-.1078E+03 .1275E-12	-.4761E+02 -.4915E+03
4	2	2	-.3545E+03 -.7440E+02	-.1342E+03 -.1431E+03	-.1342E+03 -.1431E+03
3	3	3	.2653E+03 .3100E+03	.2653E+03 .3100E+03	.2653E+03 .3100E+03
5	1	1	.7556E+03 .3189E+02	-.1282E+02 .1596E+05	-.1062E+02 .1596E+05
4	4	0	-.2661E+03 -.3707E-13	.2661E+03 -.2407E-13	.3525E+02 .2309E+03
5	3	1	-.2506E+03 -.3438E+02	-.6759E+02 -.9730E+02	.2390E+02 -.1715E+03
4	4	2	-.2386E+03 -.1338E+03	-.2386E+03 -.1338E+03	-.3839E+02 -.2674E+03
6	0	0	-.5535E+03 -.1352E-15	.2037E+02 .6232E-13	.2037E+02 .6394E-12
6	2	0	-.5513E+03 .1057E-13	-.6246E+02 .4650E-13	-.6227E+01 -.1009E+03
5	3	3	-.7637E+02 -.1999E+02	-.4194E+02 -.3316E+02	-.4194E+02 -.3316E+02

6	2	2	.4754E+02 .7638E+01	-.1307E+02 .2293E+02	-.1307E+02 .2293E+02
4	4	4	.1698E+03 .1766E+03	.1698E+03 .1766E+03	.1698E+03 .1766E+03
5	5	1	.2108E+03 .4044E+02	.2108E+03 .4044E+02	.1629E+02 .2025E+03
7	1	1	.4022E+03 .8043E+01	.1614E+03 .5632E+02	.1614E+03 .5632E+02
6	4	0	-.2310E+03 -.9005E-14	-.1091E+04 -.2054E-13	.1165E+02 .1462E+03
6	4	2	-.7130E+02 -.1923E+02	-.2336E+02 -.2889E+02	-.5429E+01 -.5757E+02
5	5	3	-.1415E+03 -.5999E+02	-.1415E+03 -.0999E+02	-.4561E+02 -.1459E+03
7	3	1	-.2312E+03 -.1773E+02	-.4488E+02 -.4136E+02	.2426E+01 -.1241E+03
6	5	0	-.2613E+03 .9736E-17	-.5763E+01 .1967E-13	-.5763E+01 .2302E-12
7	3	3	-.3237E+02 -.4298E+01	-.1342E+02 -.9995E+01	-.1342E+02 -.9995E+01
6	4	4	.1473E+02 .1086E+02	.1378E+01 .1589E+02	.1379E+01 .1503E+02
8	2	0	.3251E+02 -.3555E-15	-.6492E+01 -.4031E-13	-.9103E+01 .1042E+02
6	6	0	-.1248E+03 -.1139E-13	-.1248E+03 -.1216E-13	-.4420E+01 .1293E+03
8	2	2	.2227E+03 .1419E+02	.9804E+01 .5677E+02	.9804E+01 .5677E+02
5	5	5	.9312E+02 .9186E+02	.9312E+02 .9186E+02	.9312E+02 .9186E+02
7	5	1	.1765E+03 .1788E+02	.9061E+02 .2503E+02	.4767E+01 .1252E+03
6	6	2	.1197E+03 .3091E+02	.1197E+03 .3091E+02	.1553E+02 .1163E+03
8	4	0	-.5713E+02 -.3794E-15	-.1051E+02 -.3040E-14	.7091E+01 .2403E+02

REFERENCES

- Aberenkov I V and Heine V 1965 Phil. Mag. 12 529-37
- Almbladh C O, von Barth O, Popovic Z D and Stott M J 1976
Phys. Rev. B14 2250-4
- Anderson P W 1966 Concepts in Solids (New York: Benjamin
Press)
- Animalu A O E 1965 Phil. Mag. 11 379-88
- Animalu A O E and Heine V 1965 Phil. Mag. 12 1249-70
- Appapillai M and Williams A R 1973 J. Phys. F: Metal Phys.
3 759-71
- Ashcroft N W 1968 Phys. Rev. Lett. 21 1748-9
- Austin B J, Heine V and Sham L J 1962 Phys. Rev. 127 276-82
- Bardeen J, Cooper L N and Schrieffer J R 1957 Phys. Rev. 108
1175-1204
- Beck H and Strauss D 1975 Helv. Phys. Acta 48 655-69
- Beevers C J 1963 Acta Met. 11 1029-34
- Benedek R 1978 J. Phys. F: Metal Phys. 8 807-24
- Bergmann G and Rainer D 1973 Z. Phys. 263 59-68
- Brack M, Jennings B K and Chu Y H 1976 Phys. Lett. 65B 1-4
- Bugeat J P, Chami A C and Ligeon E 1976 Phys. Lett. 58A 127-30
- Caron L G 1972 Phys. Rev. B5 238-40
_____ 1974. Phys. Rev. B12 5025-38
- Cohen M L and Heine V 1970 Sol. St. Phys. 24 37-248

- Coulthard M 1970 J. Phys. C: Sol. St. Phys. 3 820-34
- Cowley E R 1976 Can. J. Phys. 54 2348-54
- Cowley E R and Shukla R C 1974 Phys. Rev. B9 1261-7
- Daams J M 1977 Ph.D. Thesis, McMaster University
- Daams J M and Carbotte J P 1978 Can. J. Phys. (in press)
- Dynes R C 1972 Solid St. Commun. 10 615-8
- Fetter A L and Walecka J D 1971 Quantum Theory of Many Particle Systems (New York: McGraw-Hill)
- Gaspari G D and Gyorffy B L 1972 Phys. Rev. Lett. 28 801-5
- Gilat G, Rizzi G and Cubiotti G 1969 Phys. Rev. 185 971-83
- Glyde H R and Mayne K I 1965a Phil. Mag. 12 919-37
- 1965b Phil. Mag. 12 997-1003
- Grigor'ev F V, Kormer S B, Mikhailova O L, Tolochko A P and Urlin V D 1972 JETP Lett. 16 201-4
- Gupta R P and Sinha S K 1976 in Superconductivity in d- and f-Band Metals edited by D H Douglas (Plenum: New York) 583-92
- Harris F E, Kumar L and Monkhorst H J 1973 Phys. Rev. B7 2850-66
- Harrison W A 1966 Pseudopotentials in the Theory of Metals (New York: Benjamin Press)
- Harrison W A 1970 Solid State Theory (New York: McGraw-Hill)
- Hedin L and Lundqvist B I 1971 J. Phys. C: Solid St. Phys. 4 2064-83
- Heine V 1970 Sol. St. Phys. 24 1-36
- Heine V and Aberenkov I V 1964 Phil. Mag. 9 451-65

- Heine V and Weaire D 1970 Sol. St. Phys. 24 249-463
- Hohenberg P and Kohn W 1964 Phys. Rev. 136 B864-71
- Inglesfield J E and Pendry J B 1976 Phil. Mag. 34 205-15
- Jena P and Singwi K S 1978 Phys. Rev. B17 1592-5
- Jennings B.K 1976 Ph.D. Thesis, McMaster University
- Kittel C 1963. Quantum Theory of Solids (New York: John Wiley and Sons)
- Kirzhnits D A 1957 JETP Lett. 5 64-71
- Kleinman L and Phillips J C 1959 Phys. Rev. 116 880-4
- Kohn W and Sham L J 1965 Phys. Rev. 140 A1133-88.
- Leavens C R 1970 Ph.D. Thesis, McMaster University
- _____ 1973 Solid St. Commun. 13 1607-10
- _____ 1974 Solid St. Commun. 15 1329-32
- Ma C Q and Sahni V 1977 Phys. Rev. B16 4249-55
- Mainwood A and Stoneham A M. 1976 J. Less-Common Metals 49
271-81
- McKee B T A, Triftshäuser W and Stewart A T 1972 Phys. Rev.
Lett. 28 358-60
- McMillan W L 1968 Phys. Rev. 167 331-44
- Messiah A 1961 Quantum Mechanics (Amsterdam: North Holland Publishing Co.)
- Murray G T 1961 J. Appl. Phys. 32 1045-8
- Nagara H, Miyaga H and Nakamura T 1976 Prog. Theo. Phys. 56
396-414
- Papaconstantopoulos D A and Klein B M 1977 Ferroelectrics
17 307-10

- Park D 1974 Introduction to the Quantum Theory (New York: McGraw-Hill)
- Phillips J C and Kleinman L 1959 Phys. Rev. 116 287-94
- Pines D and Nozières P 1966 The Theory of Quantum Liquids Vol 1 (New York: Benjamin Press)
- Popović Z D and Carbotte J P 1974 J. Phys. F: Metal Phys. 4 1599-607
- Popović Z D, Carbotte J P and Piercy G R 1974 J. Phys. F: Metal Phys. 4 351-60
- Popović Z D and Stott M J 1974 Phys. Rev. Lett. 33 1164-7
- Popović Z D, Stott M J, Carbotte J P and Piercy G R 1976 Phys. Rev. B13 590-602
- Rainer D and Bergmann G 1974 J. Low Temp. Phys. 14 501-19
- Schneider T 1969 Helv. Phys. Acta 42 957-89
- Schneider T and Stoll E 1971 Physica 55 702-10
- Shaw R W 1968 Phys. Rev. 174 769-81
- Shaw R W 1969a J. Phys. C: Sol. St. Phys. 2 2335-49
- Shaw R W 1969b J. Phys. C: Sol. St. Phys. 2 2350-65
- Shaw R W 1970a J. Phys. C: Sol. St. Phys. 3 1140-58
- Shaw R W 1970b Ph.D. Thesis, Stanford University
- Shaw R W and Harrison W A 1967 Phys. Rev. 163 604-11
- Shaw R W and Heine V 1972 Phys. Rev. B5 1646-50
- Shaw R W and Pynn R 1969 J. Phys. C: Sol. St. Phys. 2 2071-88
- Shyu M W, Wehling J H, Cordes M R and Gaspari G D 1971 Phys. Rev. B6 1802-1815

- Singwi K S, Sjölander A, Tosi M P and Land R H 1970 Phys. Rev. B1 1044-53
- Stoneham A M 1972a Ber. Bunsenges. Phys. Chem. 76 816-23
_____ 1972b J. Phys. F: Metal Phys. 2 417-20
- Switendick A C 1976 in Superconductivity in d- and f-Band Metals edited by D.H. Douglass (Plenum: New York) 593-605
- Vashishta P and Singwi K S 1972 Phys. Rev. B6 875-87
- Vereshchagin L F, Yakovlev E N and Timofeev Yu A 1975 JETP Lett. 21 85-6
- Vook F L, Birnbaum H K, Brown W L, Corbett J W, Crawford J H, Goland A N, Kulcinski G L, Robinson M T, Seidman D N, Young F W 1975 Rev. Mod. Phys. 47 Suppl. No. 3 S1-S44
- Whitmore M D 1975 Phys. Lett. 55A 57-8
- Williams A R 1973 J. Phys. F: Metal Phys. 3 781-4
- Williams A R and Appapillai M 1973 J. Phys. F: Metal Phys. 3 772-80
- Zaremba E, Sander L M, Shore H B and Rose J H 1977 J. Phys. F: Metal Phys. 7 1763-72
- Ziman J M 1960 Electrons and Phonons (London: Oxford University Press)